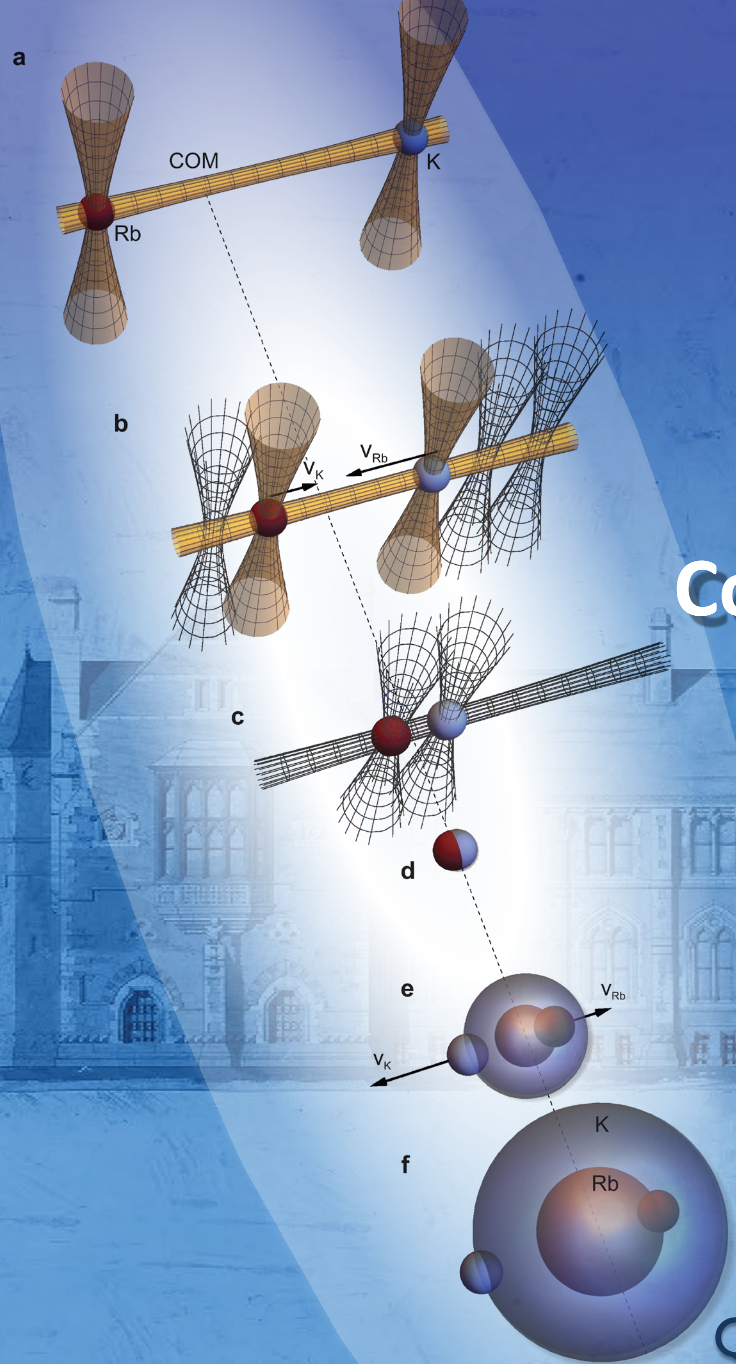

Quantum Scattering in a Collider for Ultracold Atoms

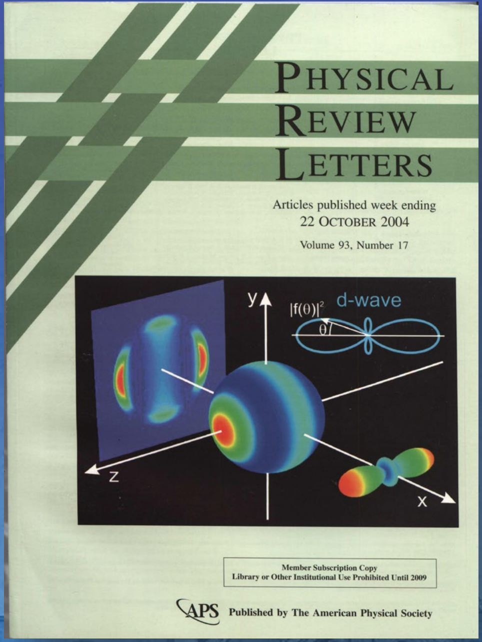
PHYSICAL REVIEW LETTERS

Articles published week ending 22 OCTOBER 2004

Volume 93, Number 17

Member Subscription Copy
Library or Other Institutional Use Prohibited Until 2009

APS Published by The American Physical Society

Otago : University

Niels Kjærgaard

Department of Physics

QSO – Centre for Quantum Science

Dodd-Walls Centre for Photonic and Quantum Technologies

UNIVERSITY of OTAGO
Te Whare Wānanga o Otāgo
NEW ZEALAND

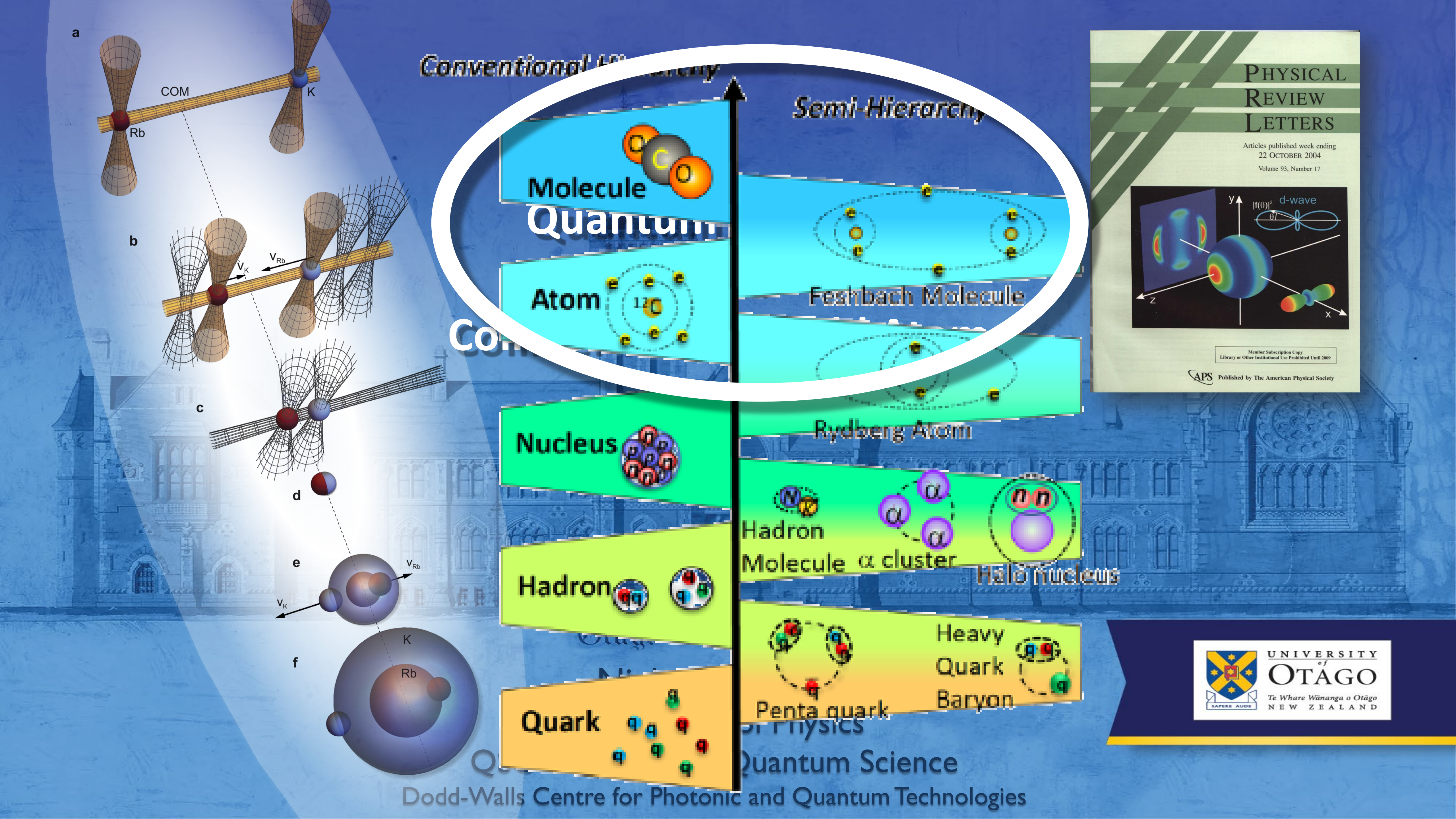
a
COM
Rb
K
b
v_K
v_{Rb}
c
d
e
f
Conventional Hierarchy
Semi-Hierarchy
Molecule
Quantum
Atom
Nucleus
Hadron
Quark
Feshbach Molecule
Rydberg Atom
Hadron Molecule
α cluster
Halo nucleus
Penta quark
Heavy Quark Baryon
Quantum Science
Dodd-Walls Centre for Photonic and Quantum Technologies
PHYSICAL REVIEW LETTERS
Articles published week ending 22 OCTOBER 2004
Volume 93, Number 17
d-wave
APS Published by The American Physical Society
UNIVERSITY of OTAGO
Te Whare Wānanga o Otāgo
NEW ZEALAND
SAPERE AUDE

Colliding indistinguishable bosons (^{87}Rb)

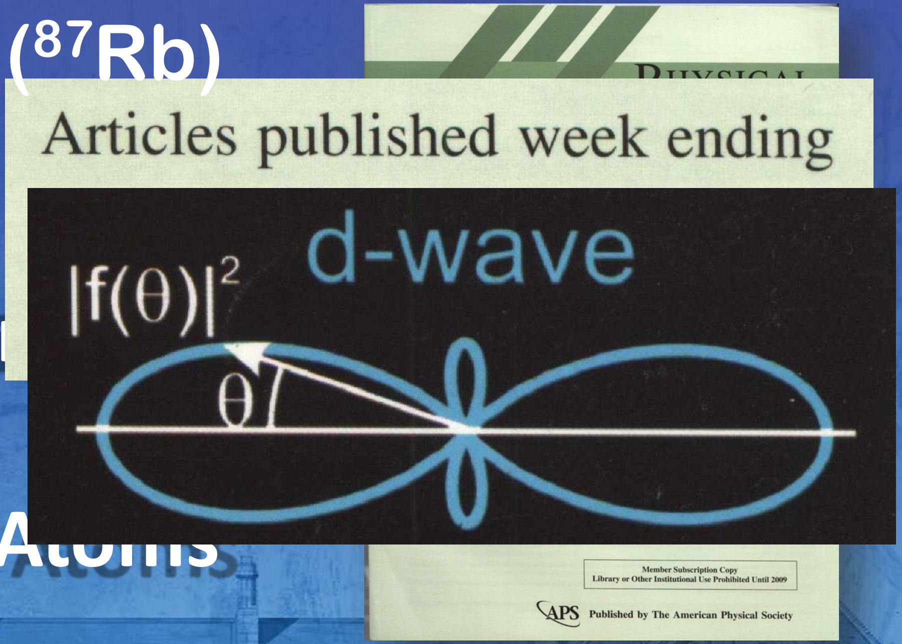

Quantum Scatteri
in a
Collider for Ultracold A

?

Otago : University

Niels Kjærgaard
Department of Physics
QSO – Centre for Quantum Science
Dodd-Walls Centre for Photonic and Quantum Technologies

UNIVERSITY of OTAGO
Te Whare Wānanga o Otāgo
NEW ZEALAND

Anatomy of an Atom (^{87}Rb): Internal structure

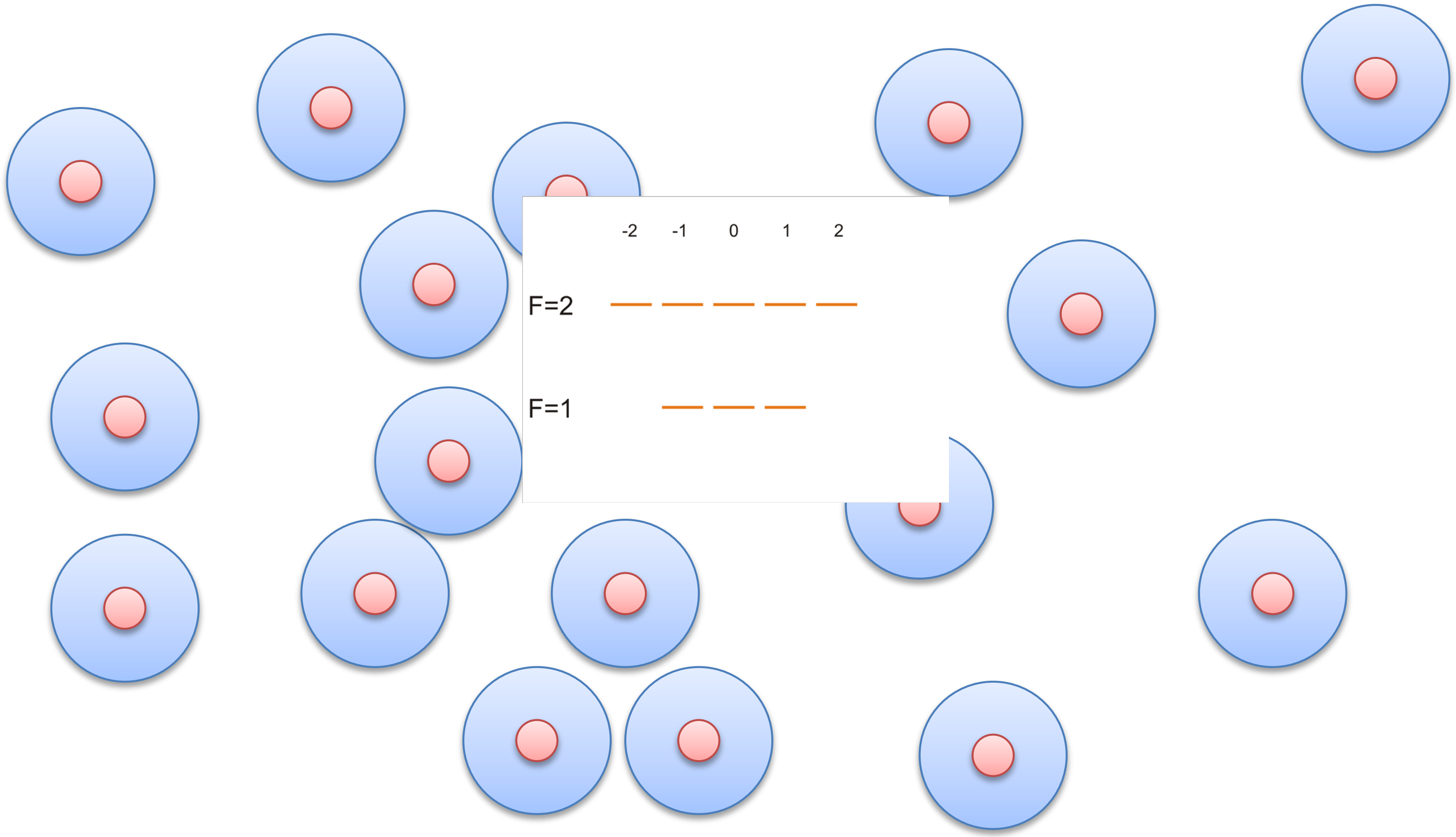

Atoms in magnetic field: Zeeman

^{87}Rb Ground state splitting in magnetic field

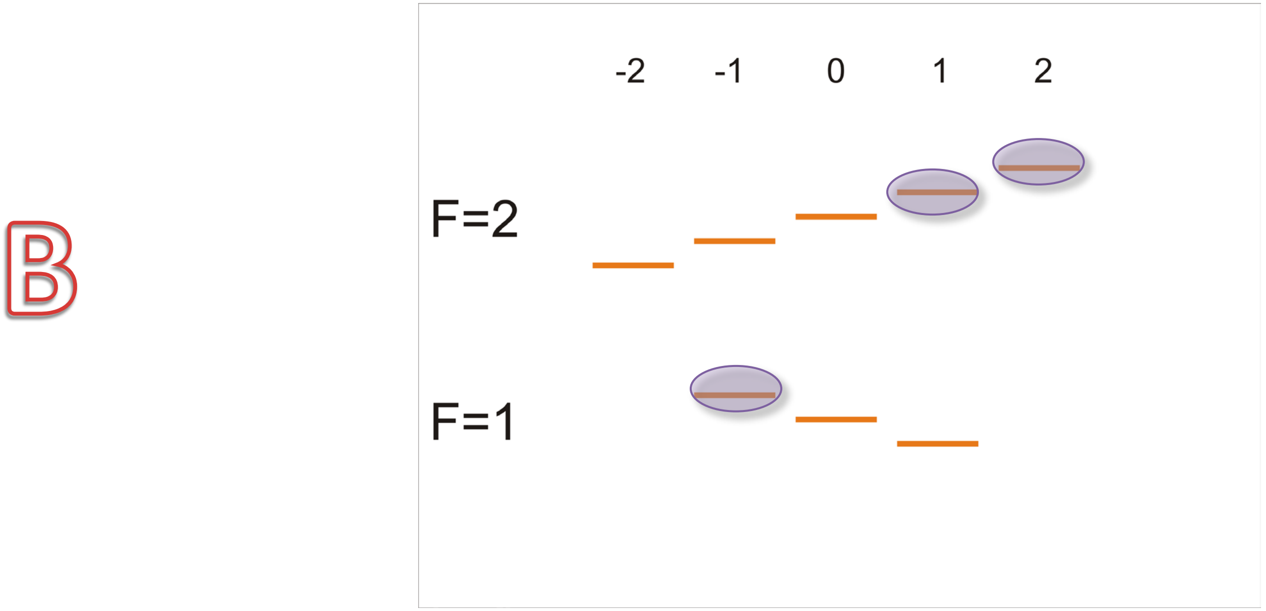

Certain states minimize their energy by seeking a low magnetic field!

Magnetic atom trap

Confinement

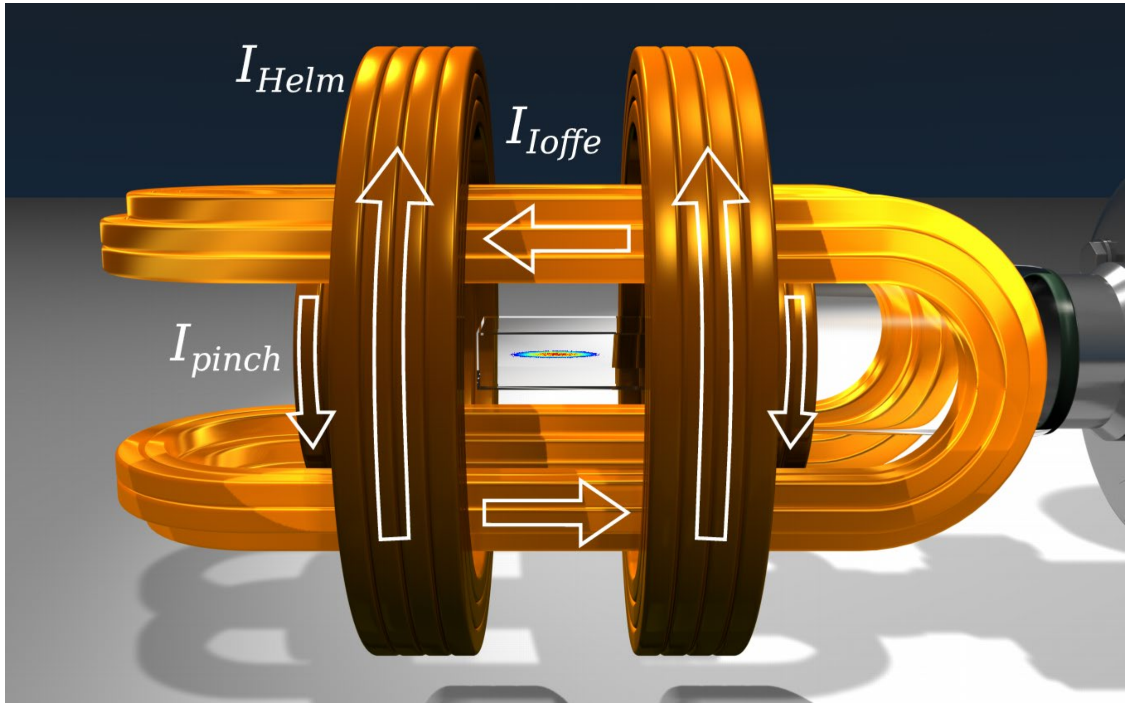

We can detect our atoms via absorption of resonant laser light

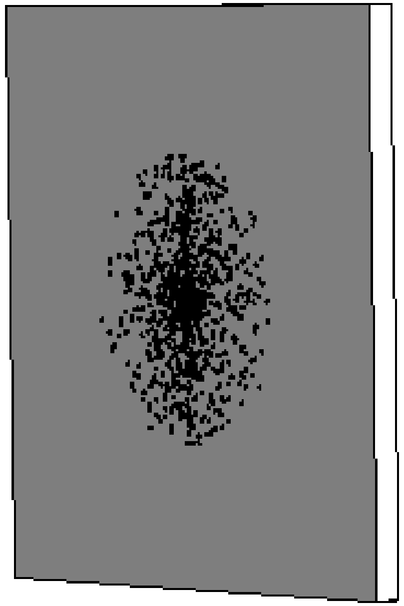

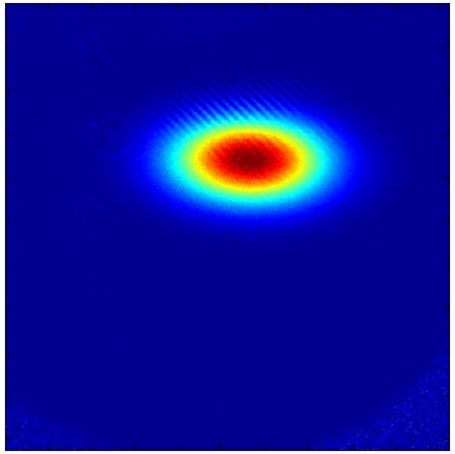

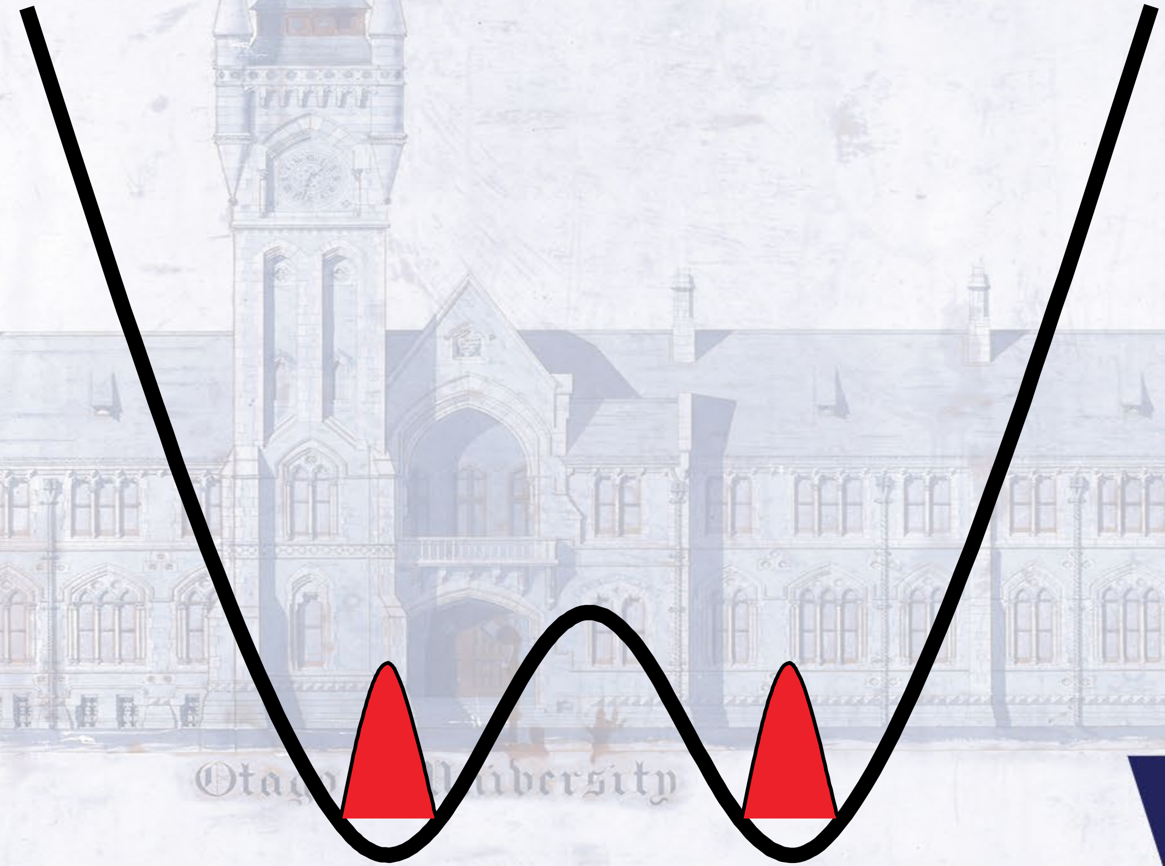

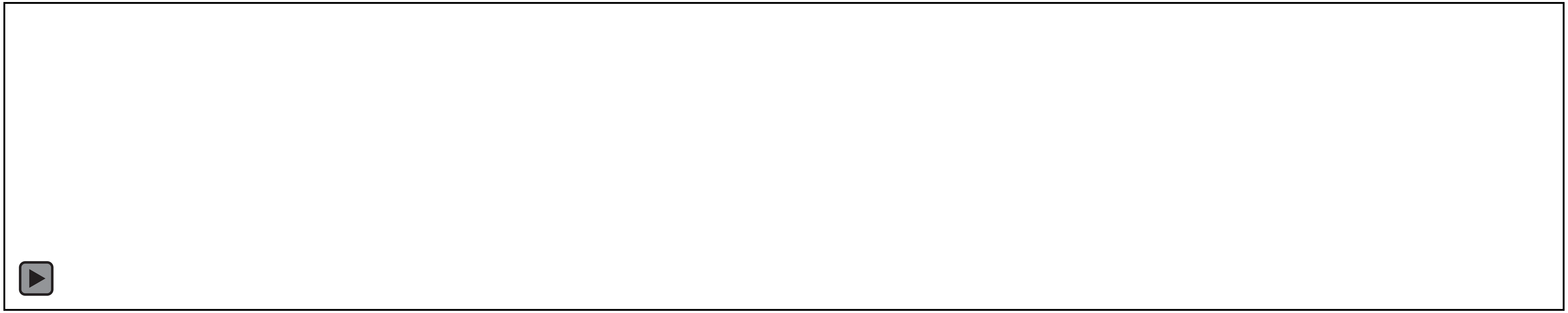

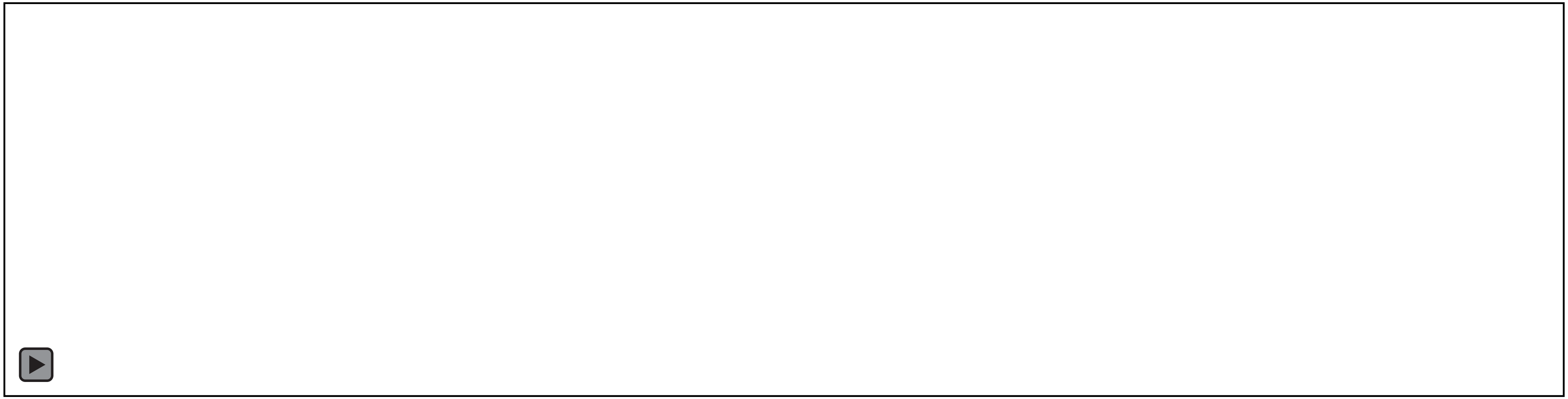

Note:
Throughout this talk energies will be stated in units of k_B

(1 μK ~ 100 peV)

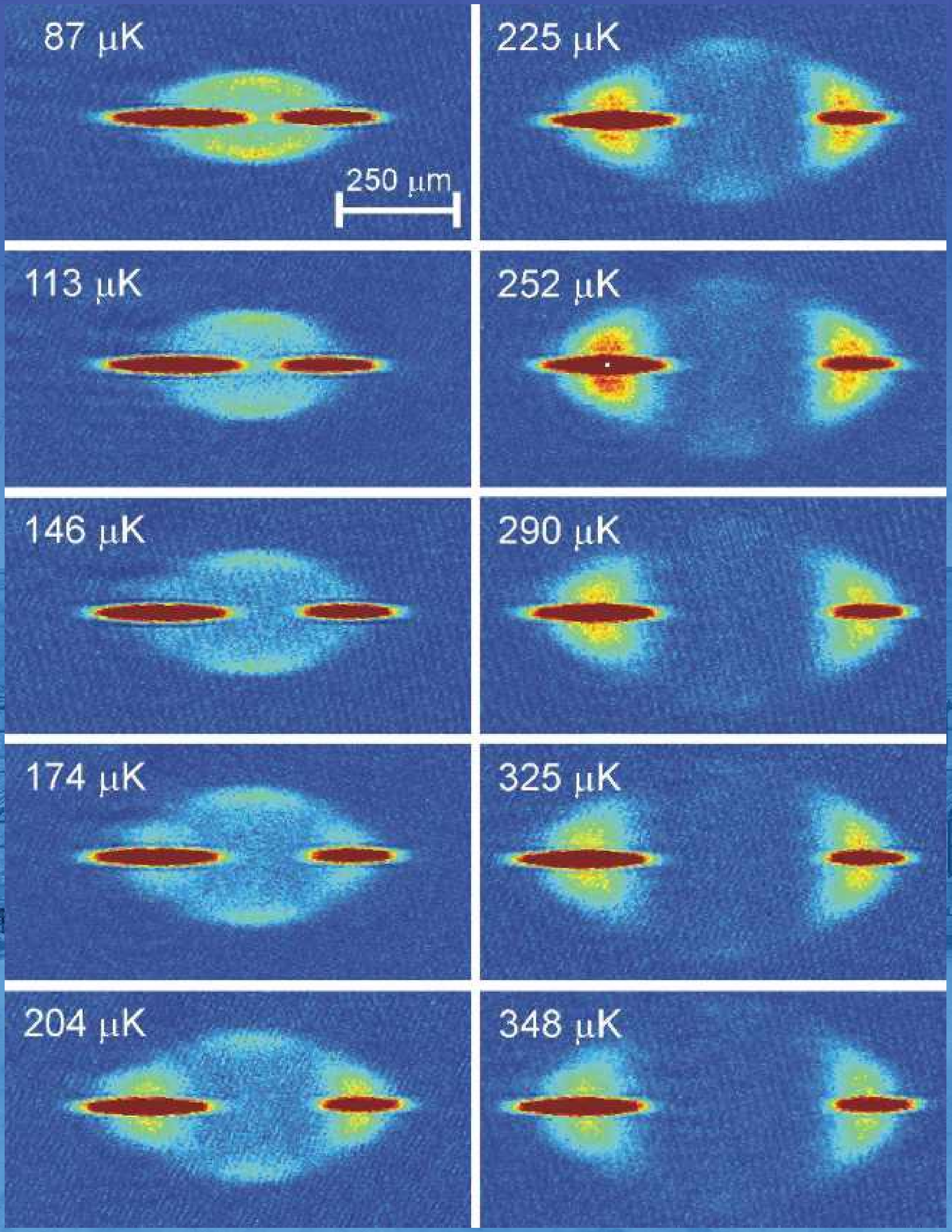
87 μK
250 μm
225 μK
113 μK
252 μK
146 μK
290 μK
174 μK
325 μK
204 μK
348 μK

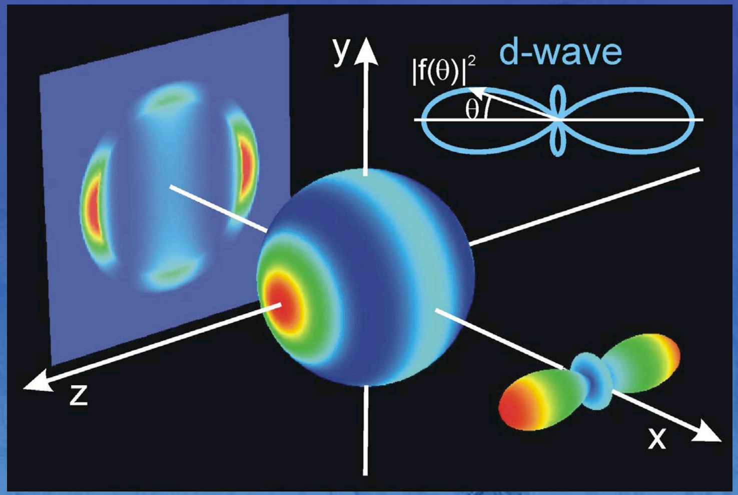
y
$|f(\theta)|^2$
d-wave
θ
z
x

s+d partial wave interference

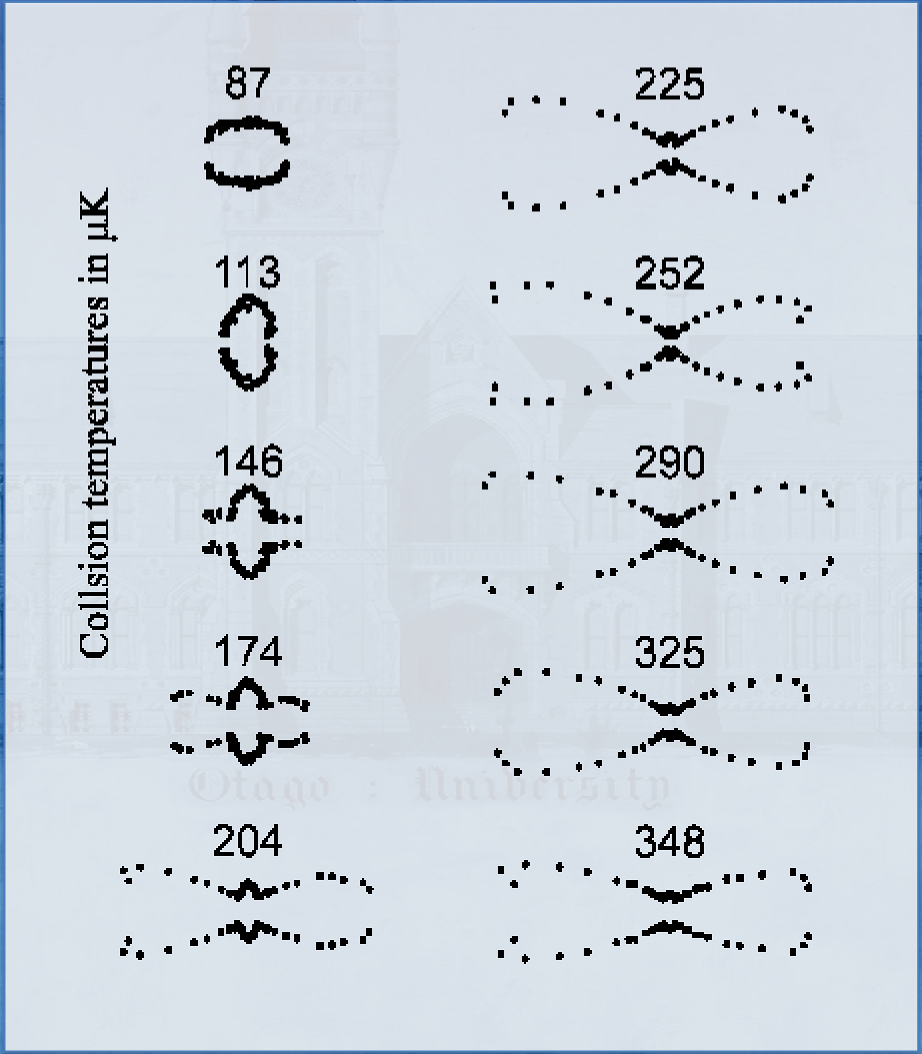

Magnetic colliders can
only be used for
magnetically
weak-field seeking states

A steerable optical tweezer platform

(can use B-field as external tuning parameter for interactions)

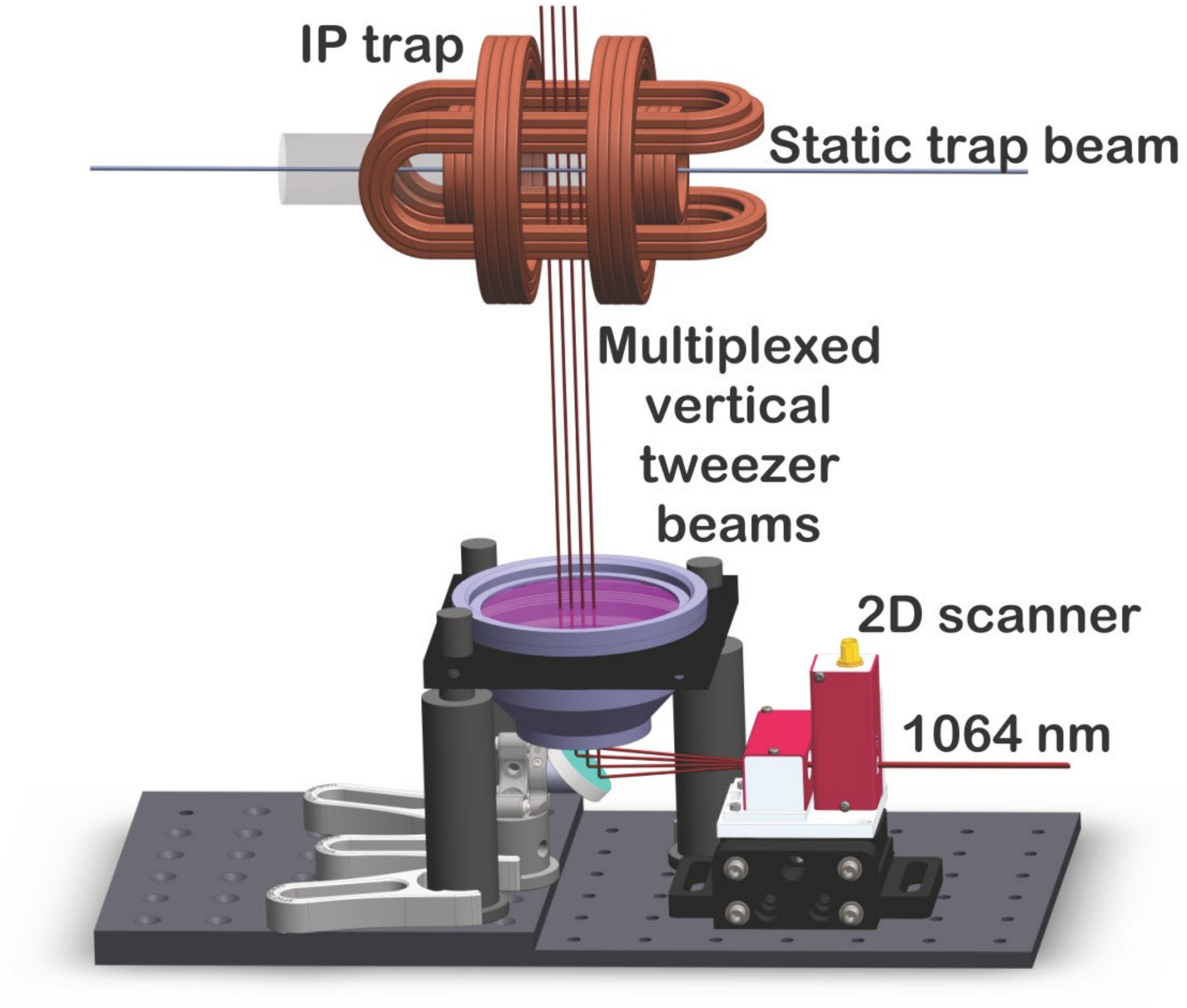

Dipole trap / Optical tweezer

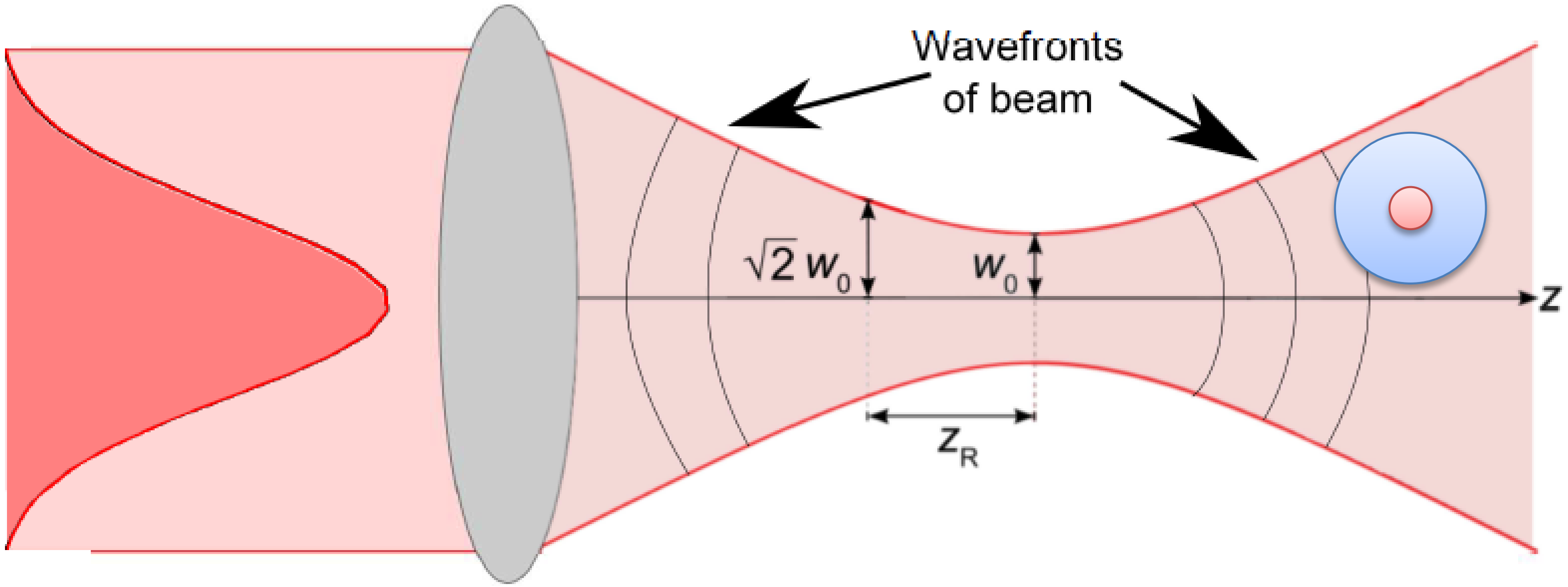

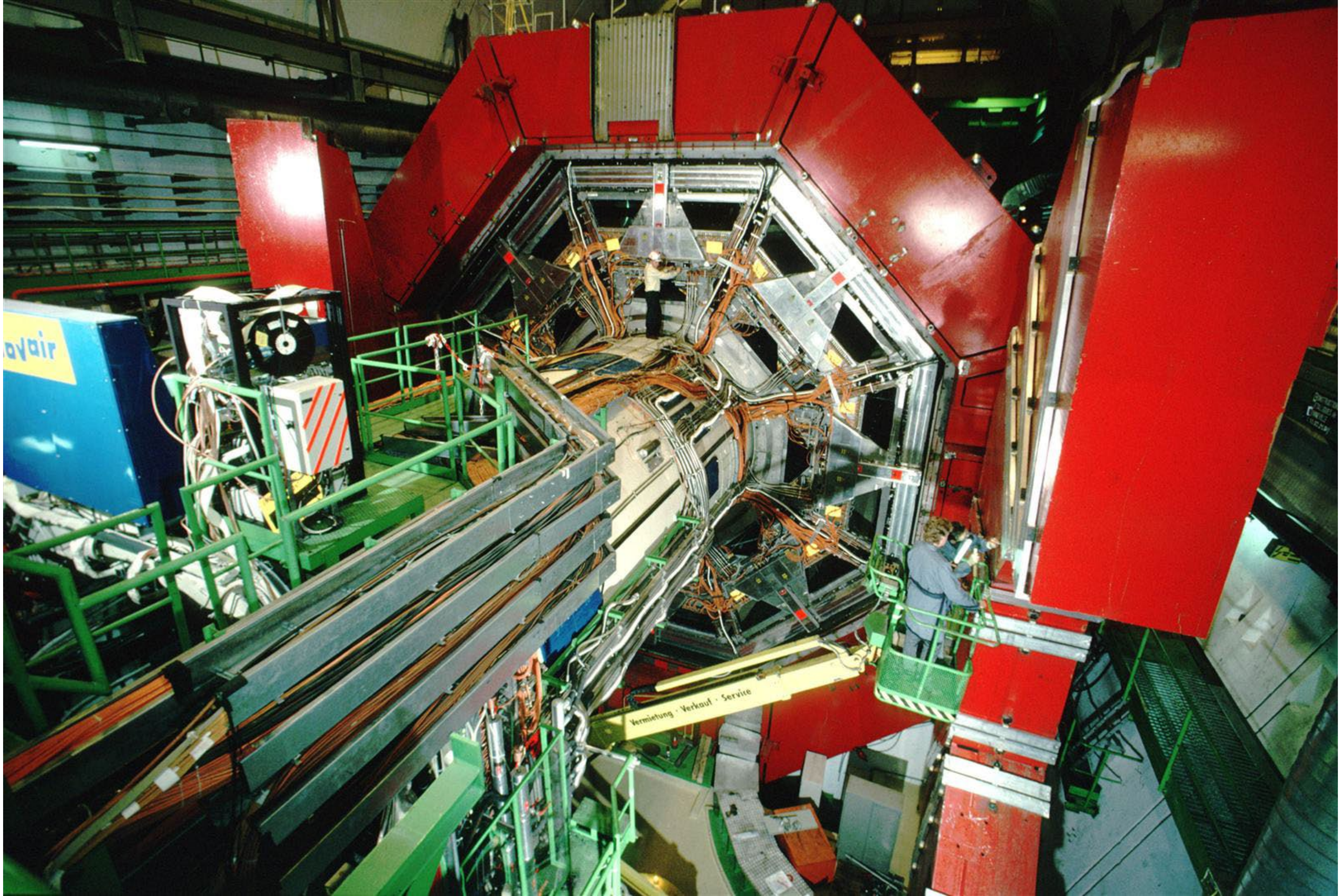
Vermietung · Verkauf · Service

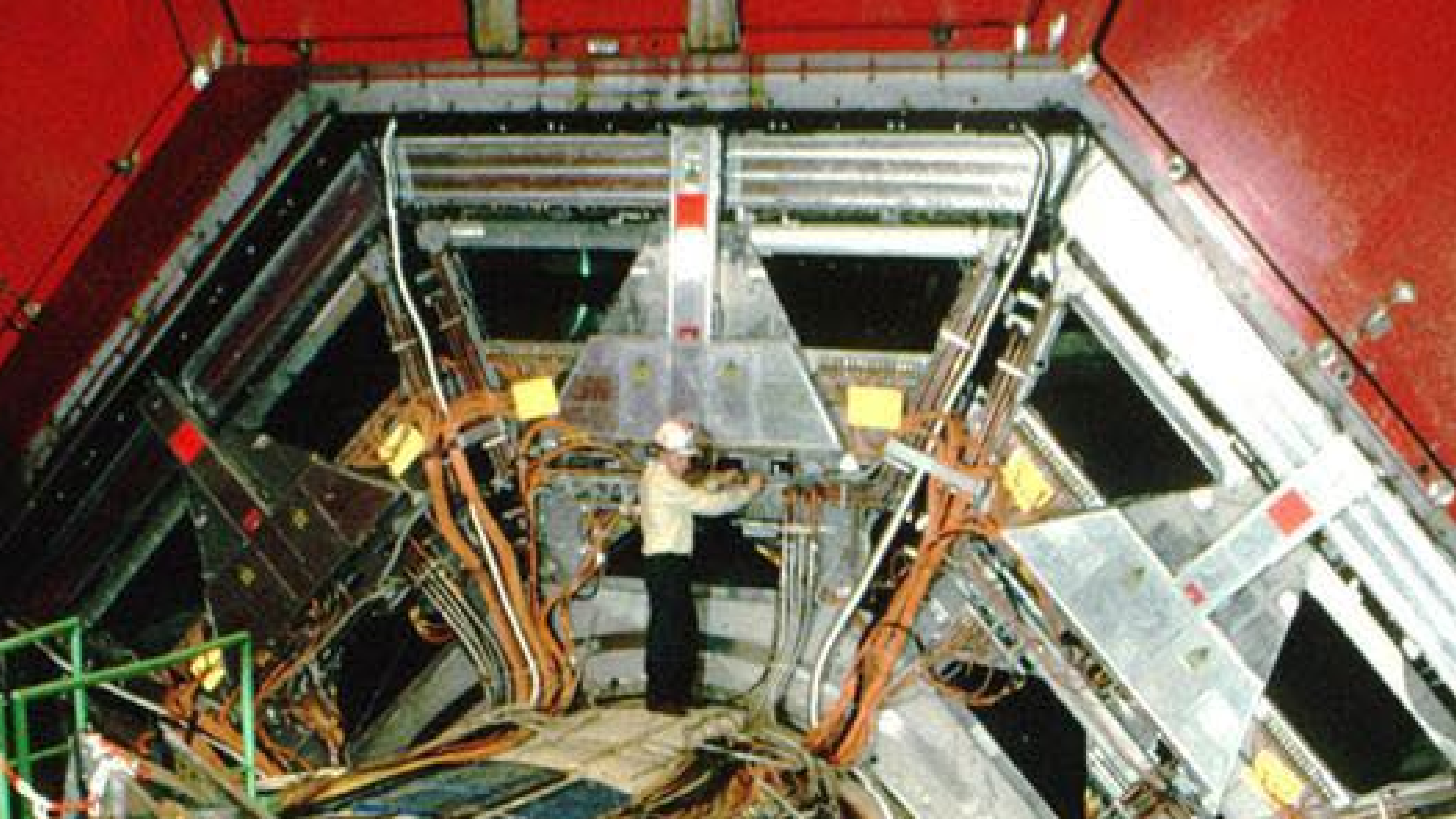

Otago ultracold atom collider

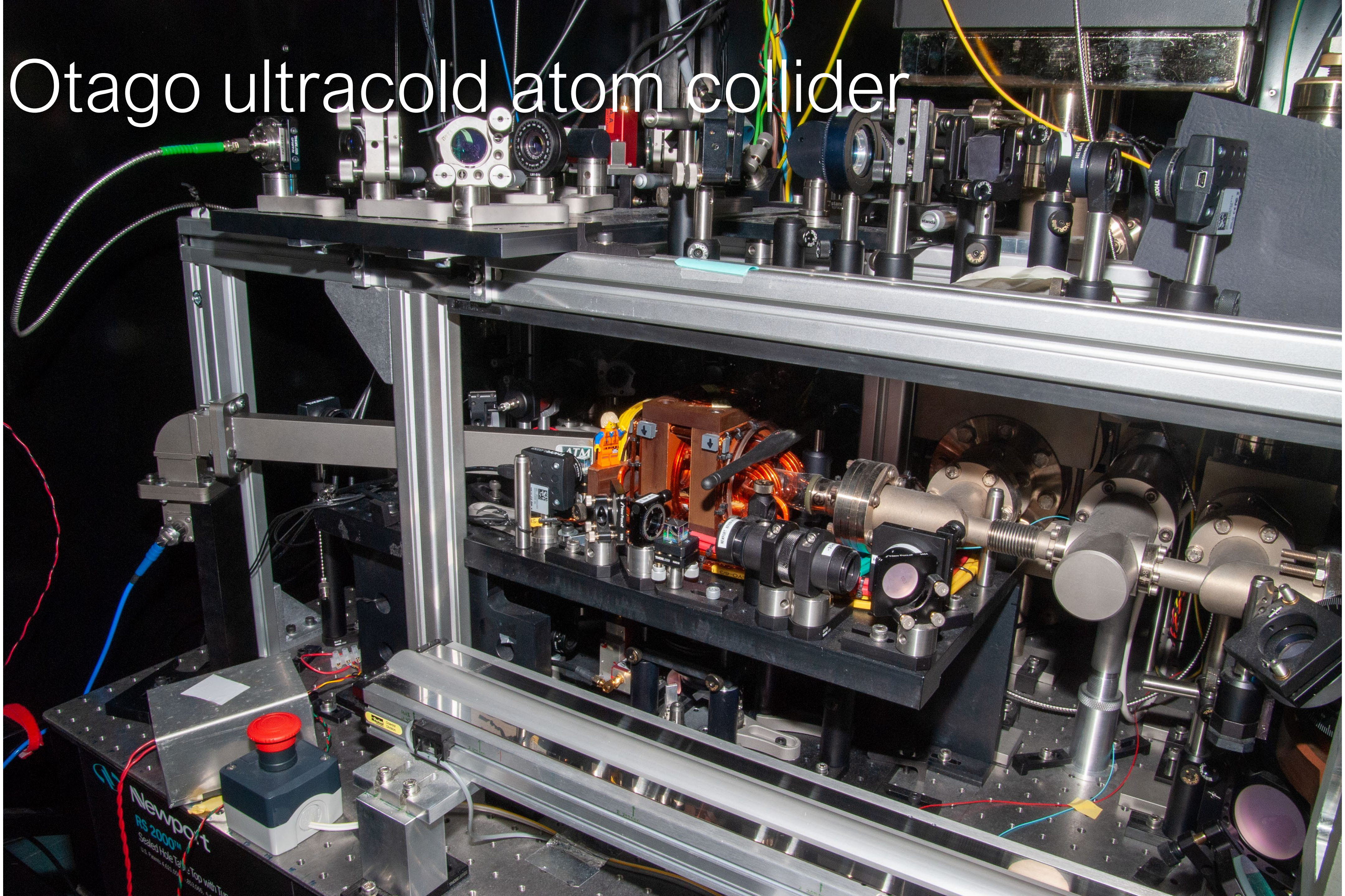


ATM

Crossed laser trap for atoms

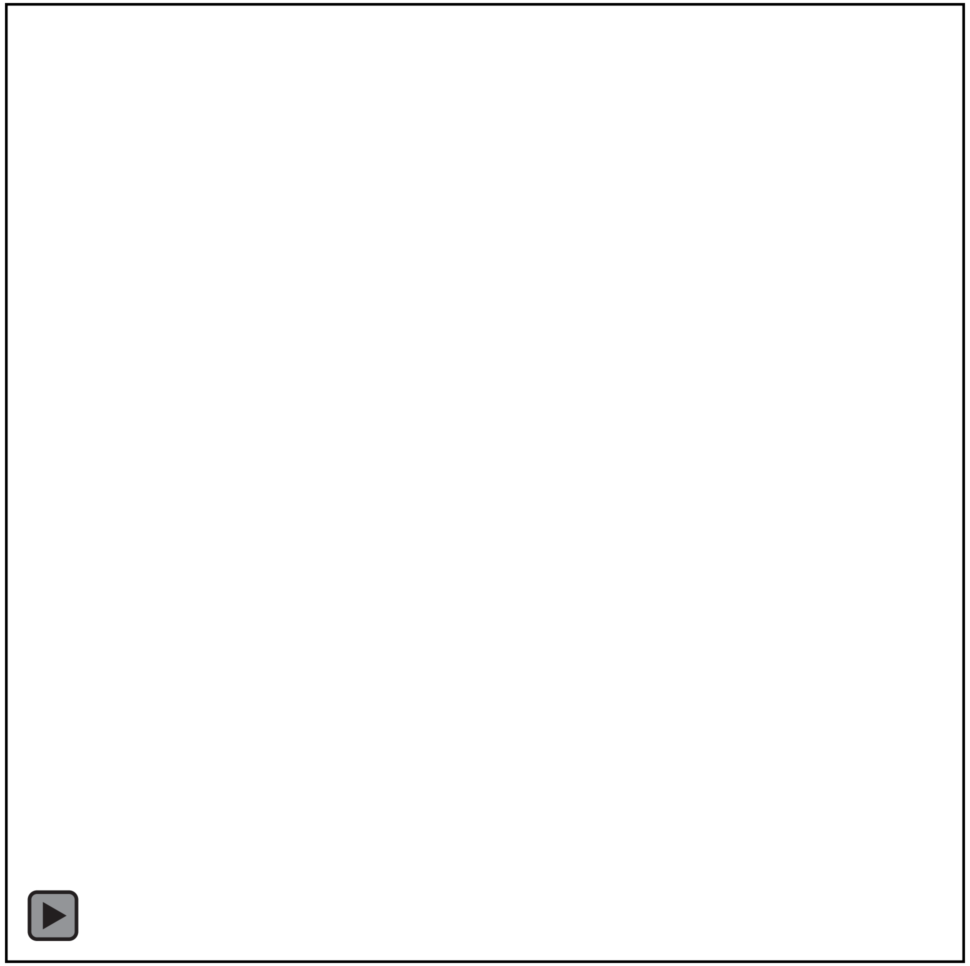

Laser beam can move atoms

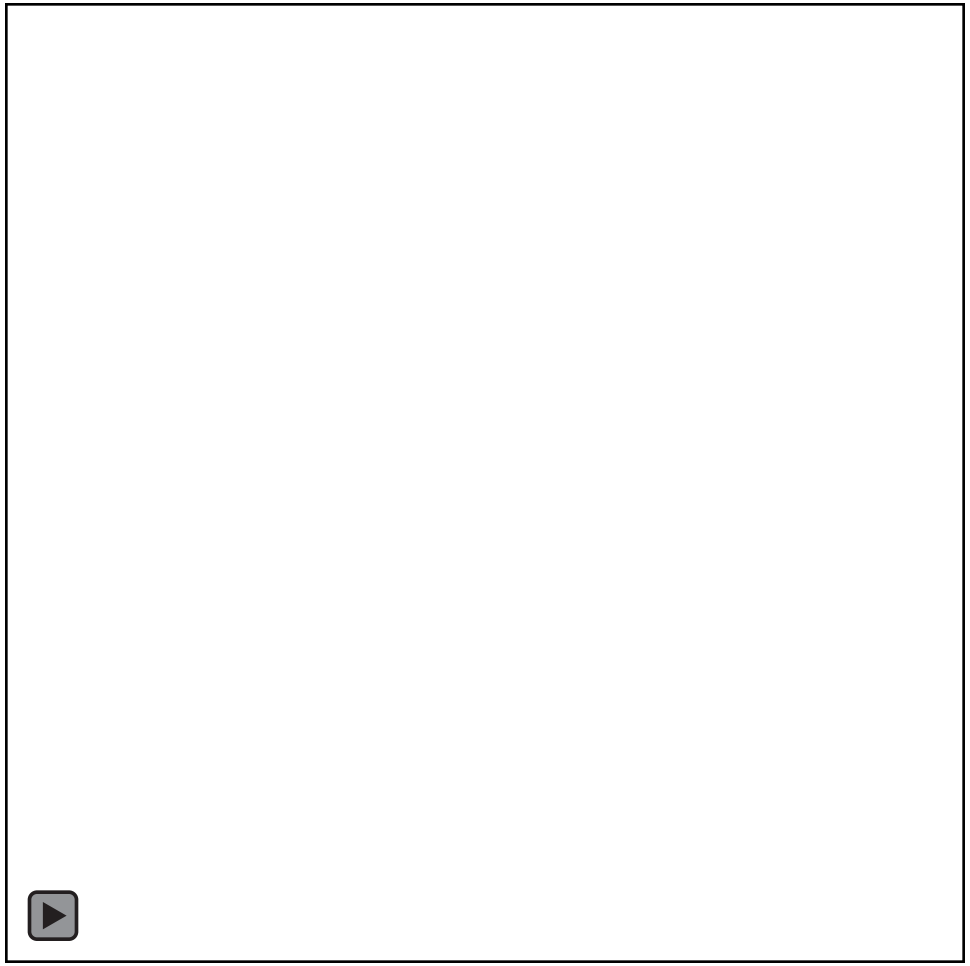

Split operation: Moving two traps

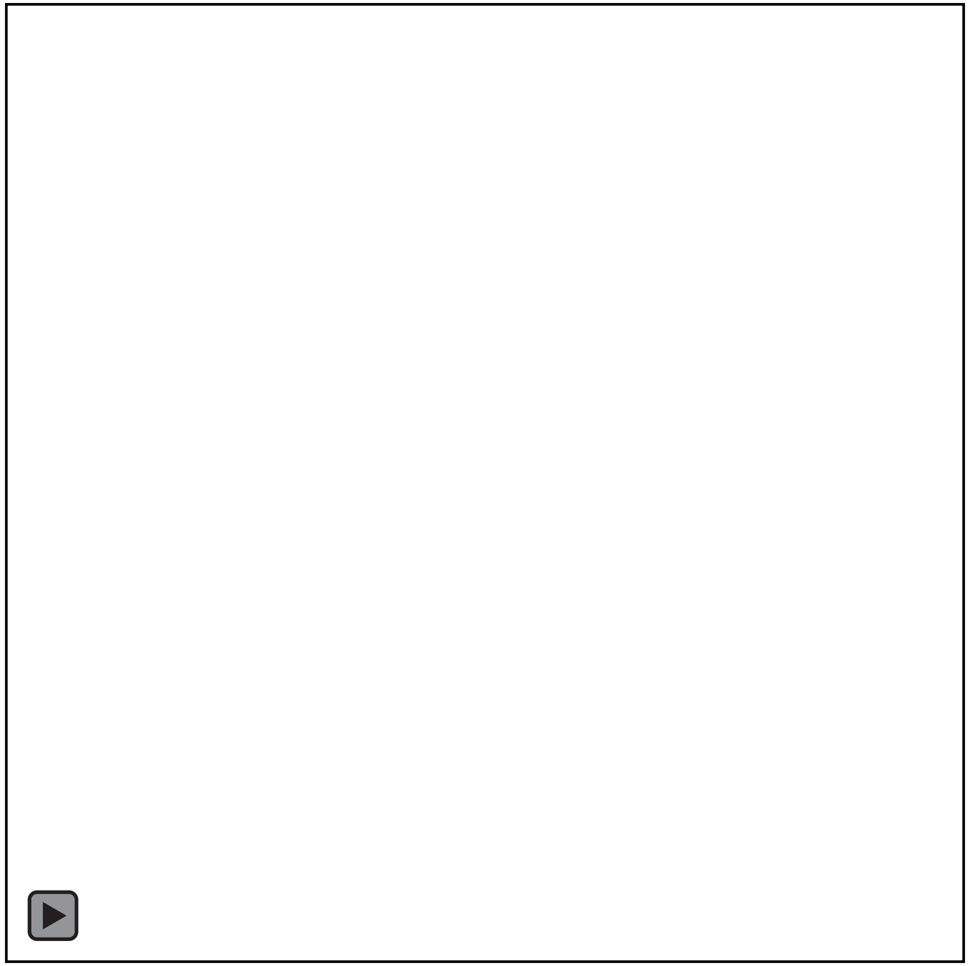

^{87}Rb (boson) angular scattering

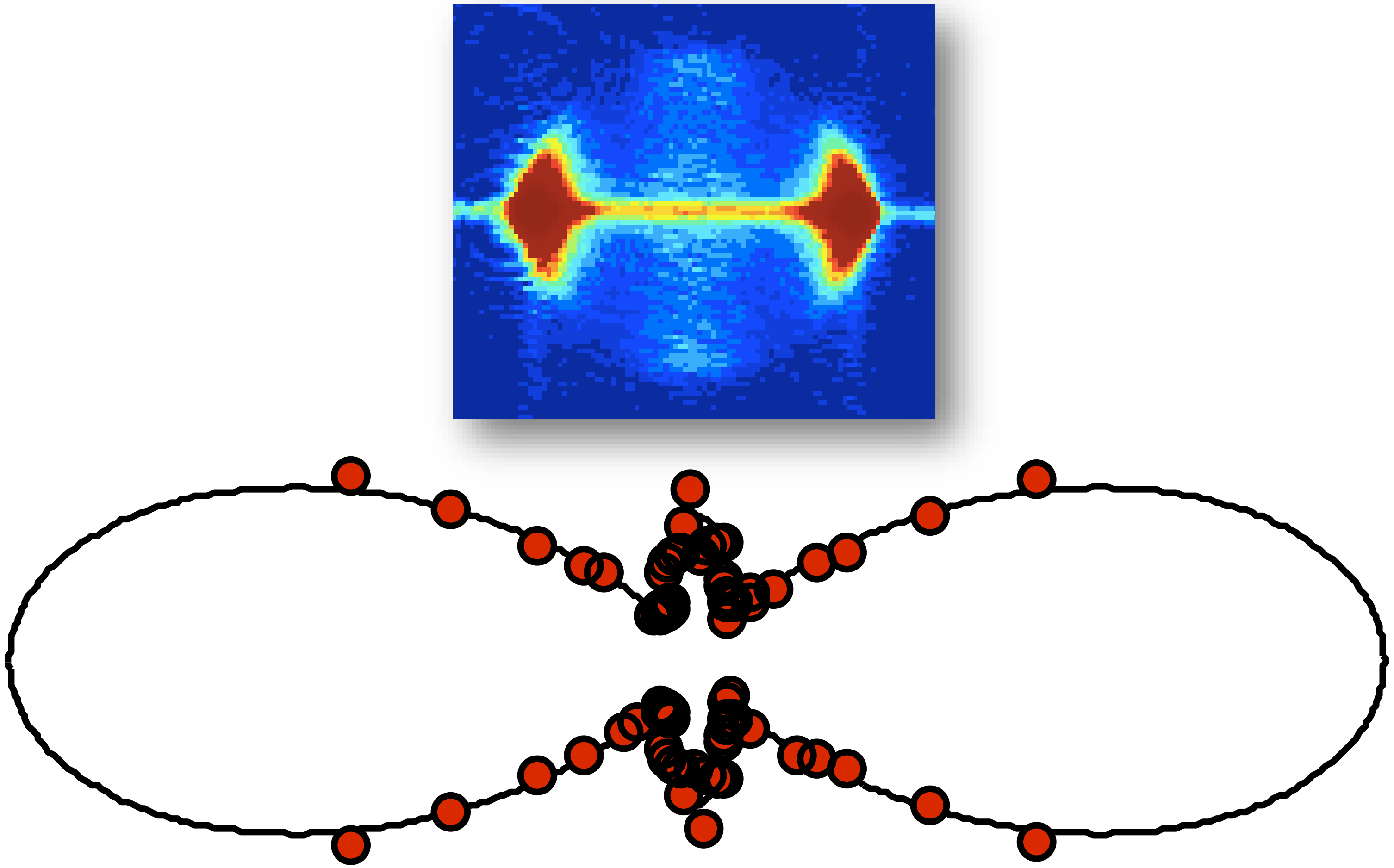

^{40}K (fermion) angular scattering

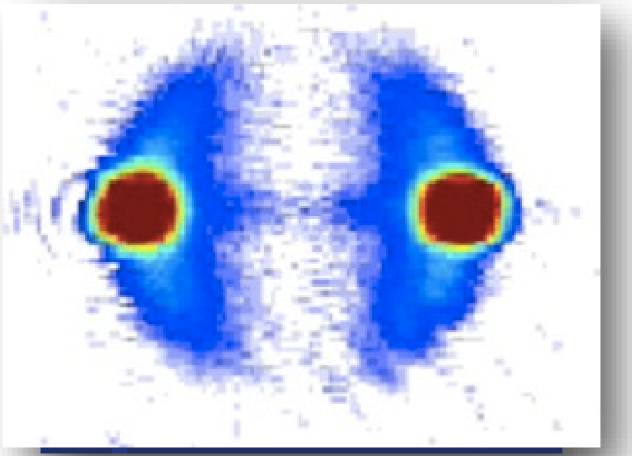

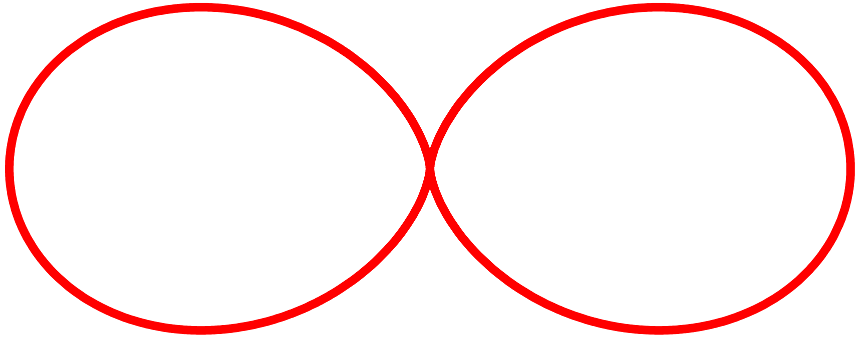

Quantum scattering

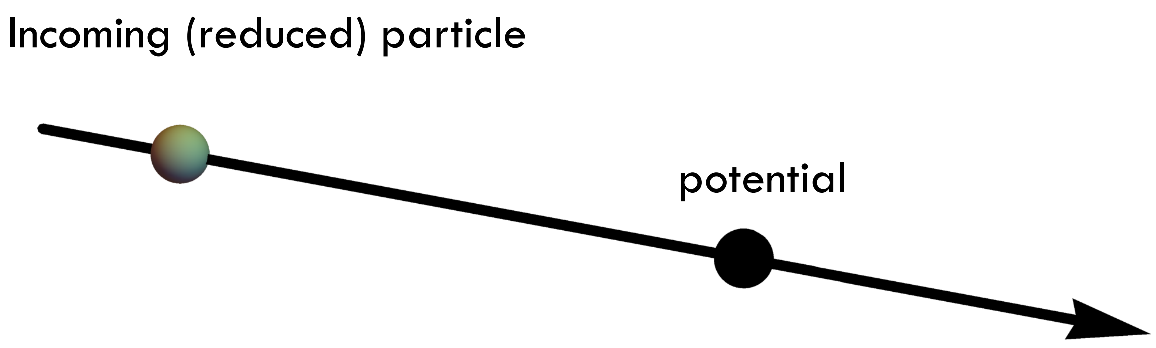

Quantum scattering

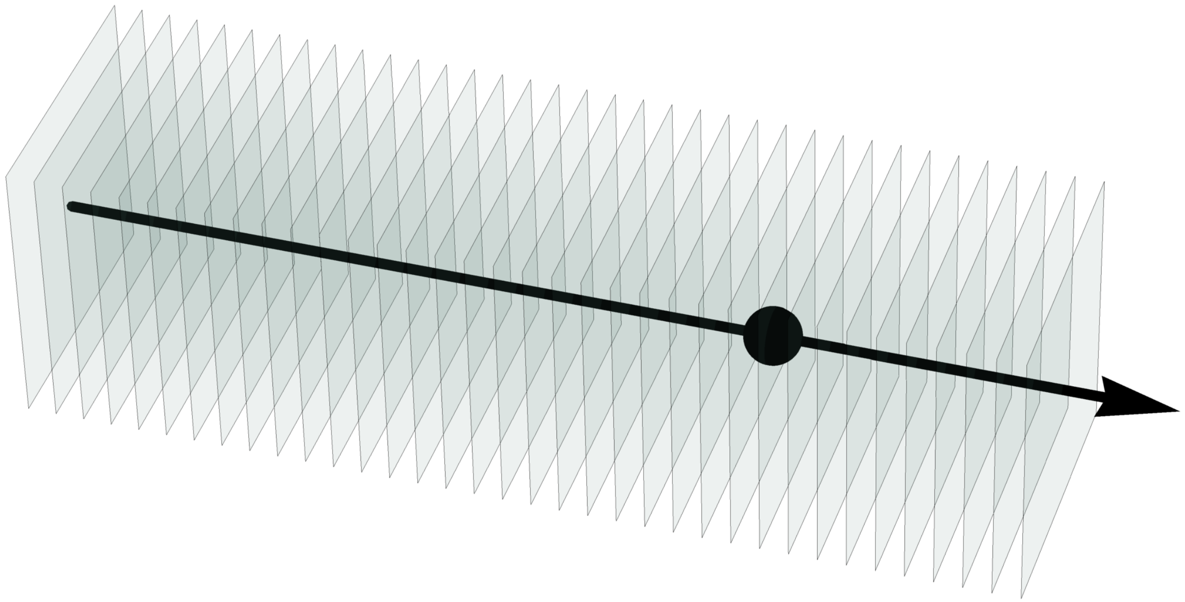

Quantum scattering

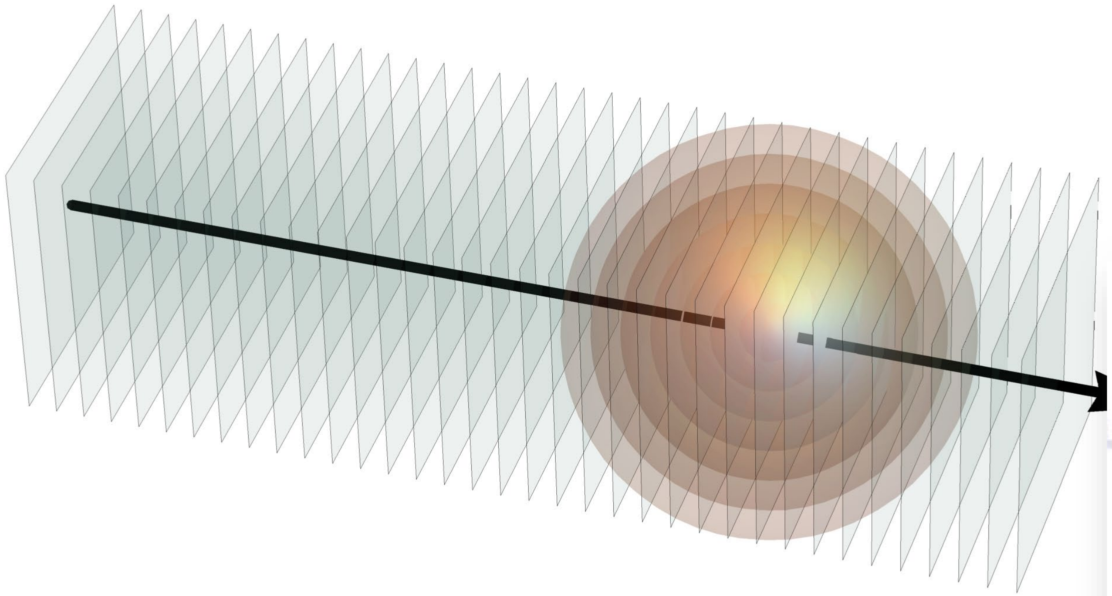

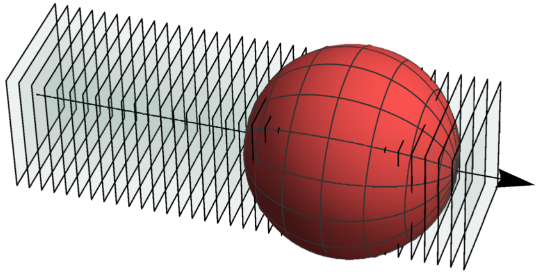

$^{40}K\left(\left|\frac{9}{2},\frac{9}{2}\right\rangle+\left|\frac{9}{2},\frac{9}{2}\right\rangle\right)$

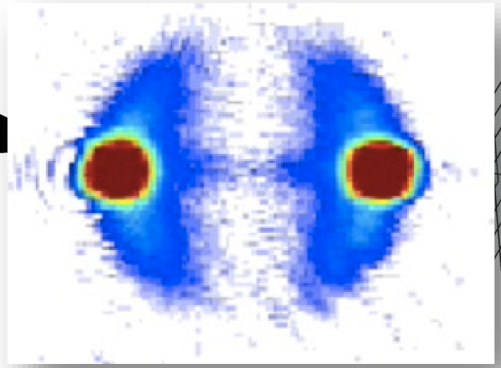

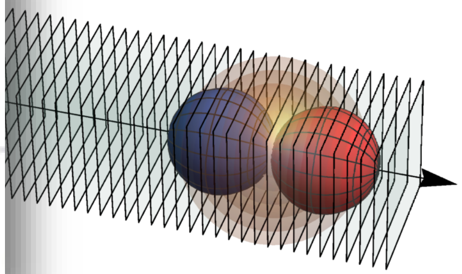

$^{87}Rb(|2,2\rangle+|2,2\rangle)$

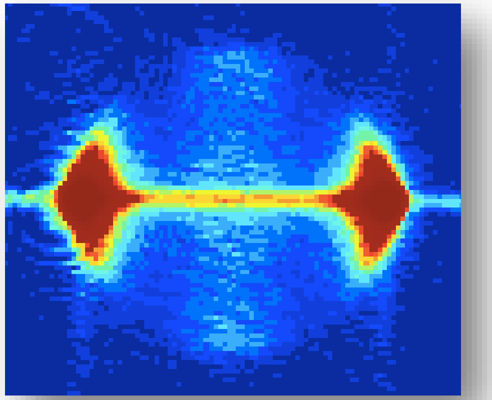

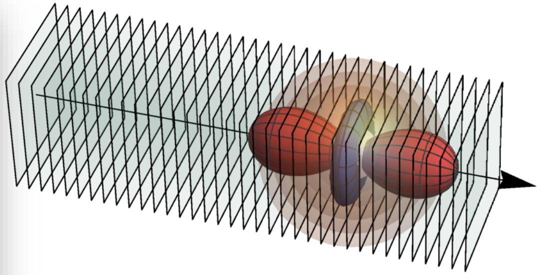

Quantum scattering

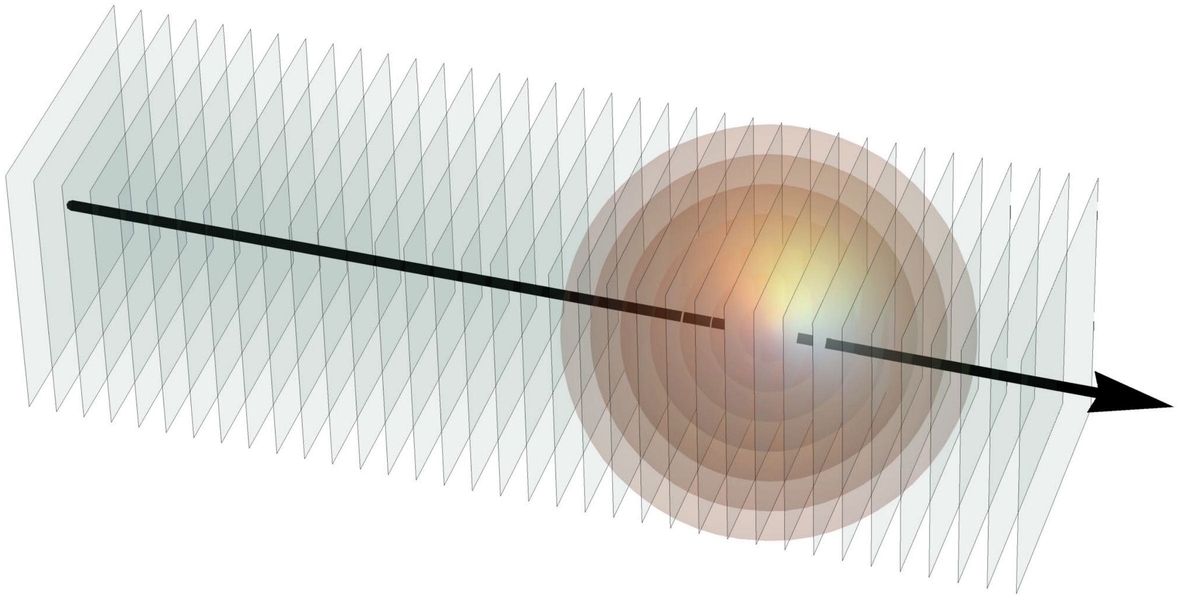

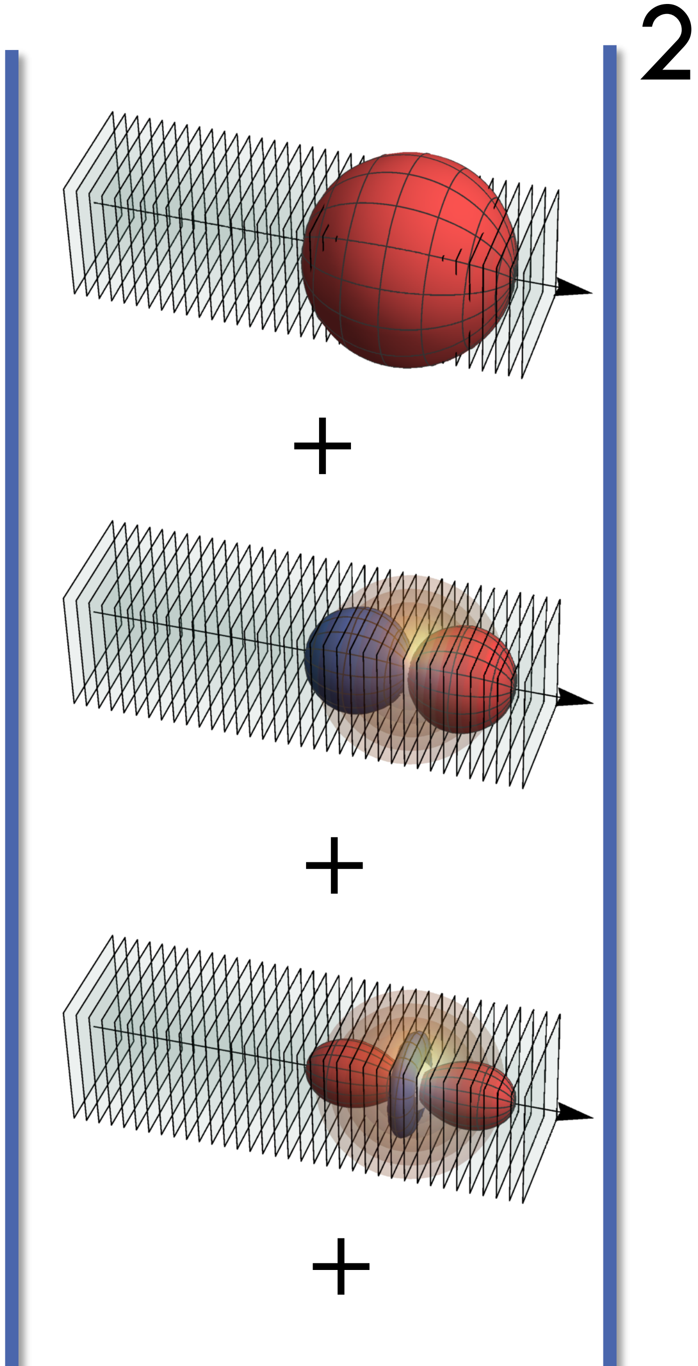

Example: s+p wave interference

$^{87}\mathrm{Rb}(|2,2\rangle+|1,-1)$

constructive

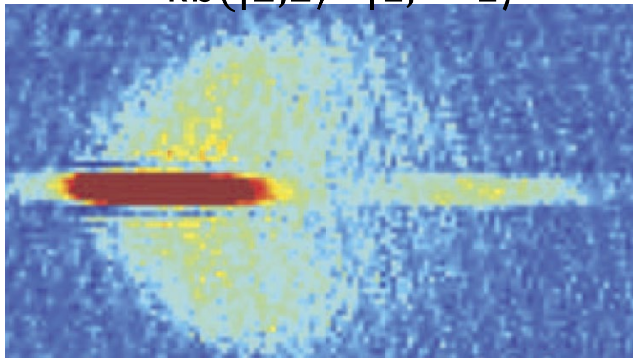

destructive

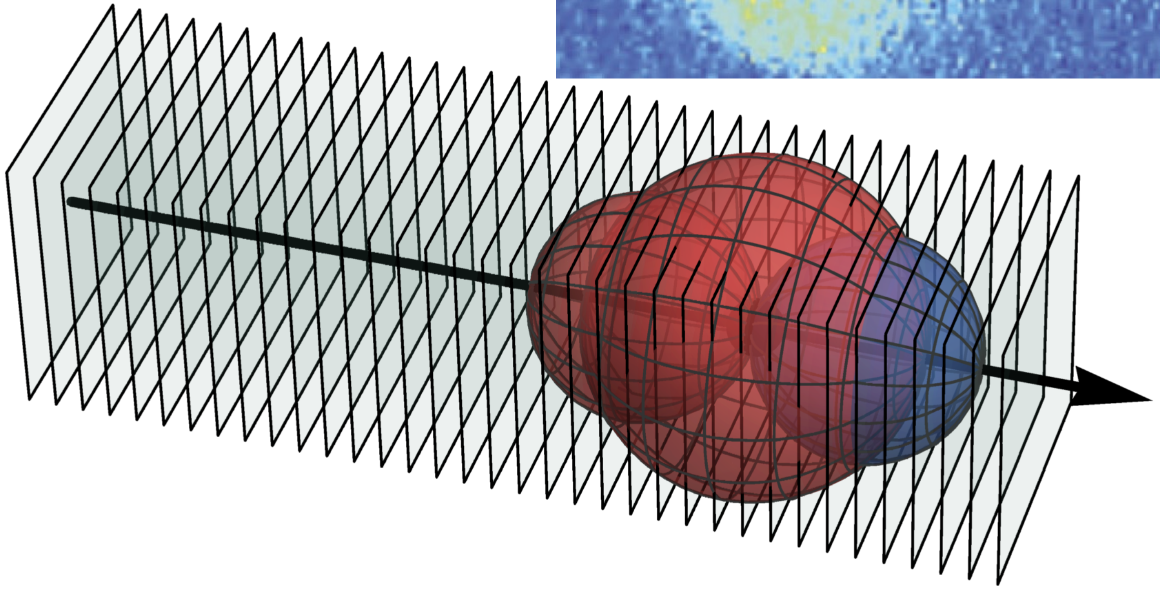

Round up the usual suspects

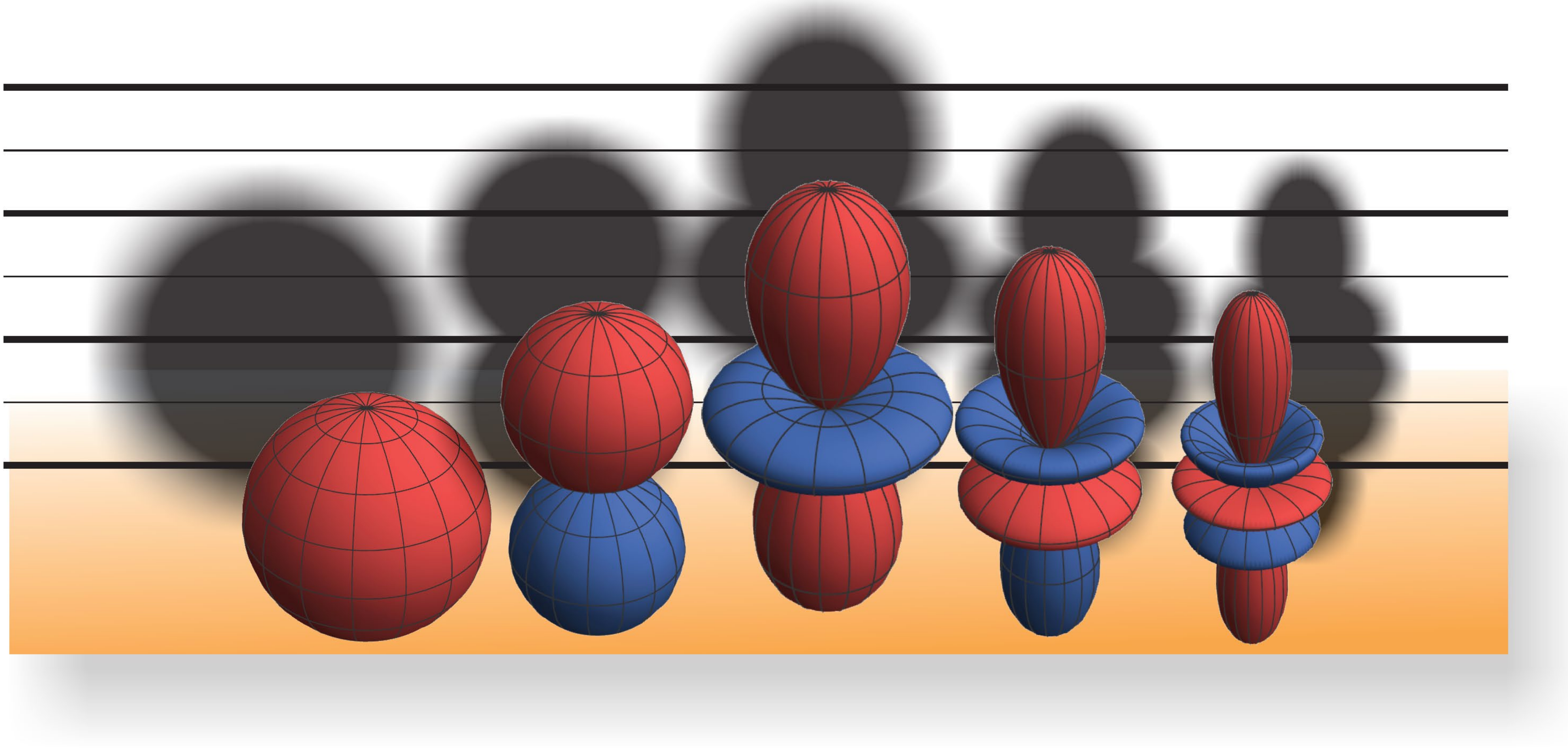

Round up the usual suspects

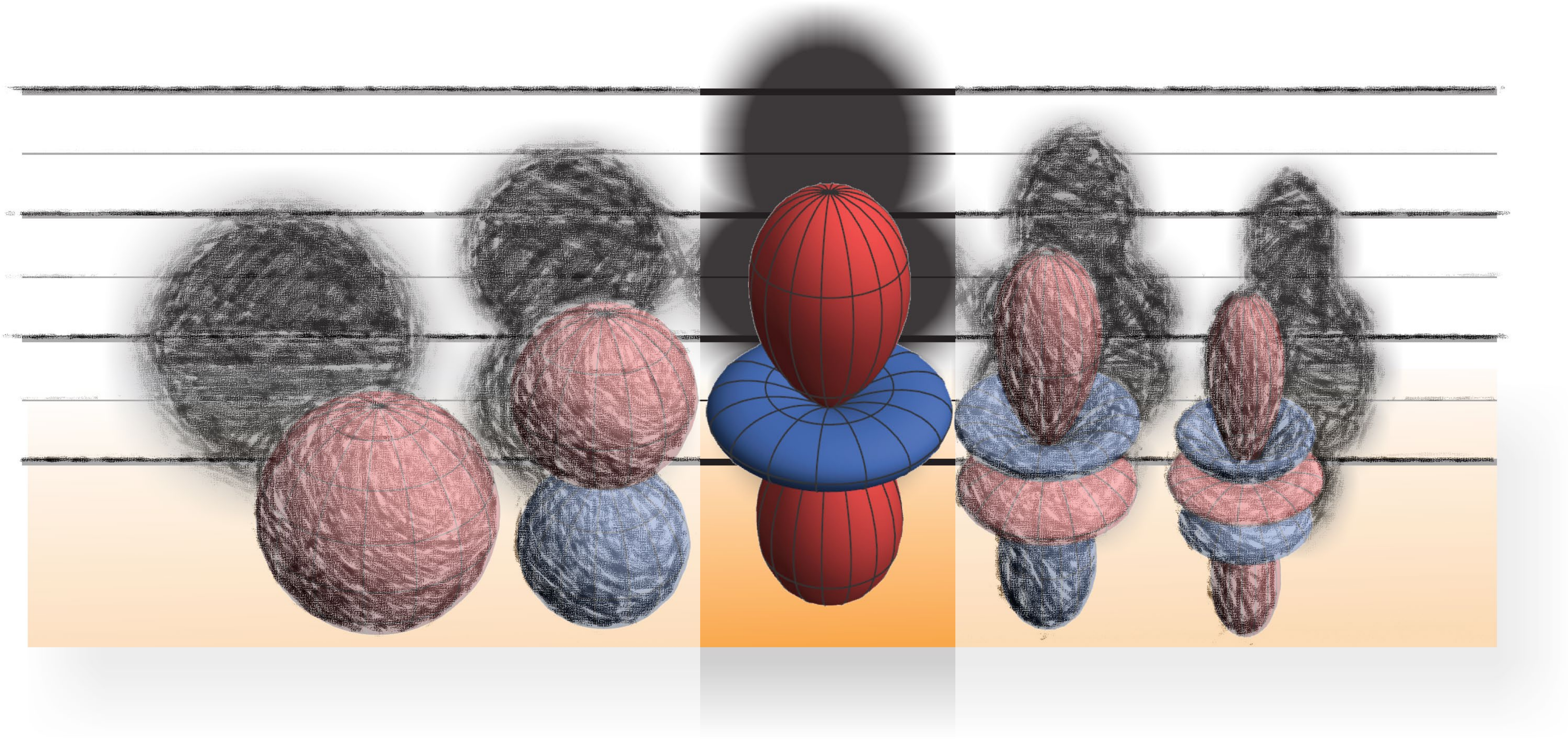

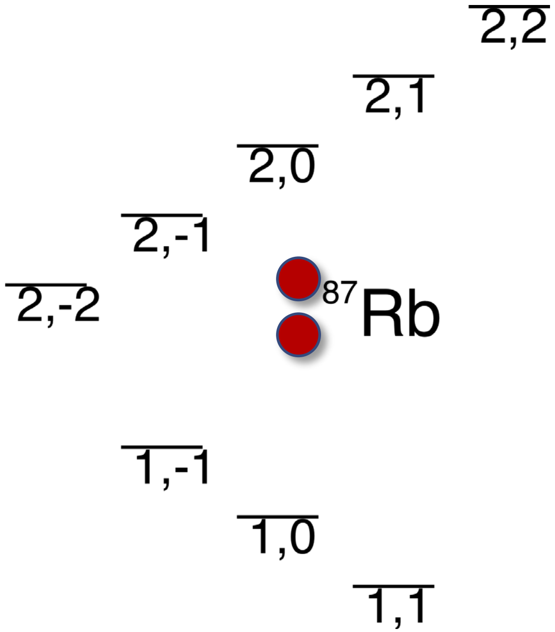
2,2
2,1
2,0
2,-1
2,-2
87Rb
1,-1
1,0
1,1

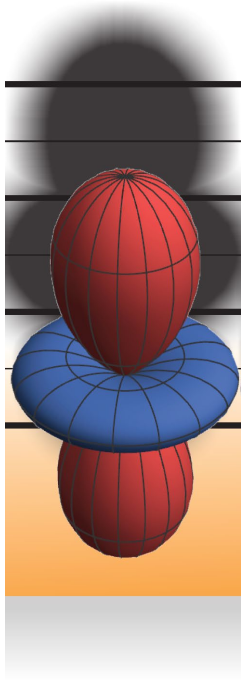

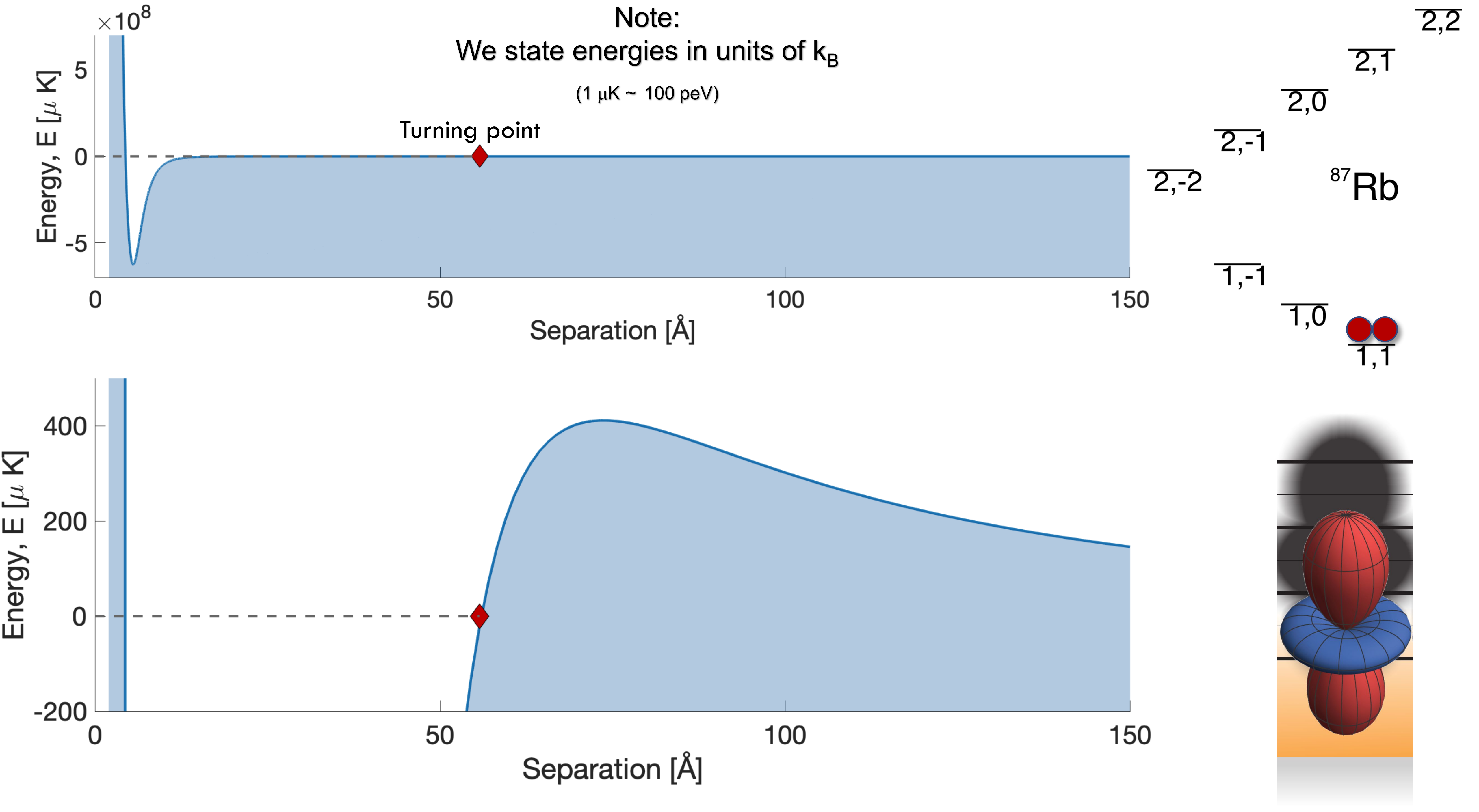
Note:
We state energies in units of k_B
(1 μK ~ 100 peV)
Turning point
$\times 10^8$
Energy, E [μ K]
5
0
-5
0
50
100
150
Separation [Å]
2,2
2,1
2,0
2,-1
2,-2
^{87}Rb
1,-1
1,0
1,1
Energy, E [μ K]
400
200
0
-200
0
50
100
150
Separation [Å]

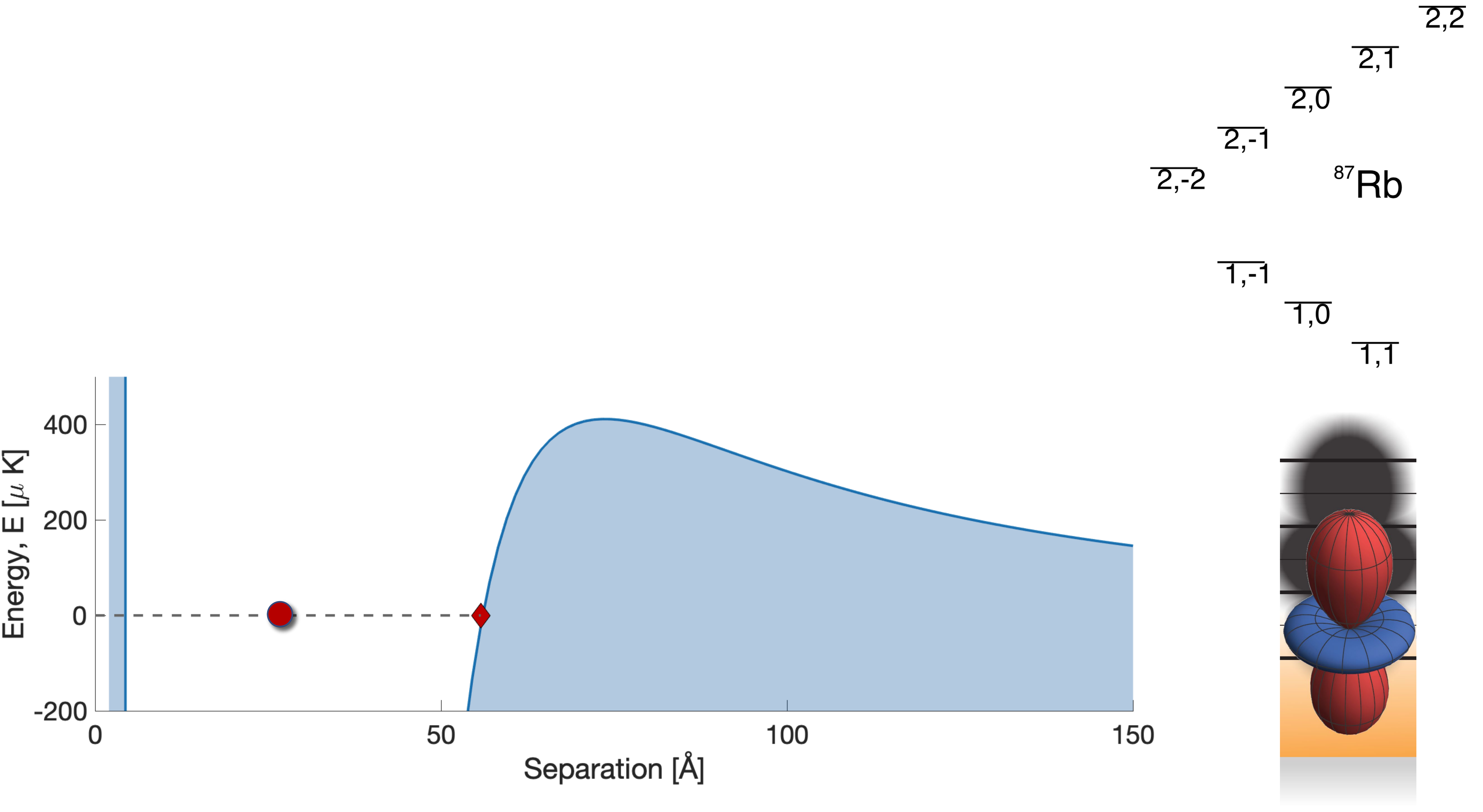

2,2
2,1
2,0
2,-1
2,-2
^{87}Rb
1,-1
1,0
1,1
400
200
0
-200
Energy, E [μ K]
0
50
100
150
Separation [Å]

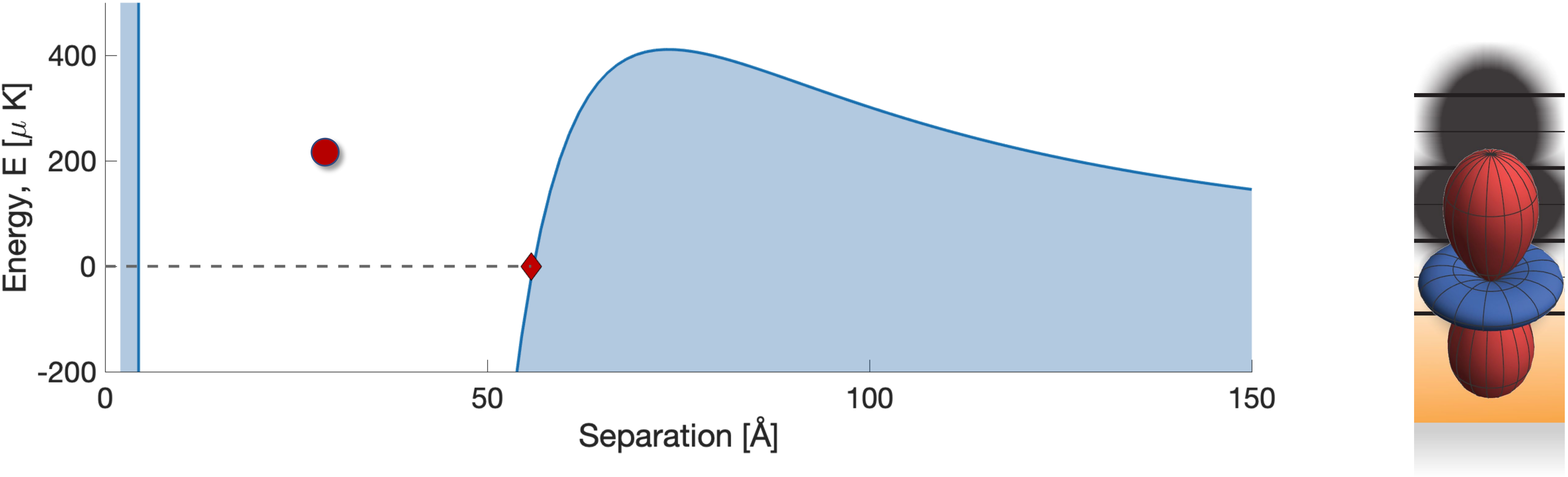

Energy, E [μ K]
400
200
0
-200
0
50
100
150
Separation [Å]

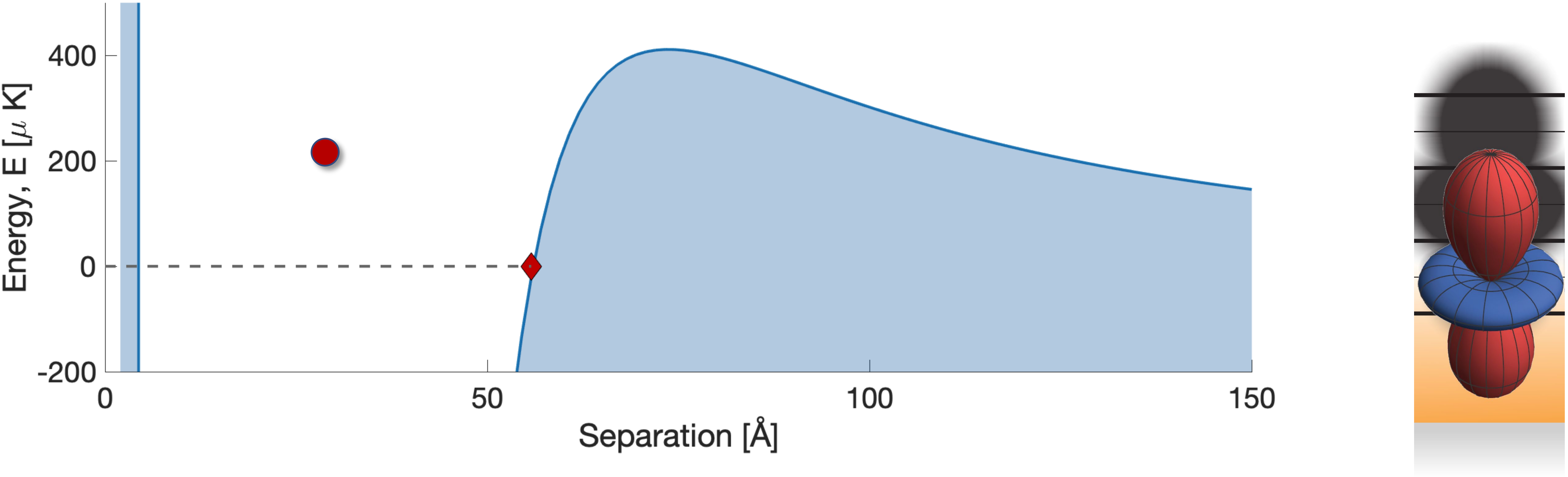
Energy, E [μ K]
400
200
0
-200
0
50
100
150
Separation [Å]

Wave functions above threshold

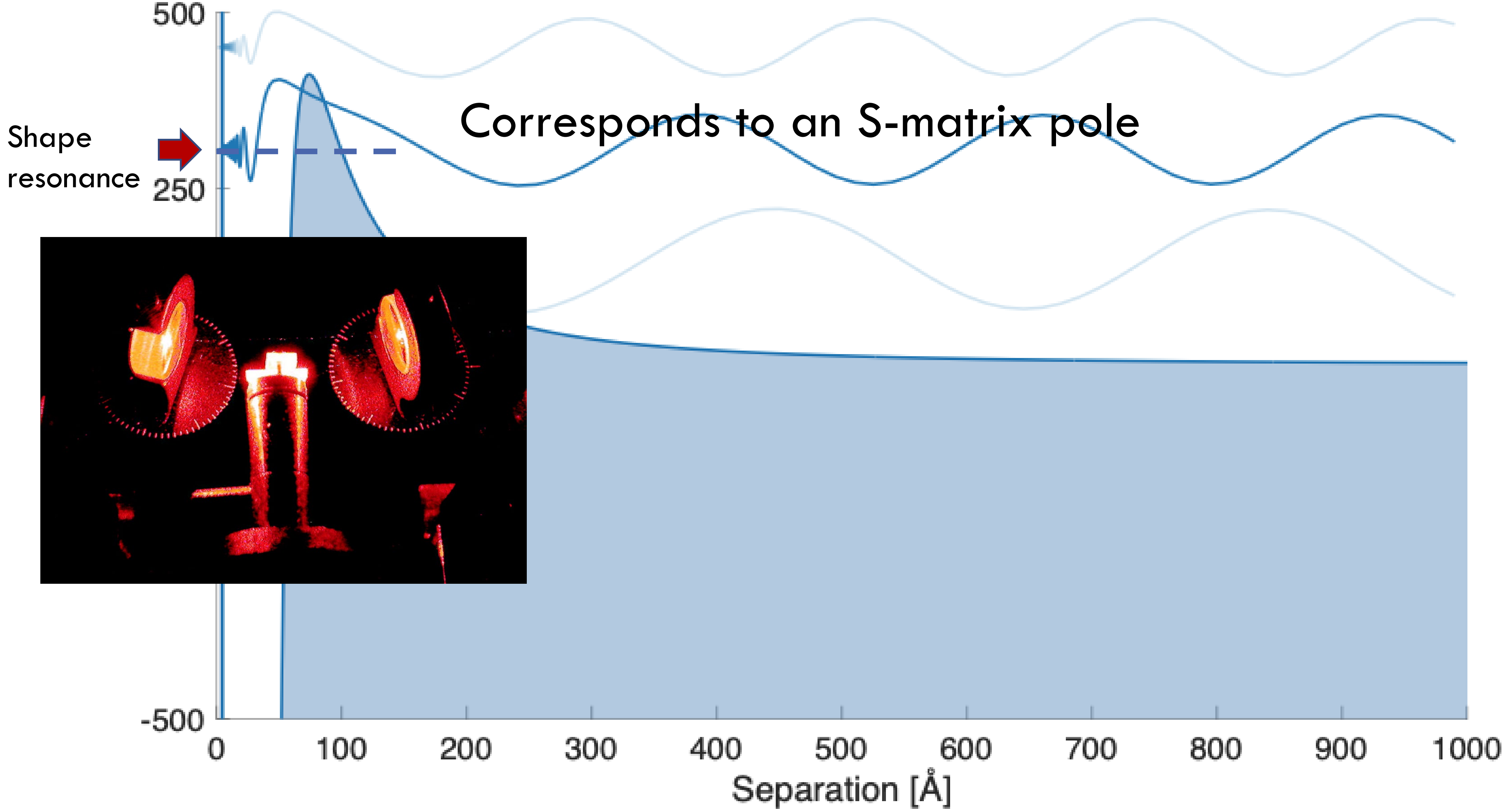

Free space radial solution (to Schrödinger eq.)

$$E = \frac{\hbar^2 k^2}{2\mu}$$

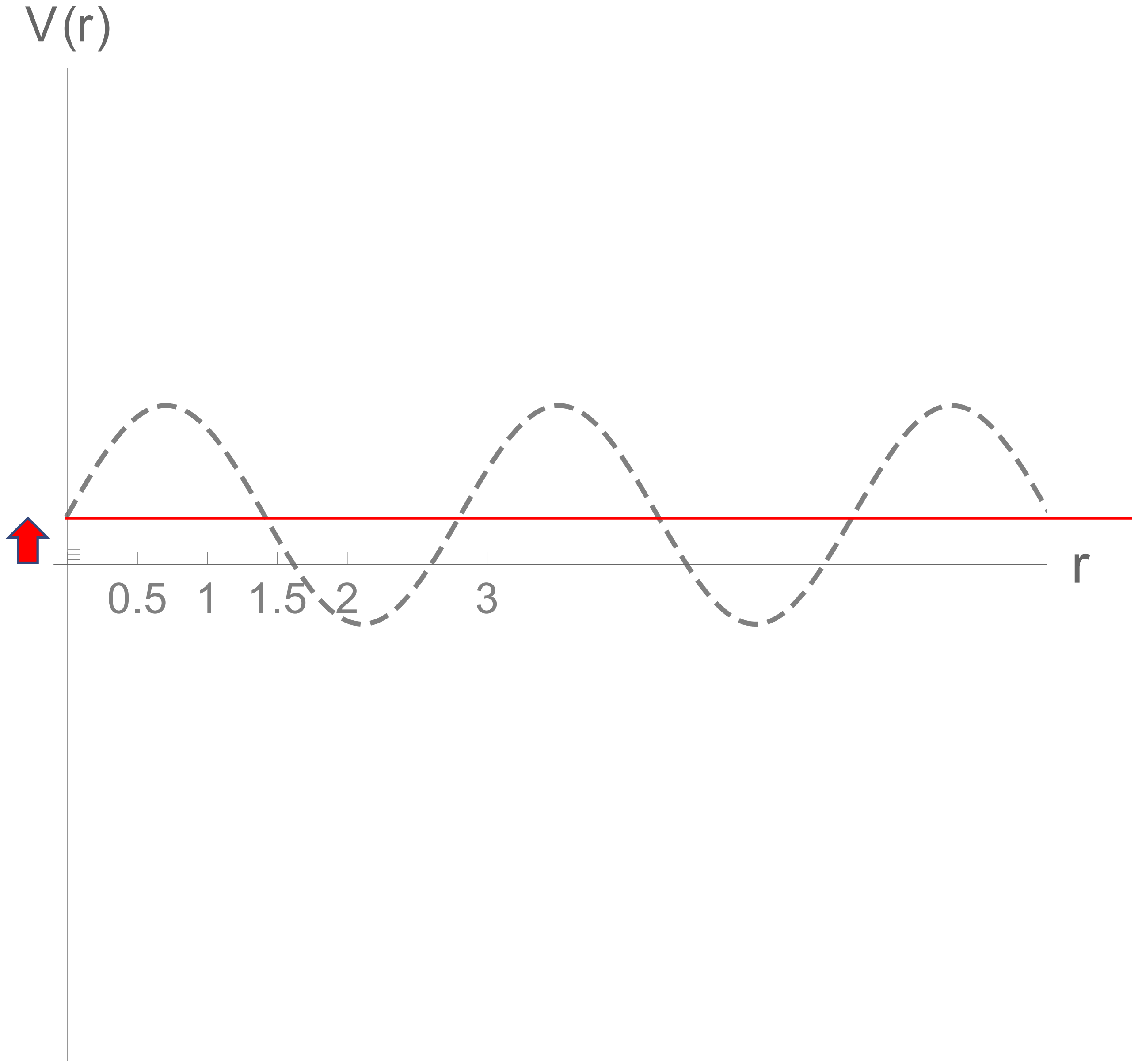

Add well

$$\ell = 0$$

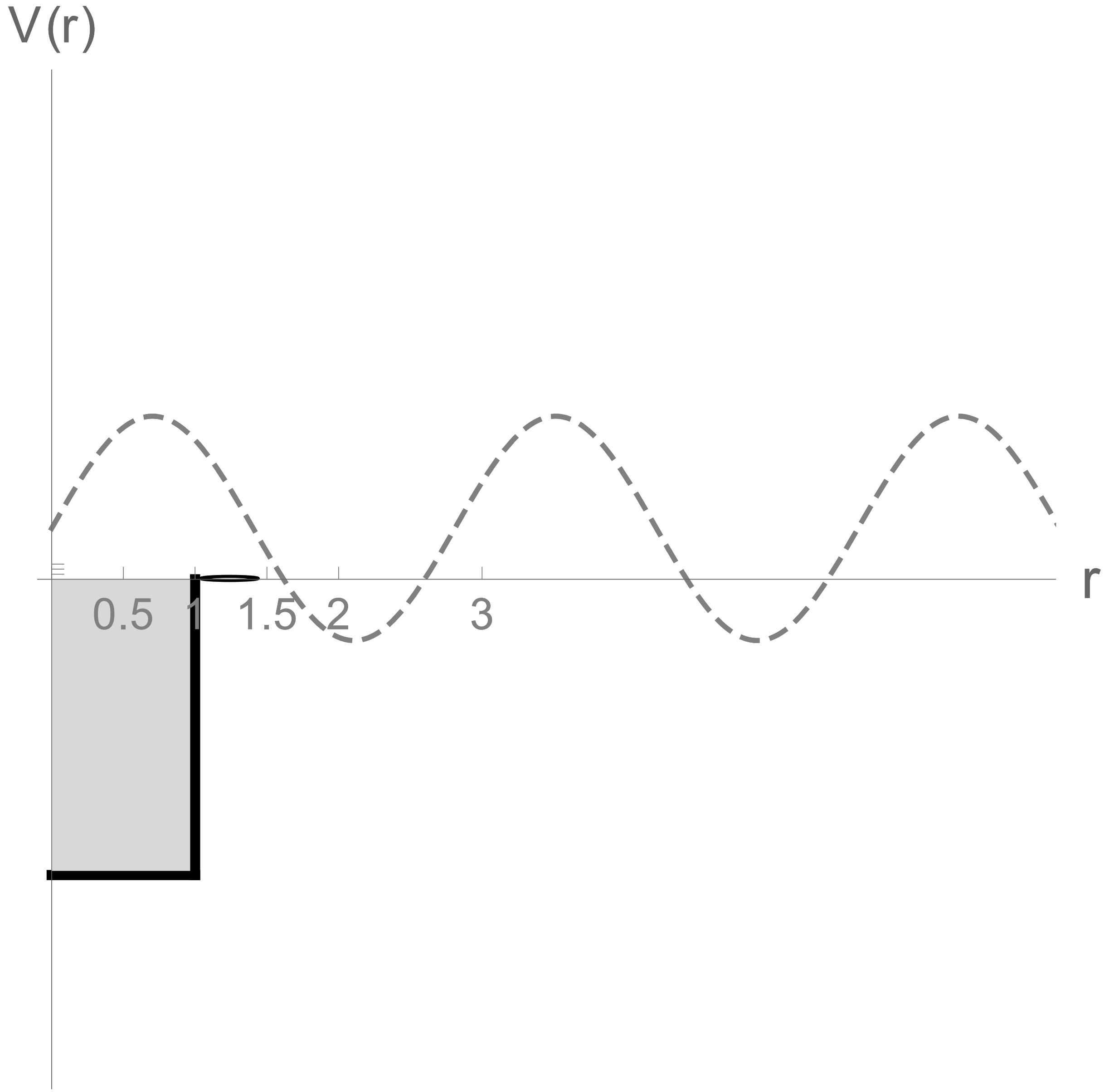

Phase shift with respect to free space

$$S_0(k) = e^{2i\delta_0(k)}$$

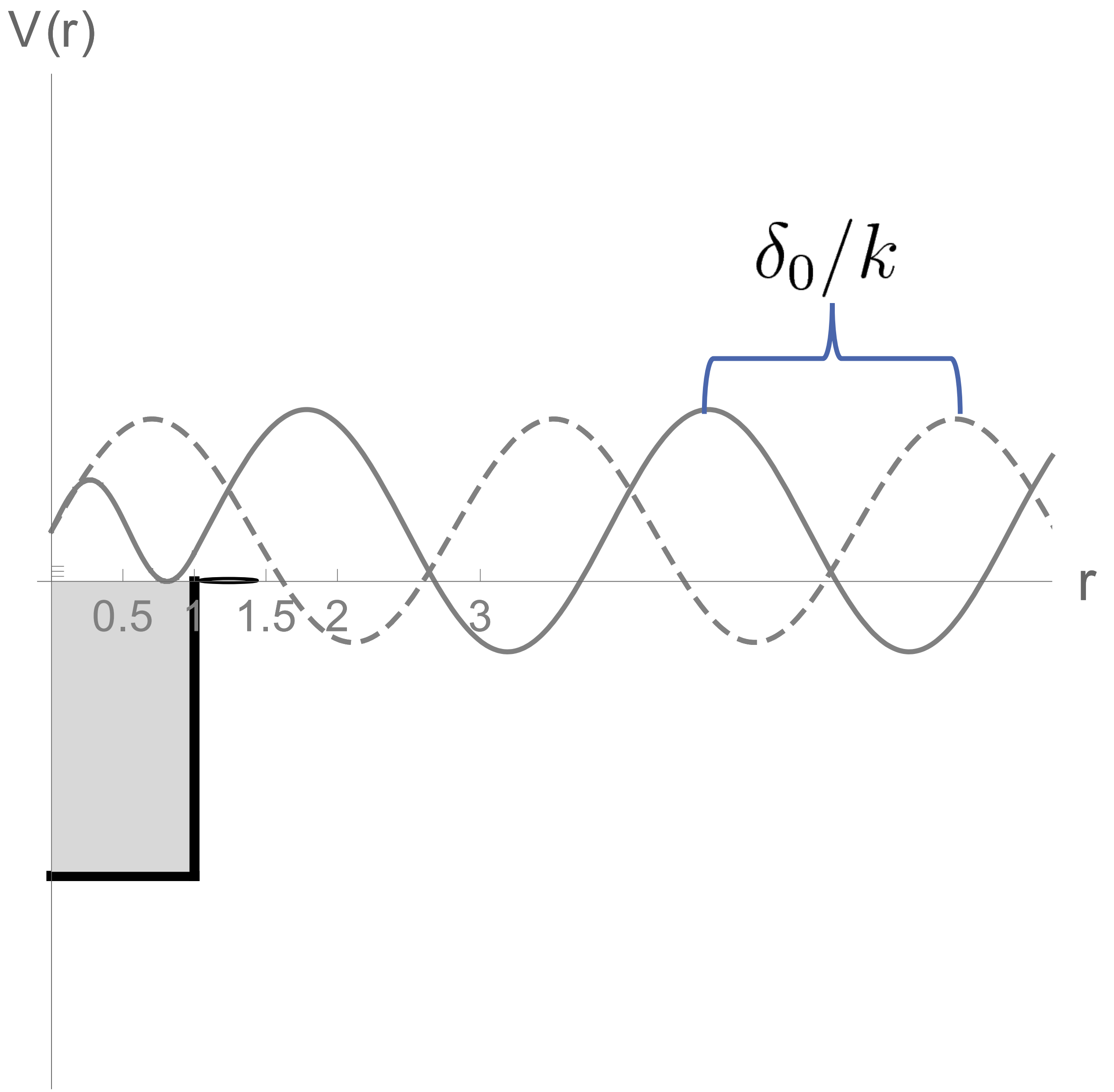

Bound state solutions – pure exp. decay

$$S_0(k) = e^{2i\delta_0(k)}$$

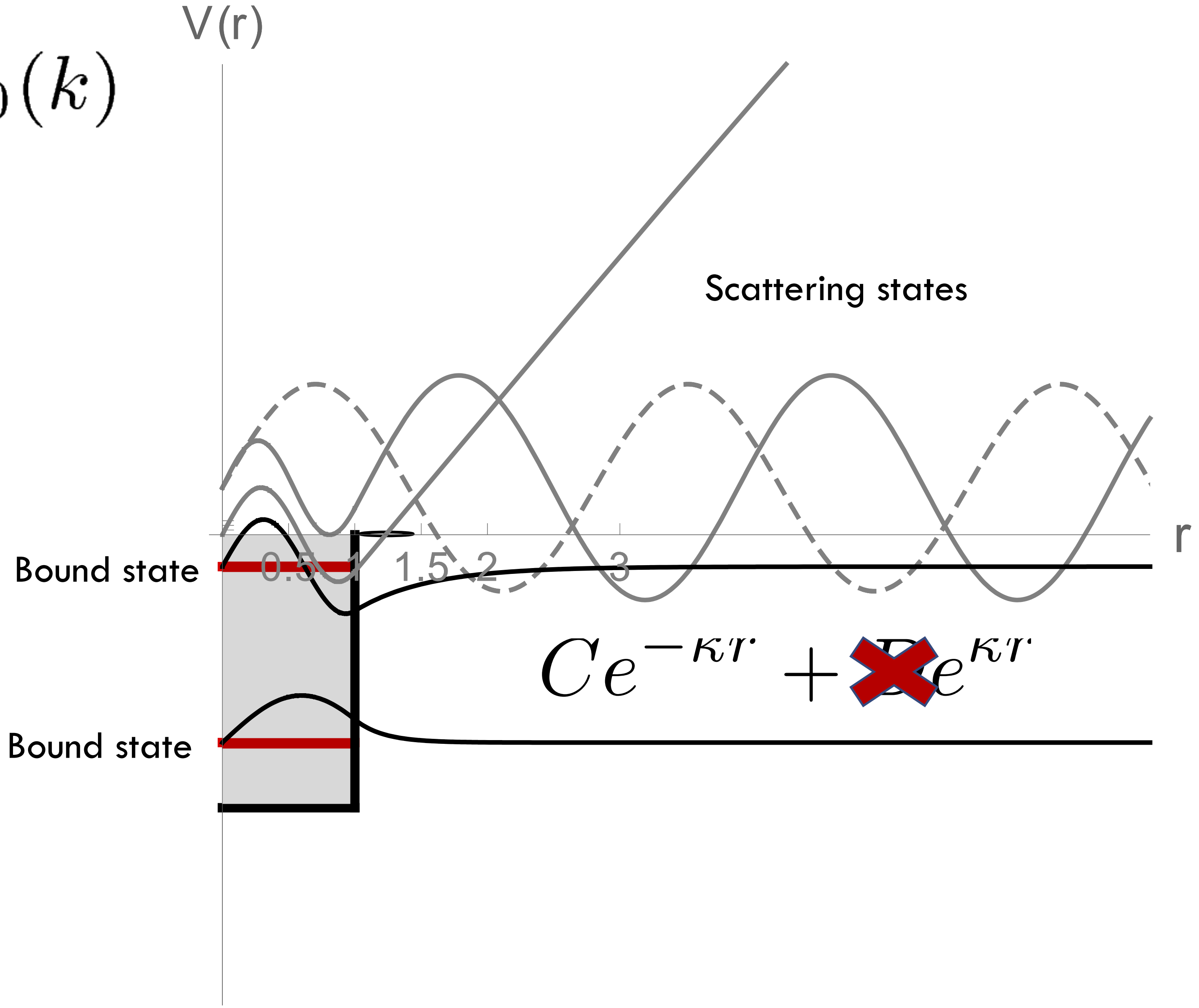

Antibound state

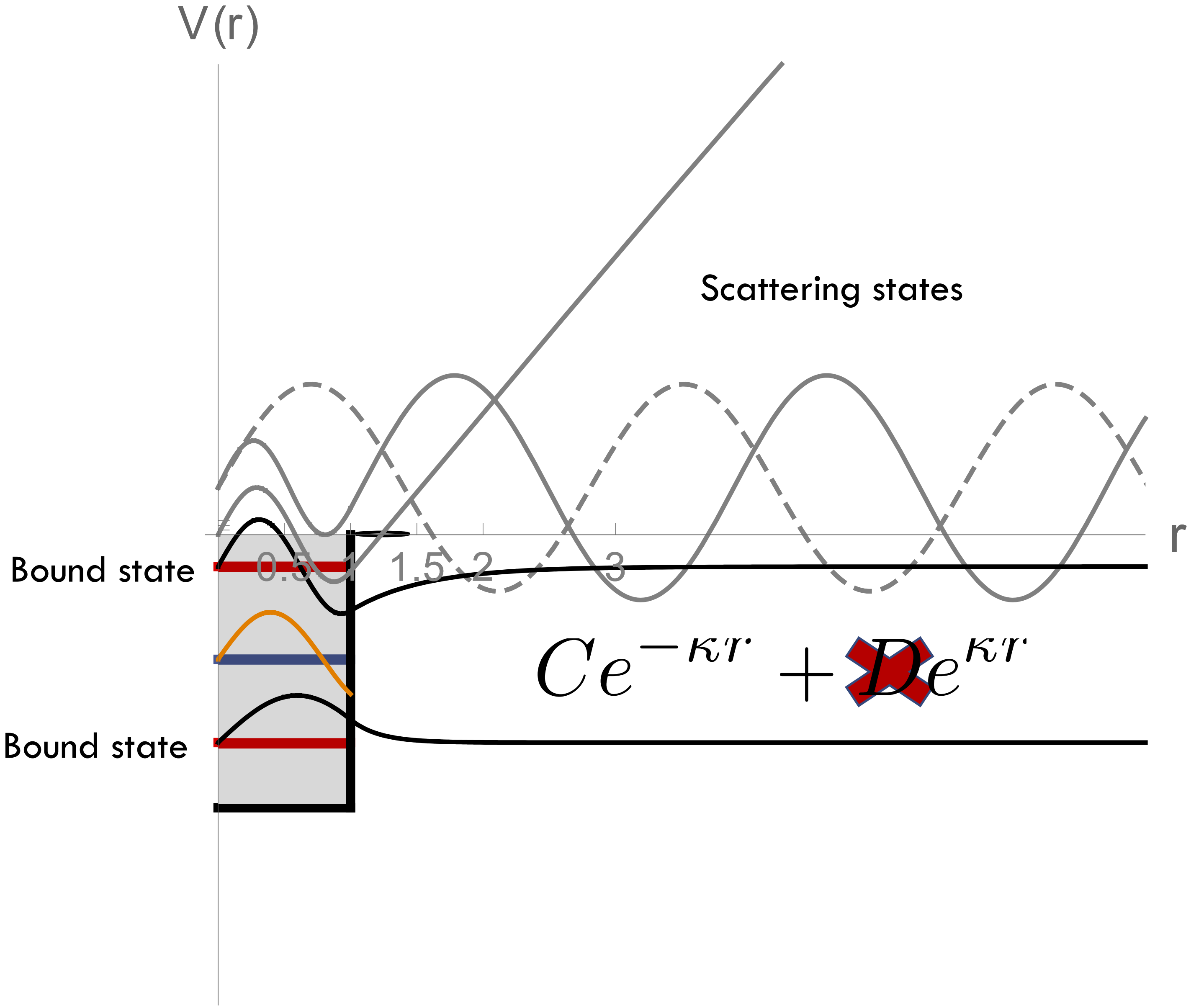

Antibound state – pure exp. growth

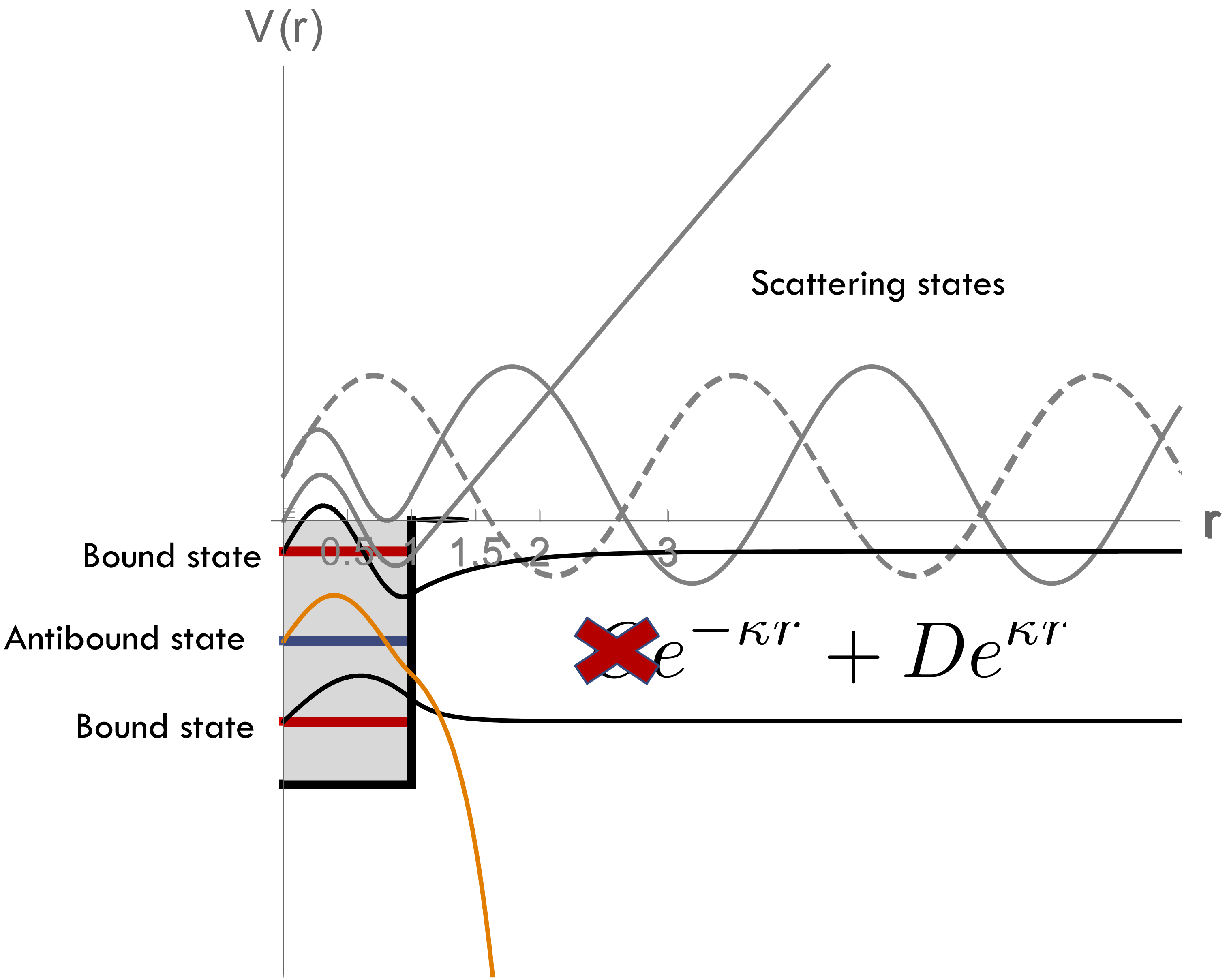

Scattering Matrix

$$S_0(k) = e^{2i\delta_0(k)}$$

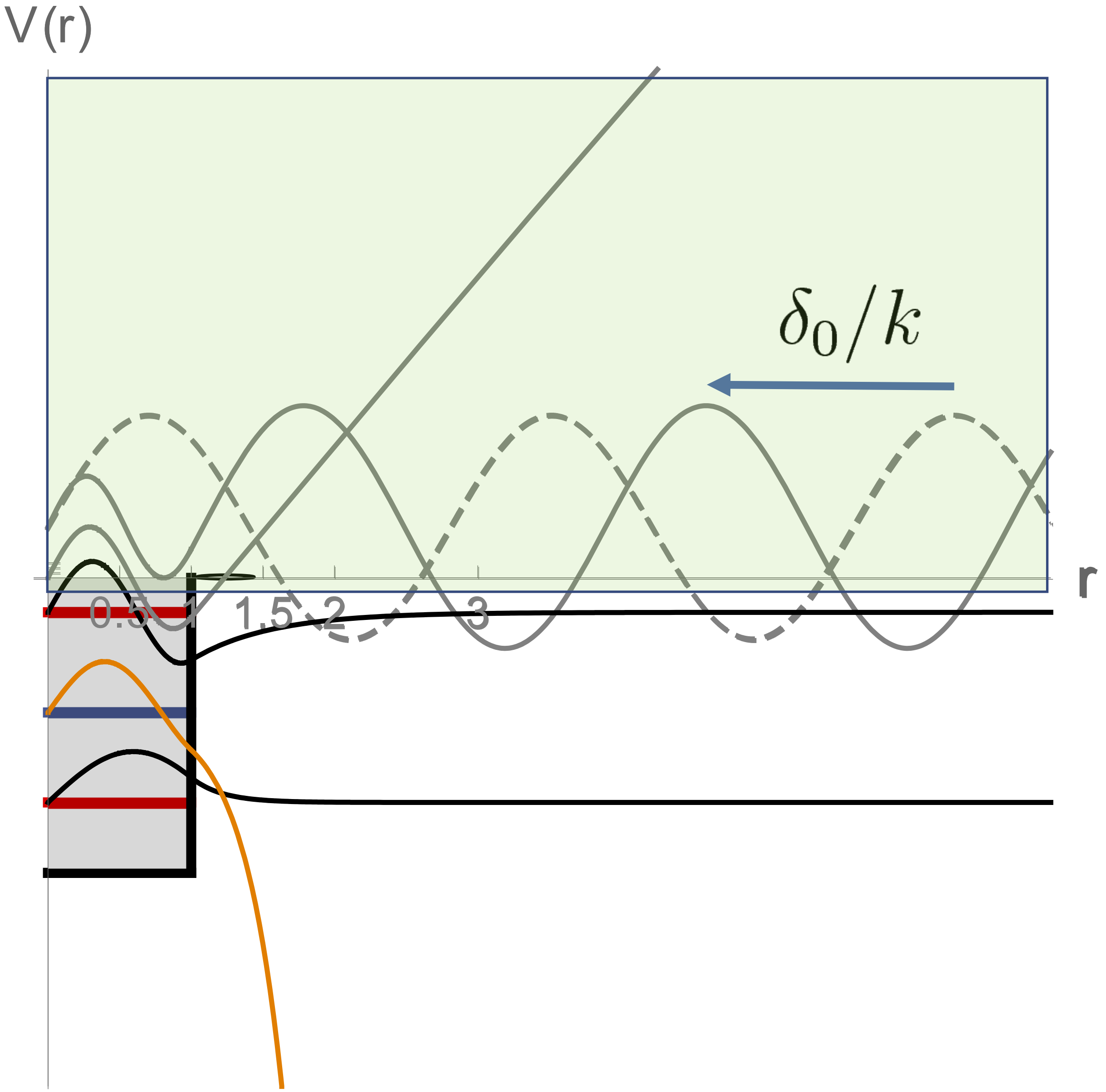

Scattering Matrix

$$S_0(k) = e^{2i\delta_0(k)}$$

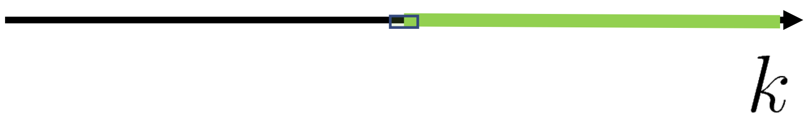

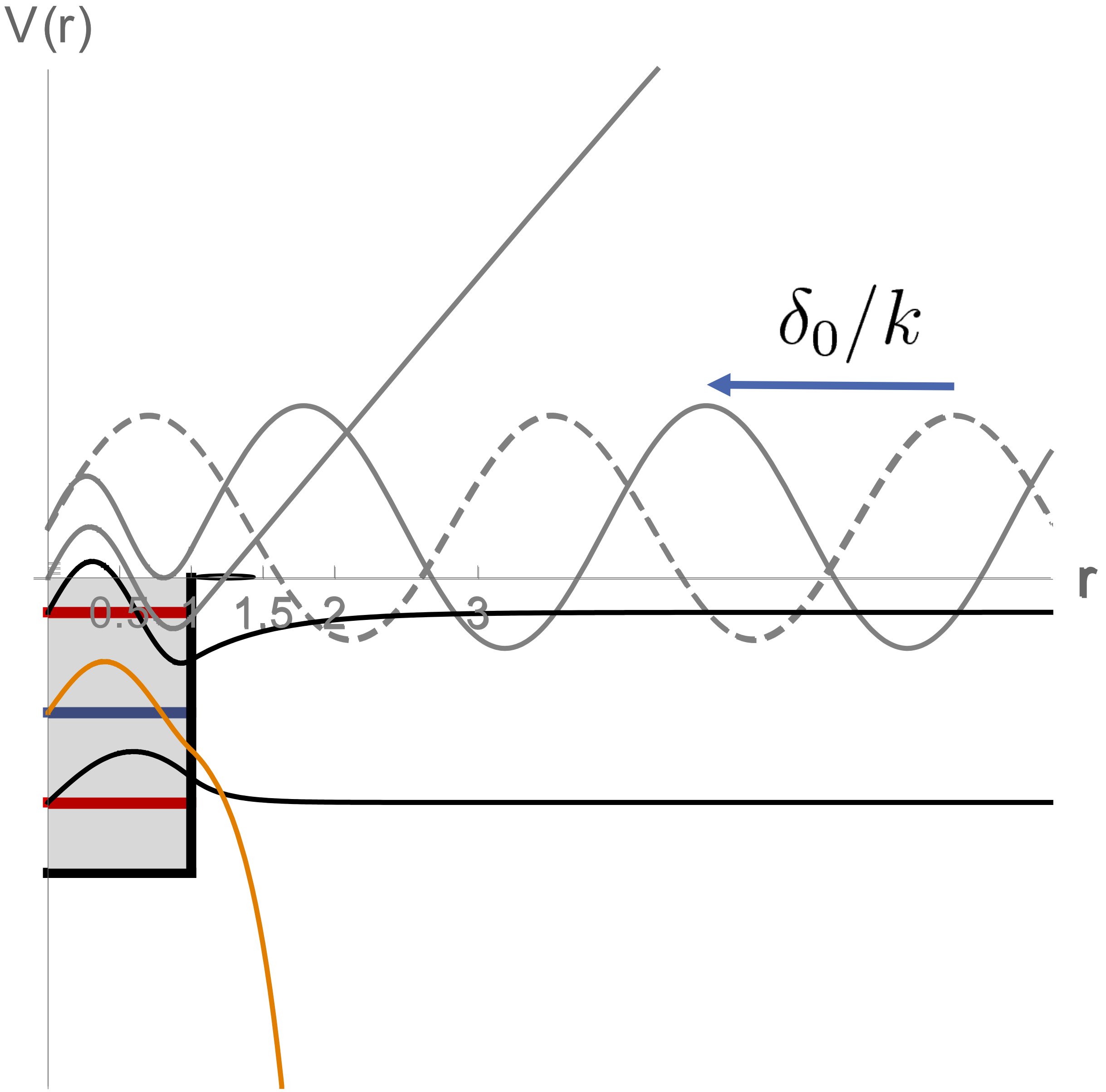

Analytic continuation S-matrix

$$S_0(k) = e^{2i\delta_0(k)}$$

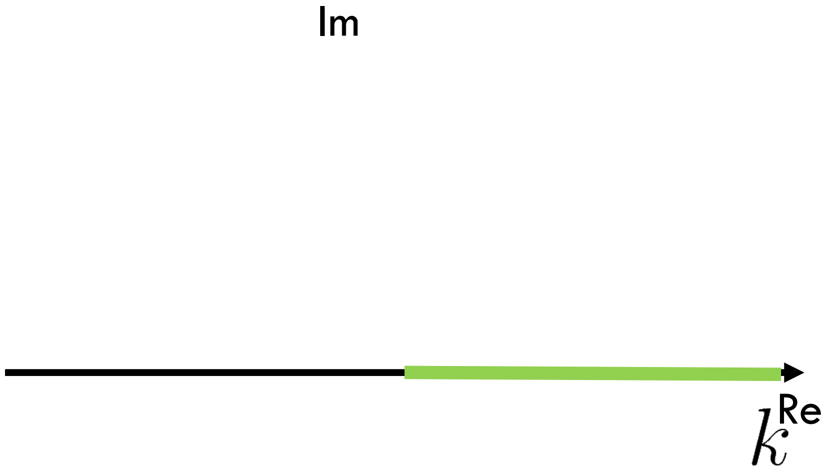

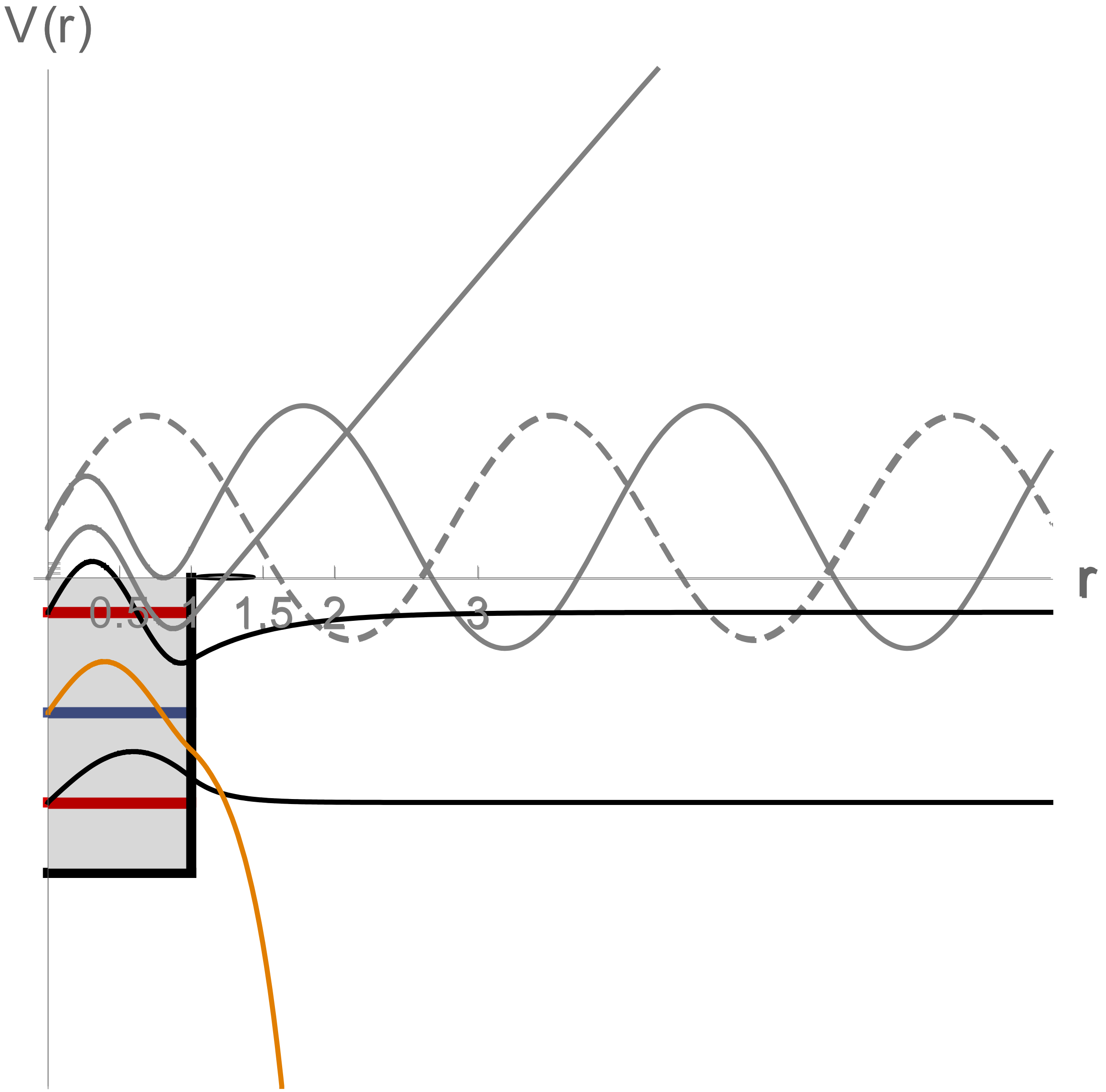

Analytic continuation S-matrix

$$S_0(k) = e^{2i\delta_0(k)}$$

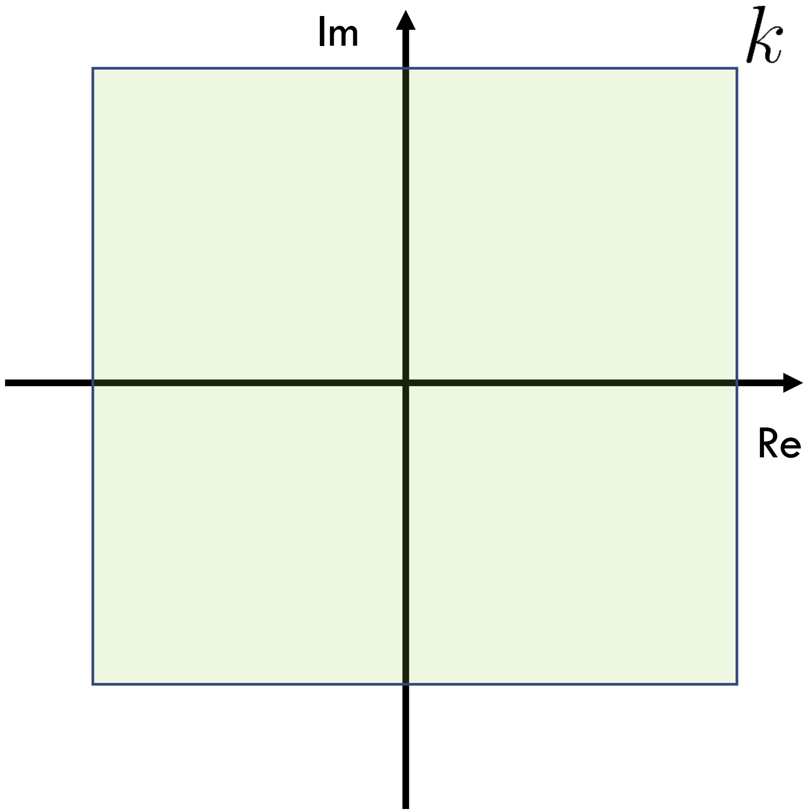

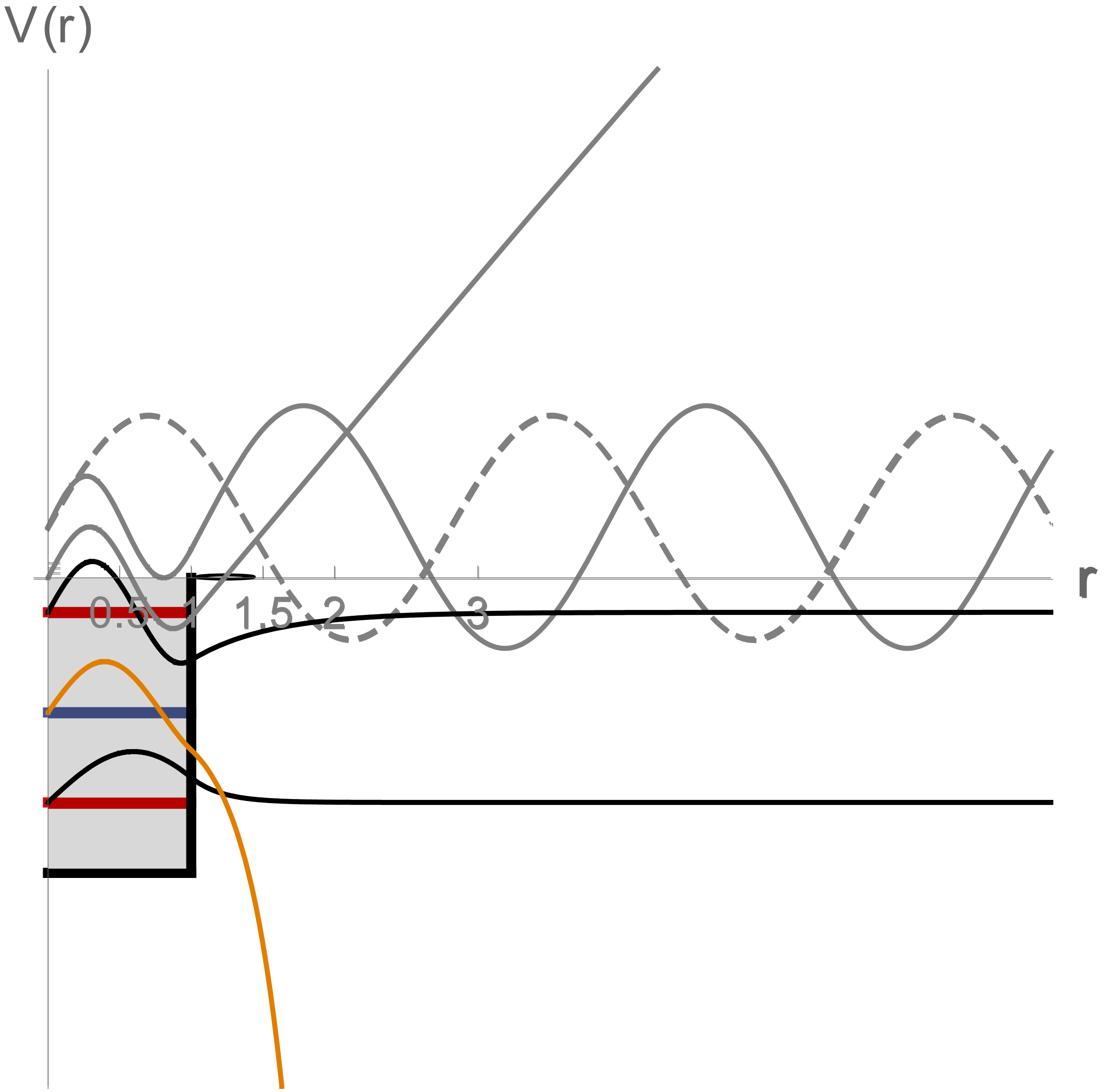

Bound and antibound states ⇔ poles on imaginary axis of analytically continued S-matrix

$$S_0(k) = e^{2i\delta_0(k)}$$

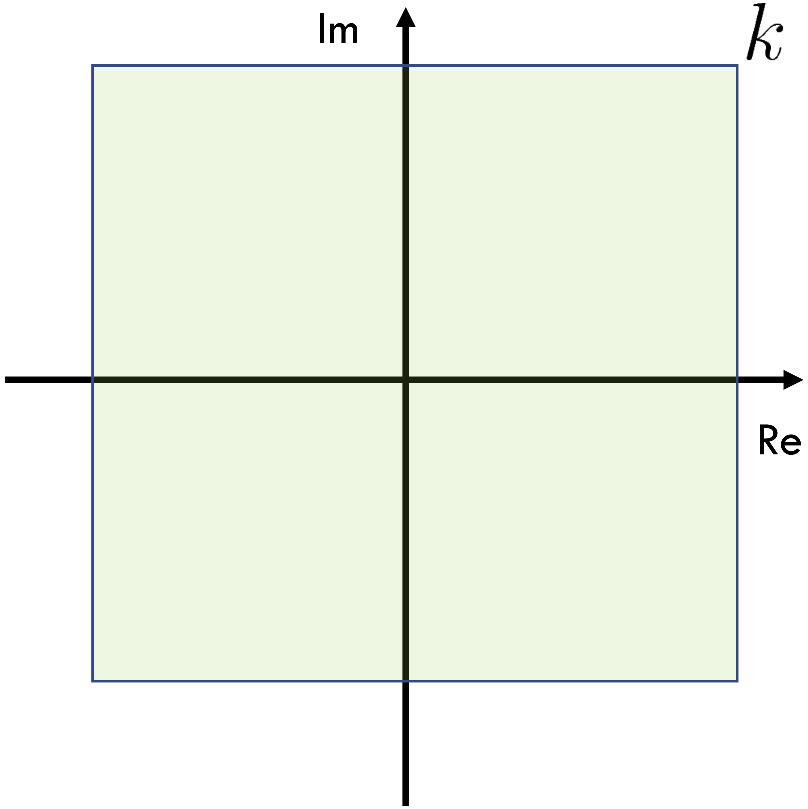

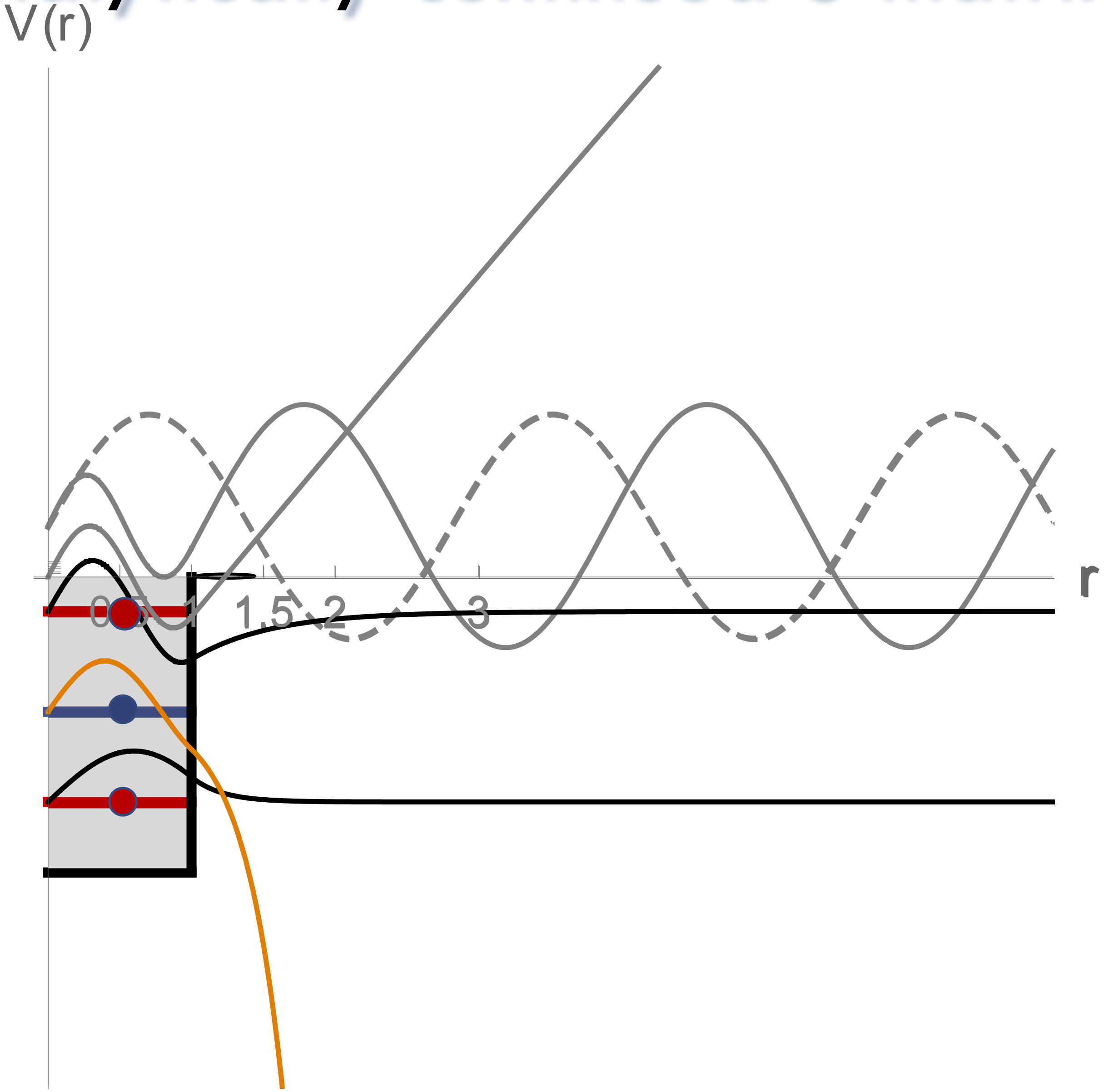

Bound and antibound states ⟺ poles on imaginary axis of analytically continued S-matrix

$$S_0(k) = e^{2i\delta_0(k)}$$

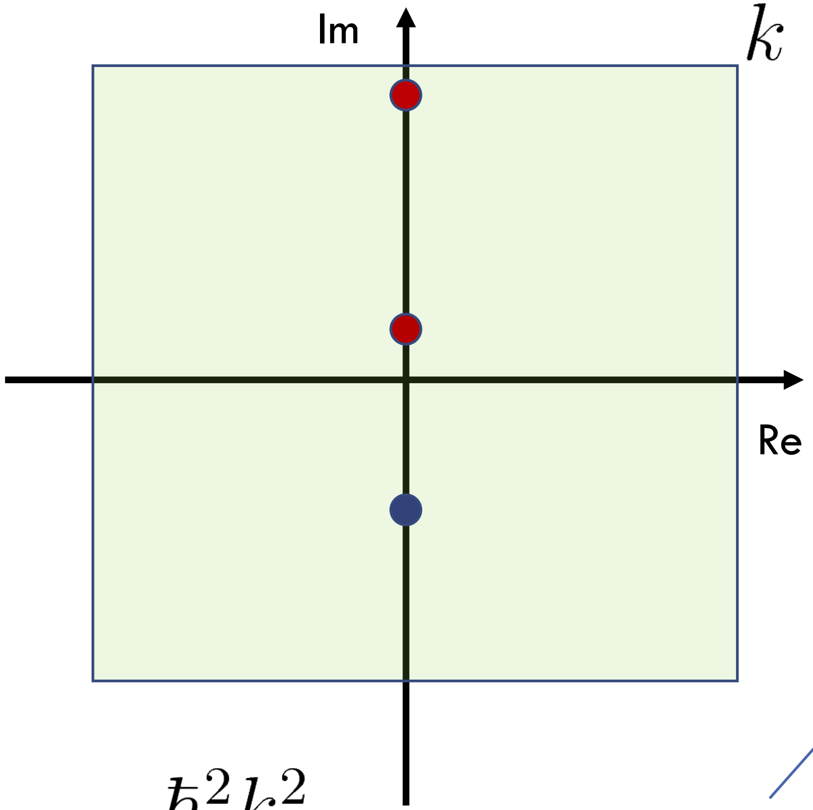

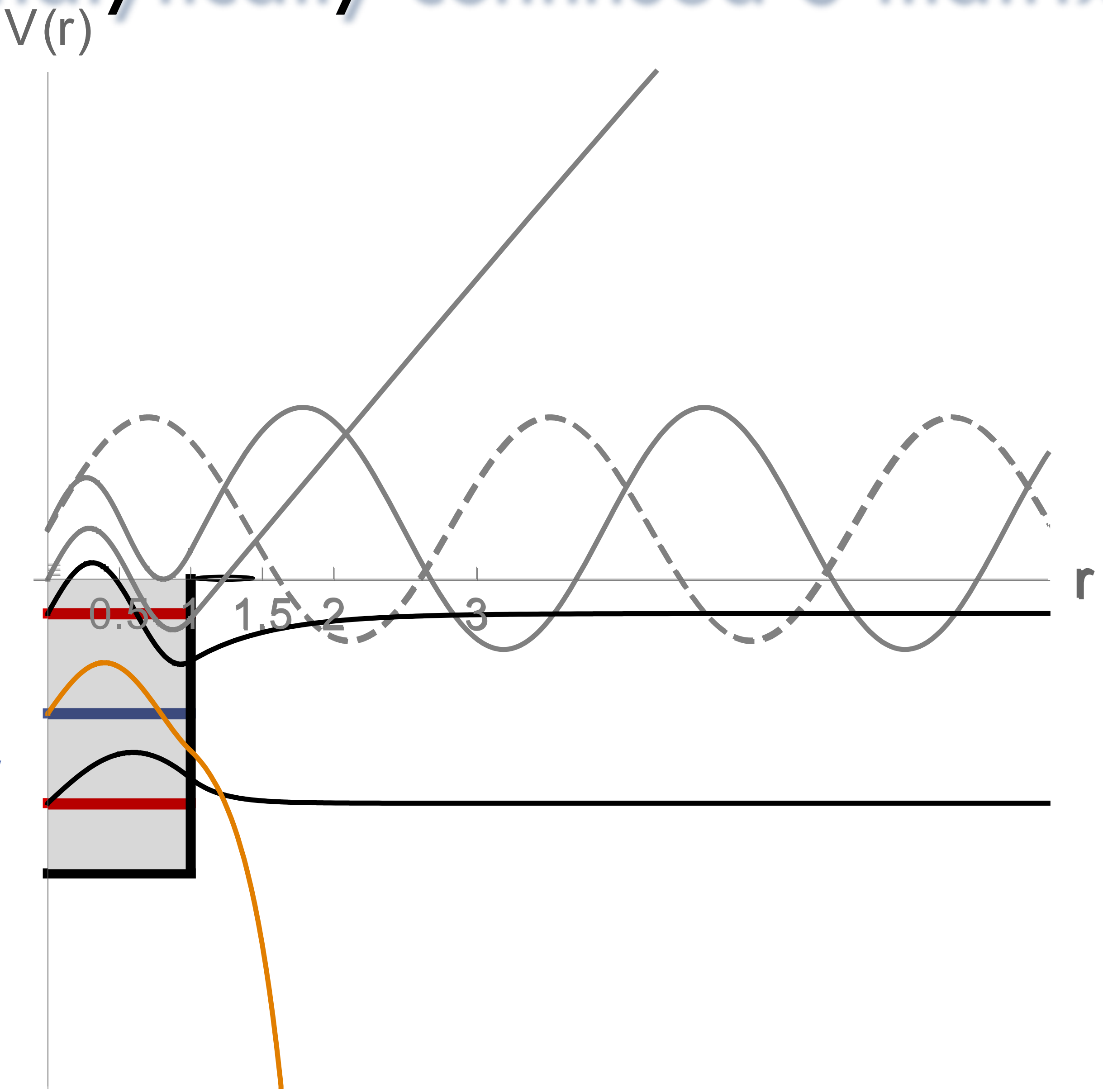

$$E = \frac{\hbar^2 k^2}{2\mu}$$

$(\pm ik \Rightarrow E < 0)$✓

Weakening potential: effect in complex *k* and *E* planes

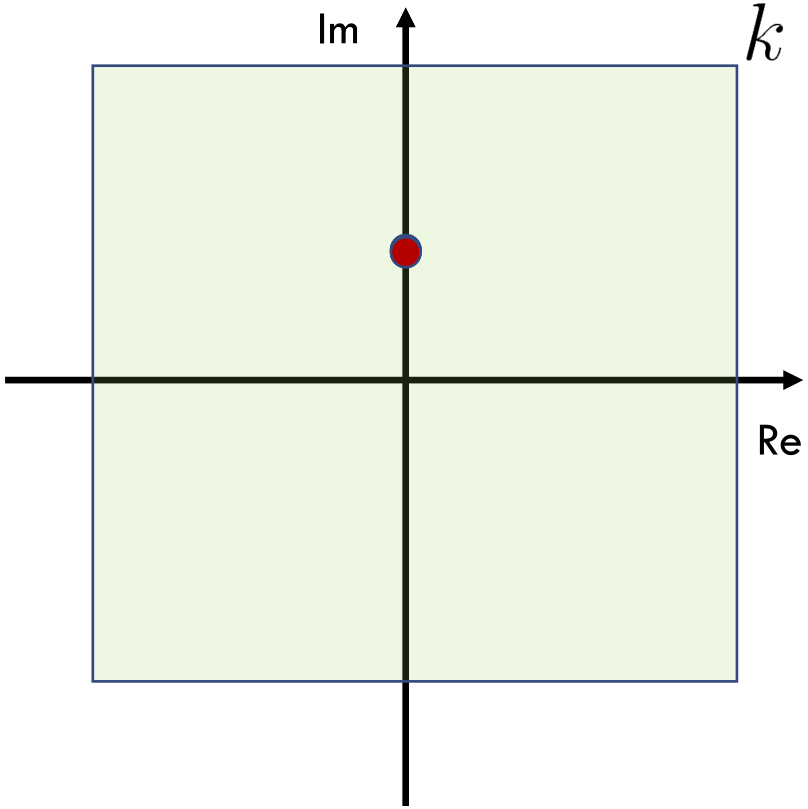

$$E = \frac{\hbar^2 k^2}{2\mu}$$

Weakening potential: effect in complex *k* and *E* planes

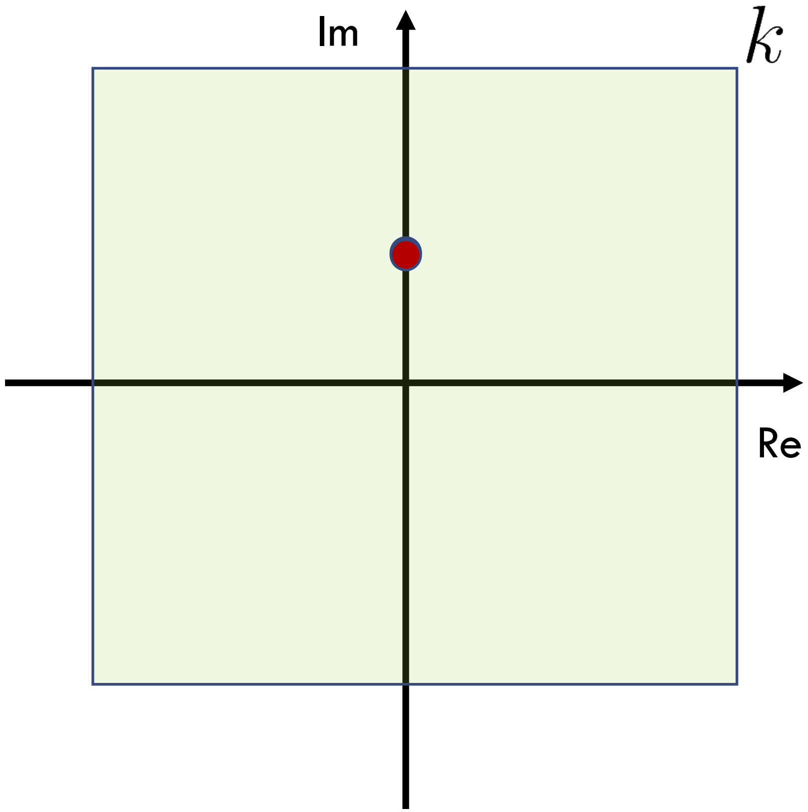

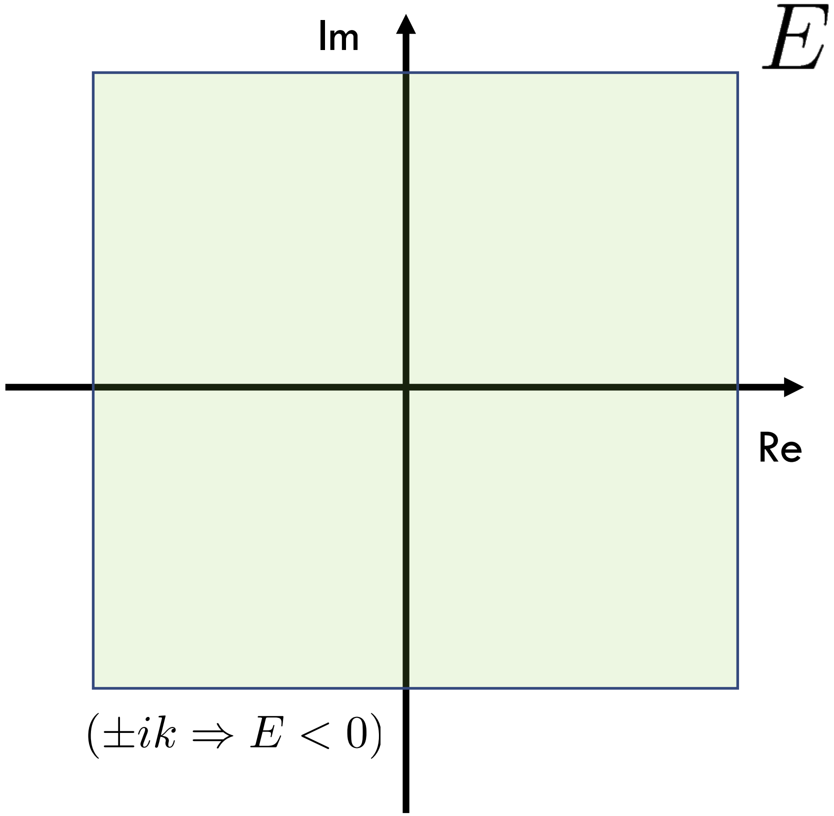

$$E = \frac{\hbar^2 k^2}{2\mu}$$

Weakening potential: effect in complex *k* and *E* planes

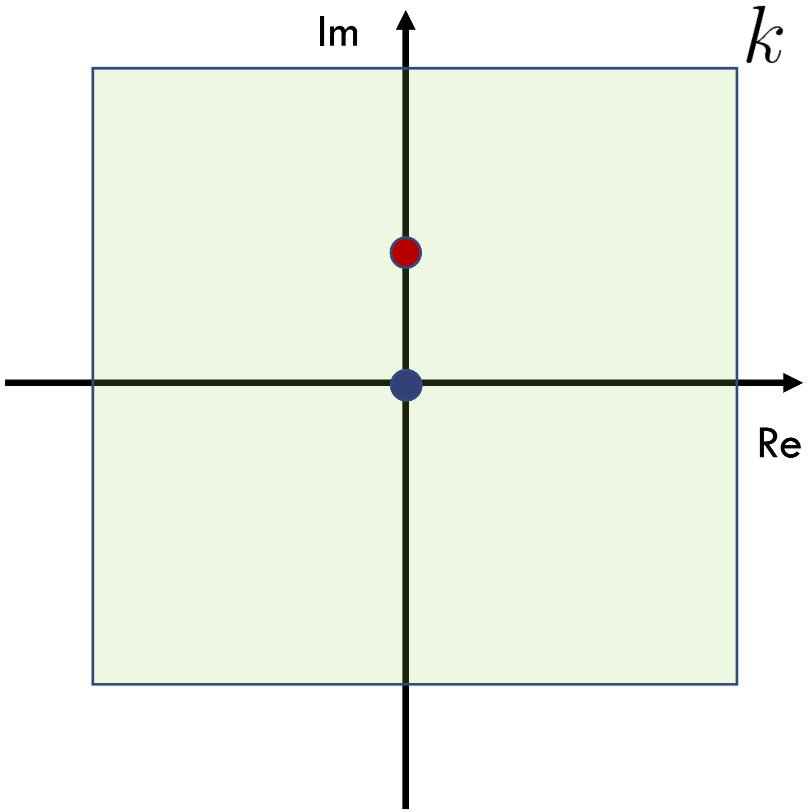

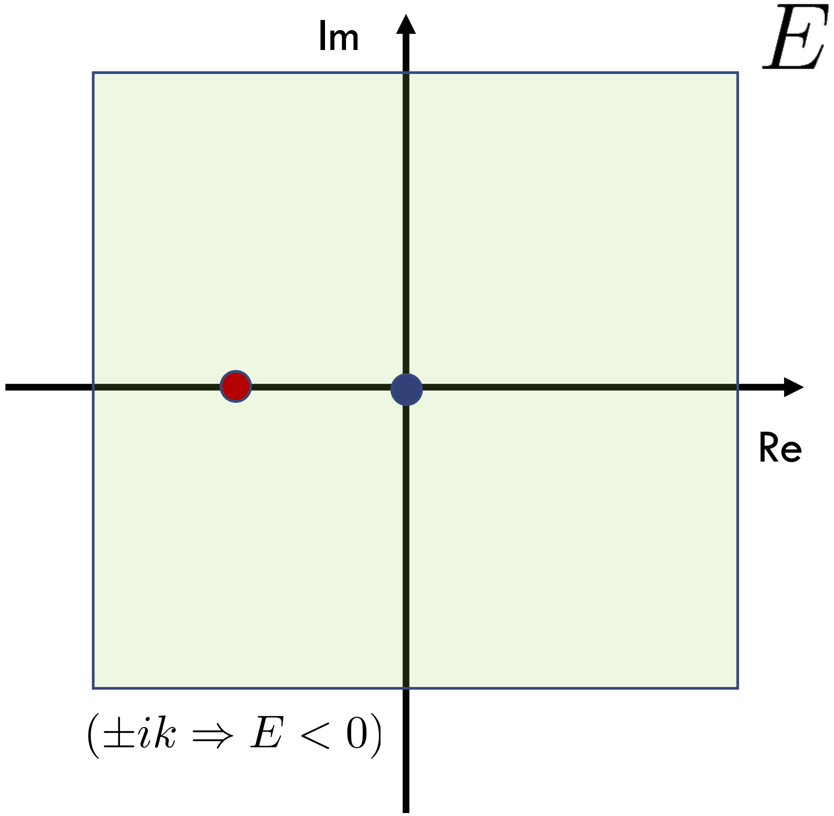

$$E = \frac{\hbar^2 k^2}{2\mu}$$

Weakening potential: effect in *E* plane

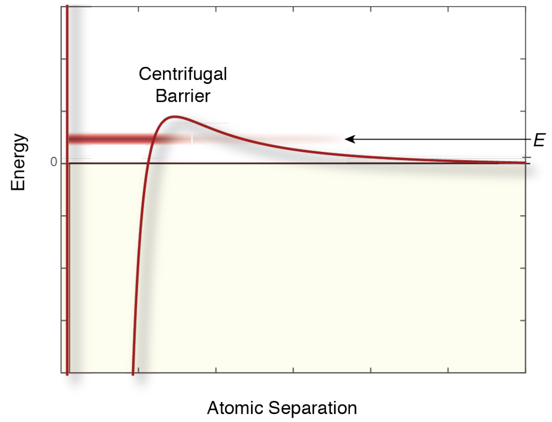

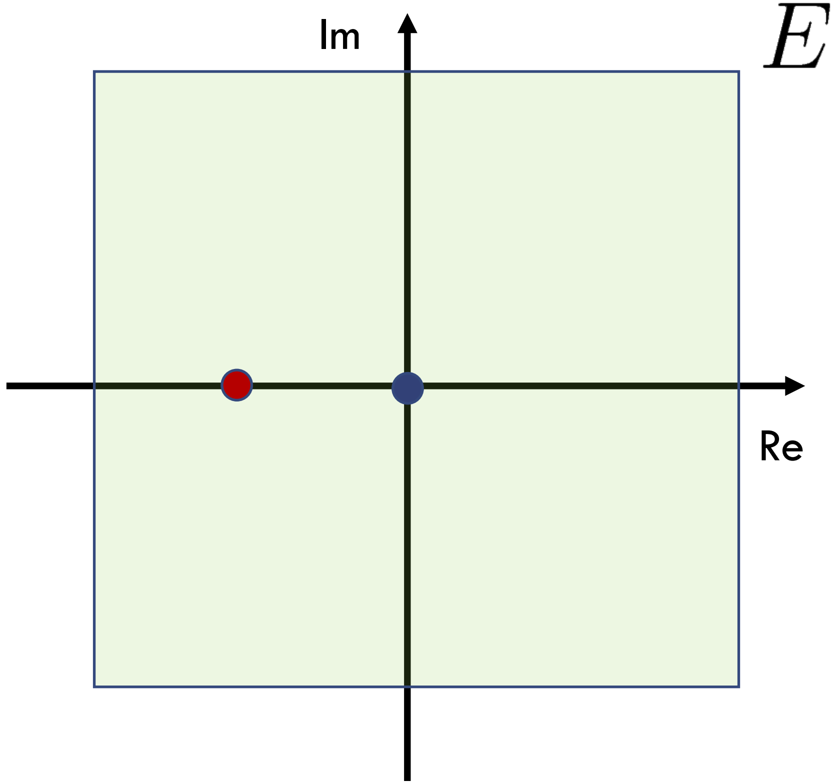

$$\ell = 0$$

Resonance state

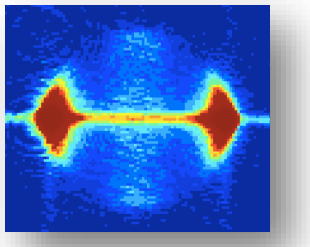

Atomic Pole Dance

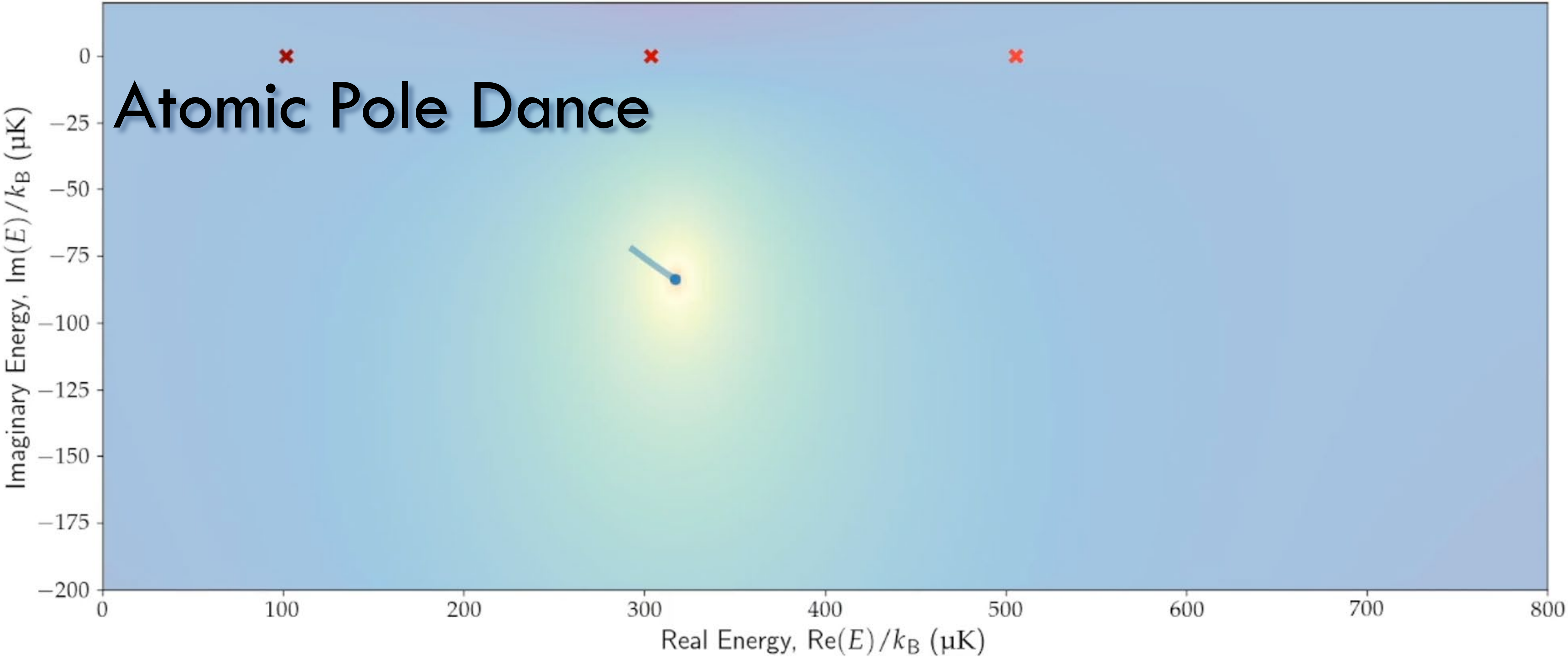

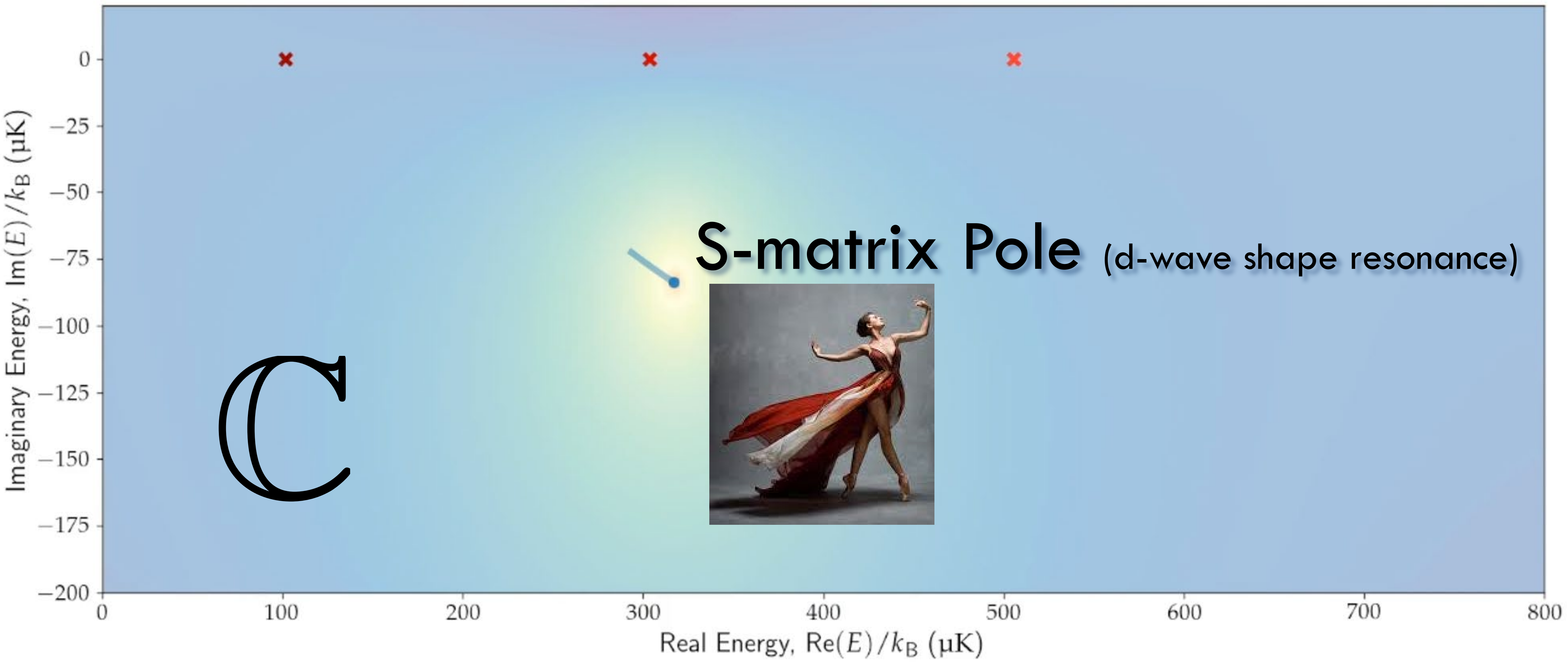

S-matrix Pole (d-wave shape resonance)
$\mathbb{C}$
Imaginary Energy, $\mathrm{Im}(E)/k_\mathrm{B}$ (μK)
0
−25
−50
−75
−100
−125
−150
−175
−200
Real Energy, $\mathrm{Re}(E)/k_\mathrm{B}$ (μK)
0
100
200
300
400
500
600
700
800

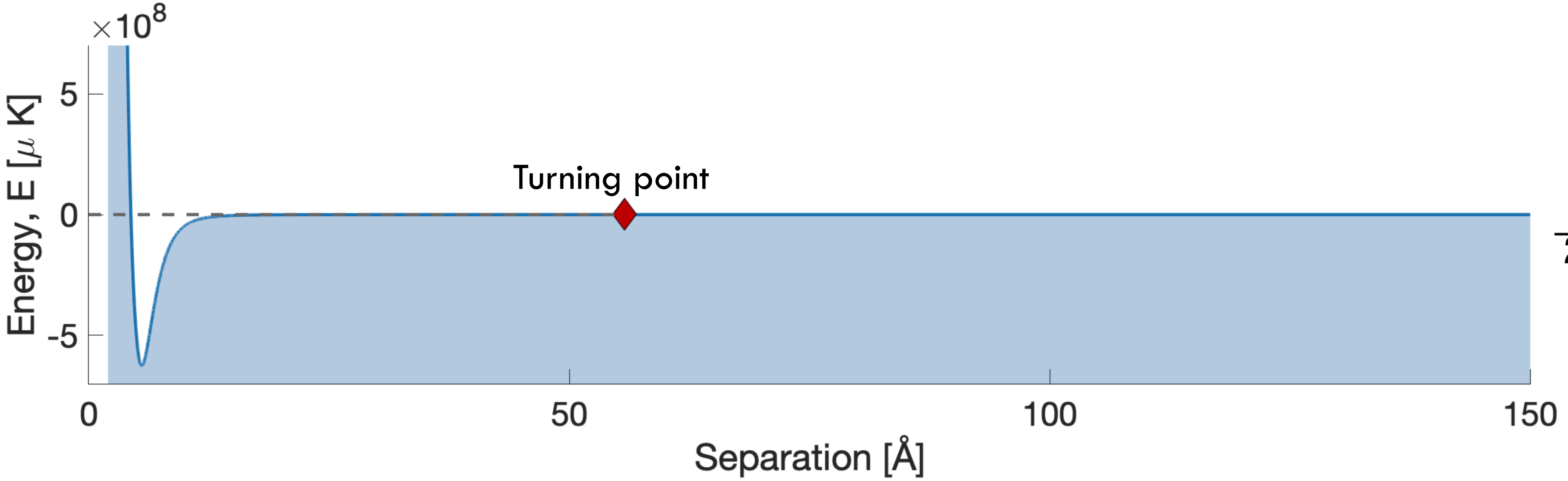
×10^8
Energy, E [μ K]
5
0
-5
Turning point
0
50
100
150
Separation [Å]

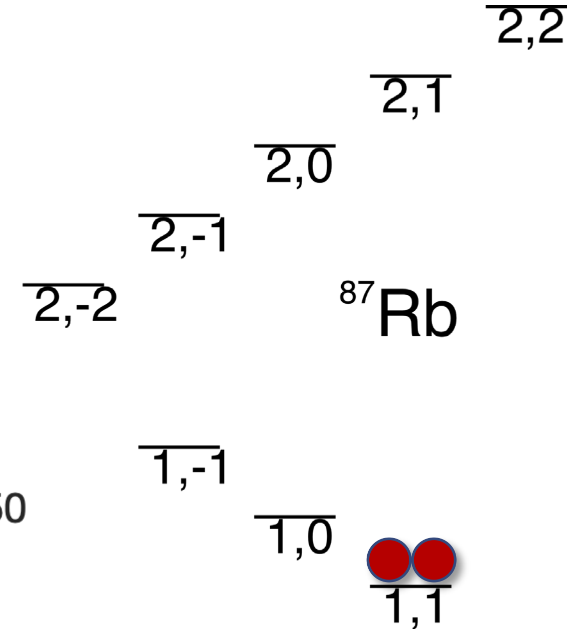
2,2
2,1
2,0
2,-1
2,-2
87Rb
1,-1
1,0
1,1

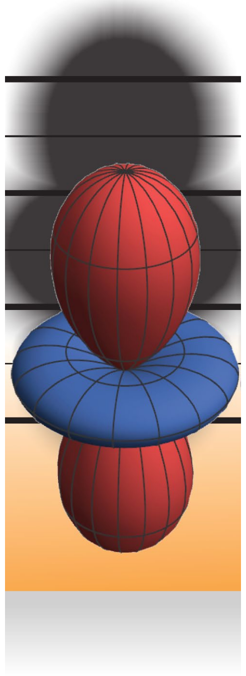

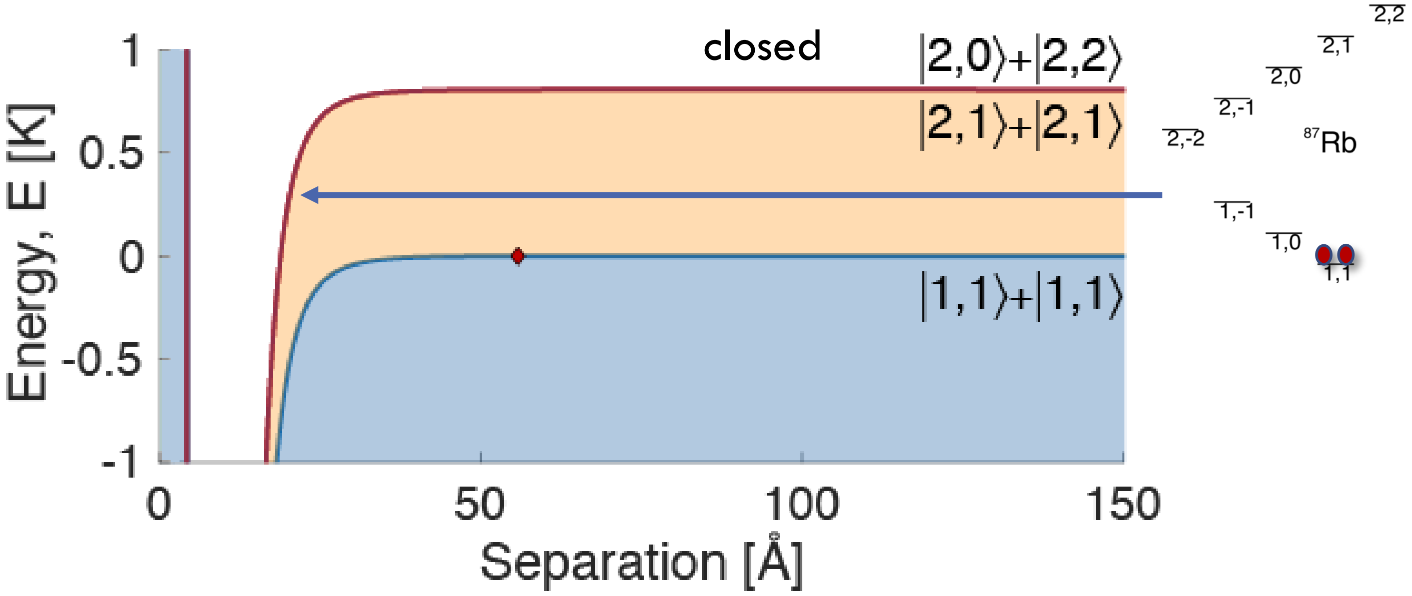
closed
|2,0⟩+|2,2⟩
|2,1⟩+|2,1⟩
|1,1⟩+|1,1⟩
Energy, E [K]
1
0.5
0
-0.5
-1
0
50
100
150
Separation [Å]
2,2
2,1
2,0
2,-1
2,-2
87Rb
1,-1
1,0
1,1

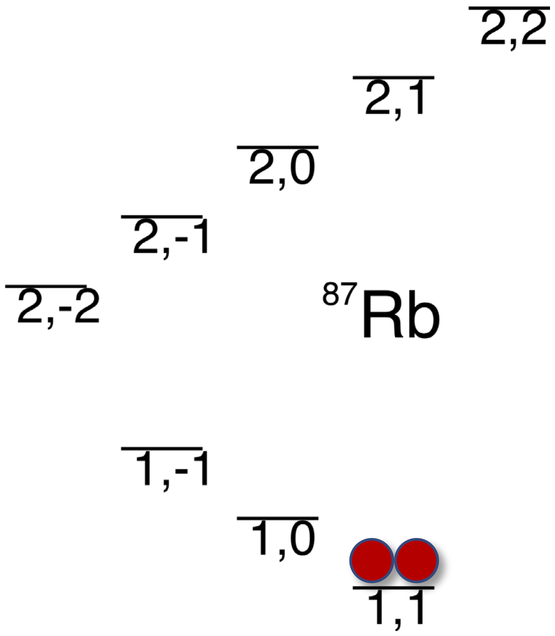
2,2
2,1
2,0
2,-1
2,-2
87Rb
1,-1
1,0
1,1

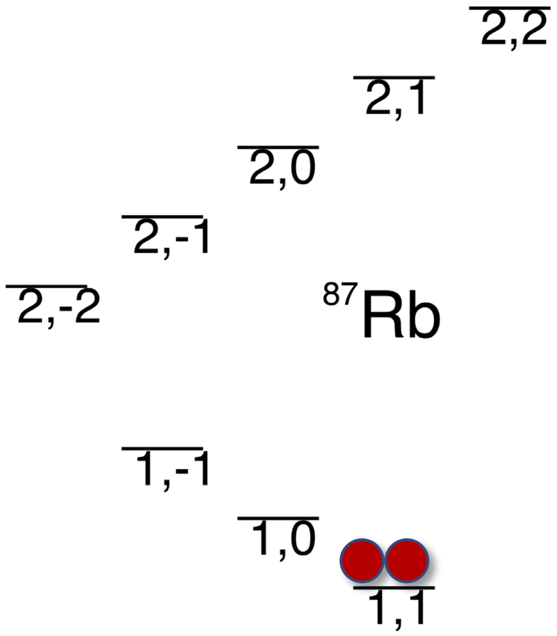
2,2
2,1
2,0
2,-1
2,-2
87Rb
1,-1
1,0
1,1

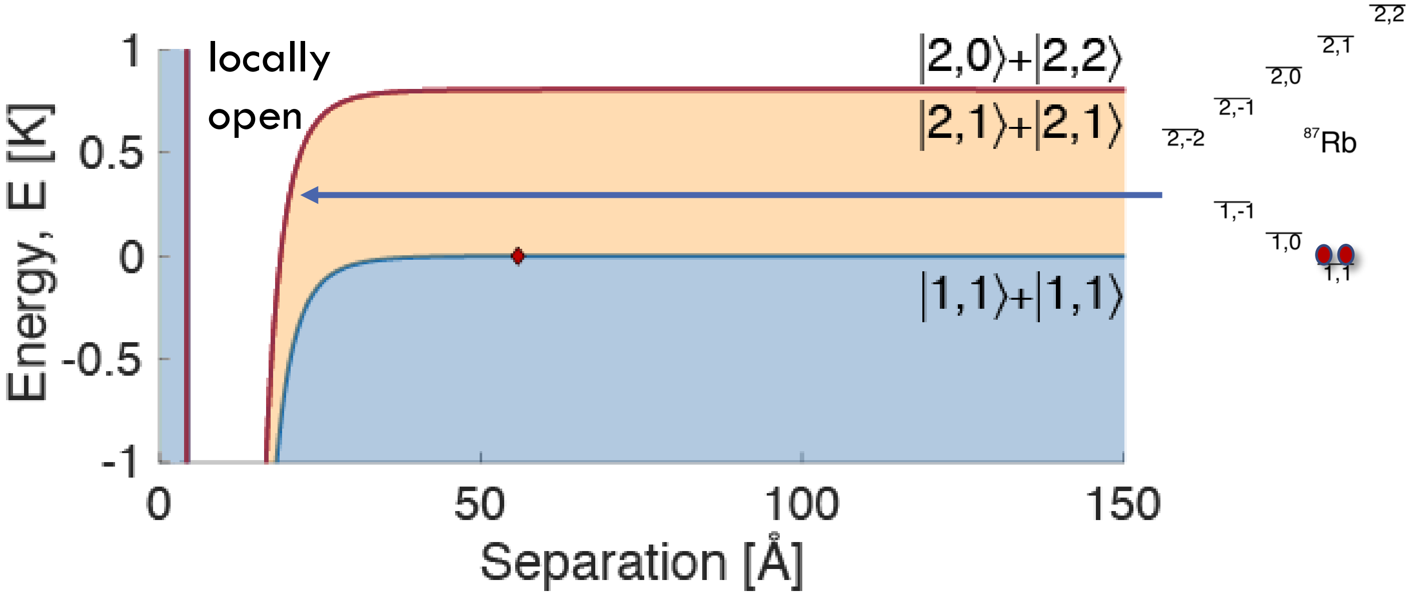
locally
open
|2,0⟩+|2,2⟩
|2,1⟩+|2,1⟩
|1,1⟩+|1,1⟩
Energy, E [K]
1
0.5
0
-0.5
-1
0
50
100
150
Separation [Å]
2,2
2,1
2,0
2,-1
2,-2
87Rb
1,-1
1,0
1,1

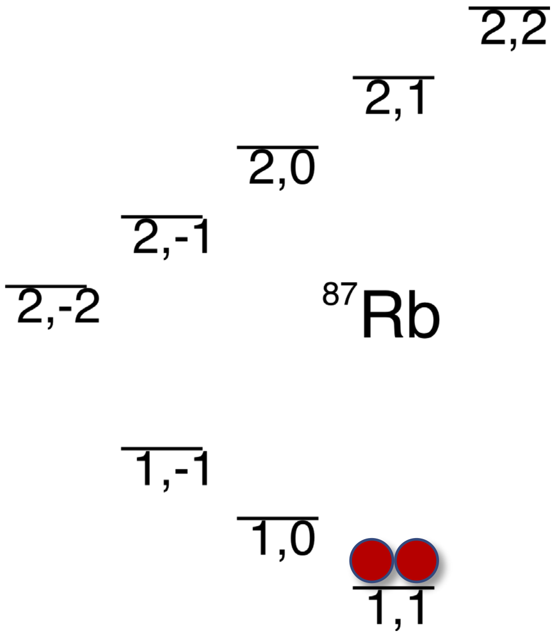
2,2
2,1
2,0
2,-1
2,-2
87Rb
1,-1
1,0
1,1

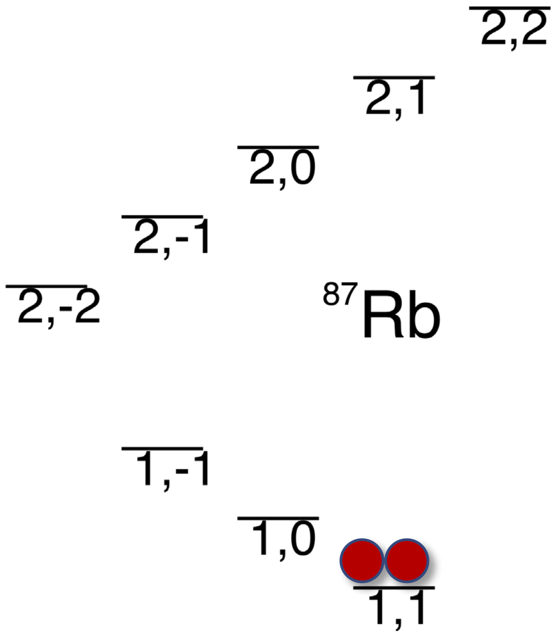
2,2
2,1
2,0
2,-1
2,-2
87Rb
1,-1
1,0
1,1

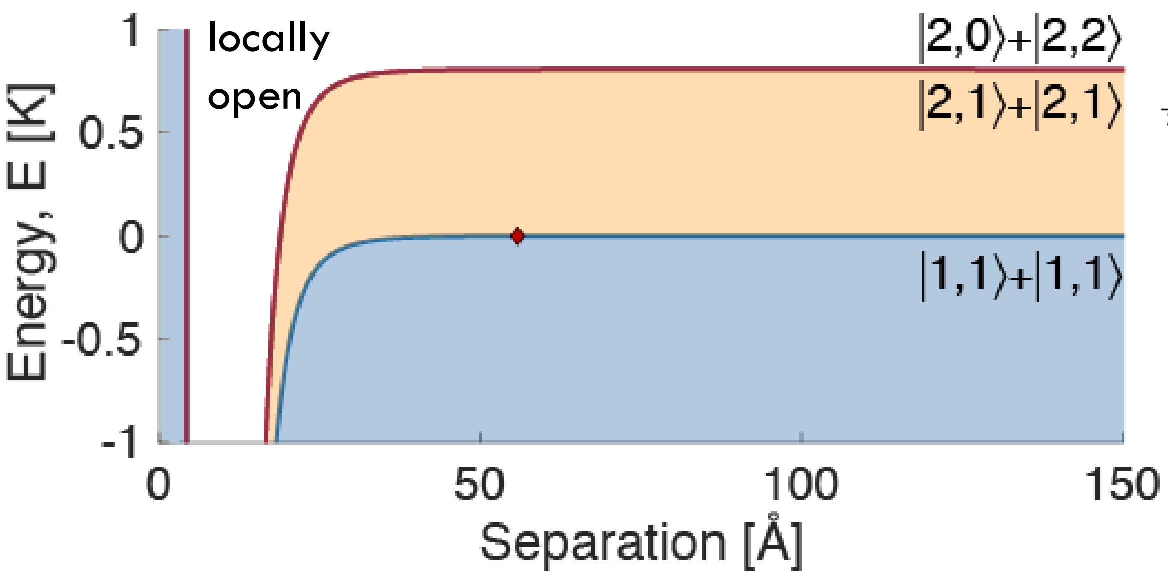

locally
open
|2,0⟩+|2,2⟩
|2,1⟩+|2,1⟩
|1,1⟩+|1,1⟩
Energy, E [K]
1
0.5
0
-0.5
-1
0
50
100
150
Separation [Å]

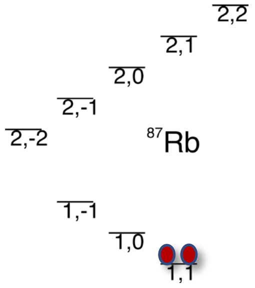

2,2
2,1
2,0
2,-1
2,-2
87Rb
1,-1
1,0
1,1

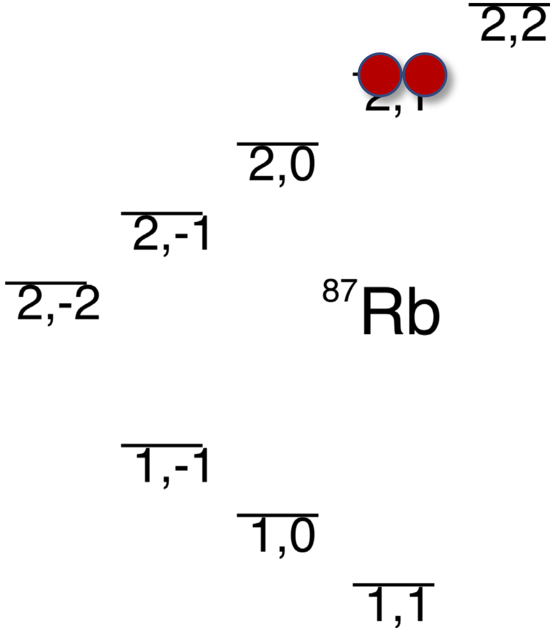

2,2
2,1
2,0
2,-1
2,-2
87Rb
1,-1
1,0
1,1

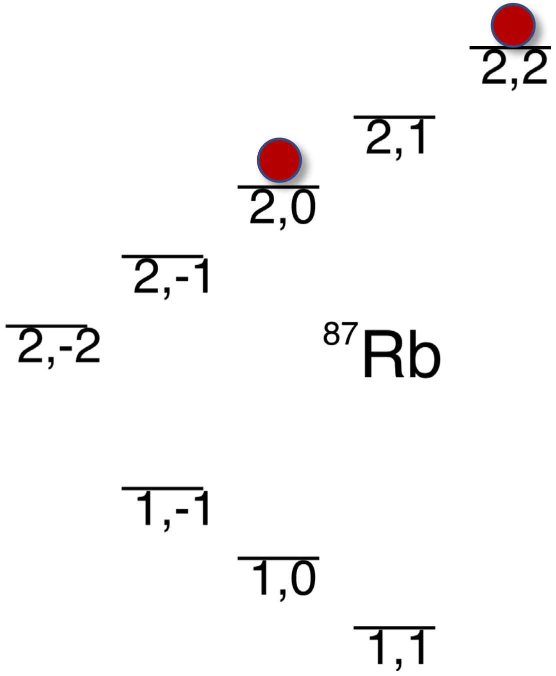

2,2
2,1
2,0
2,-1
2,-2
87Rb
1,-1
1,0
1,1

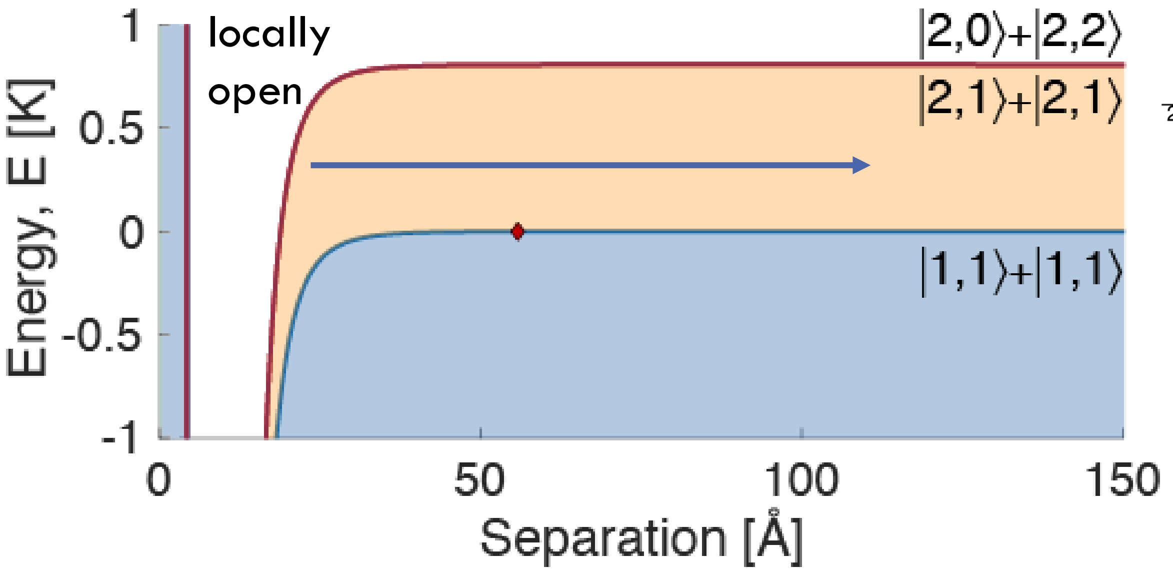
locally
open
|2,0⟩+|2,2⟩
|2,1⟩+|2,1⟩
|1,1⟩+|1,1⟩
Energy, E [K]
1
0.5
0
-0.5
-1
0
50
100
150
Separation [Å]

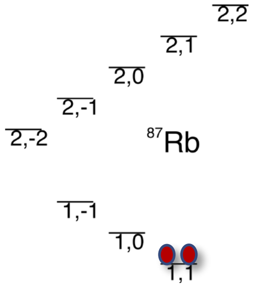
2,2
2,1
2,0
2,-1
2,-2
87Rb
1,-1
1,0
1,1

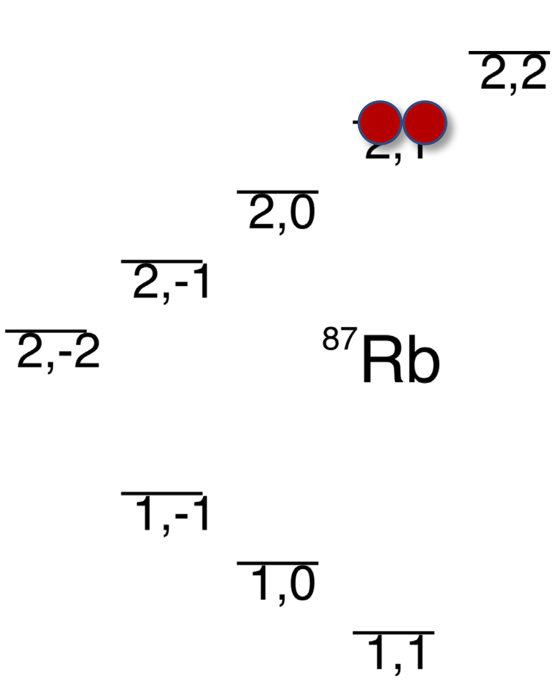
2,2
2,1
2,0
2,-1
2,-2
87Rb
1,-1
1,0
1,1

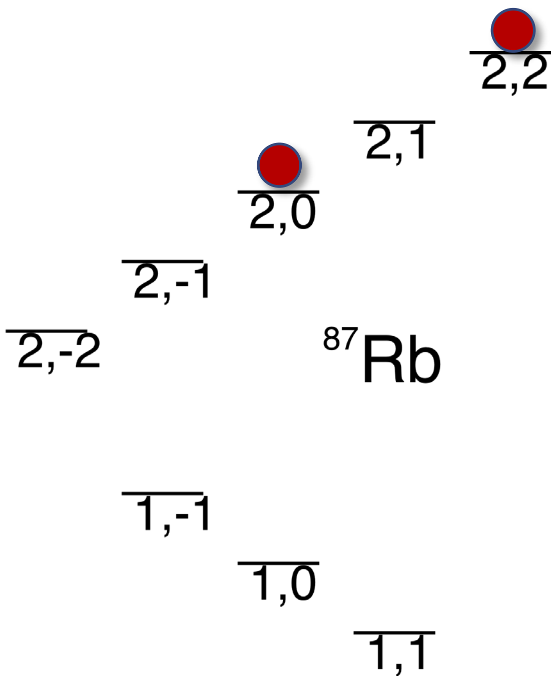
2,2
2,1
2,0
2,-1
2,-2
87Rb
1,-1
1,0
1,1

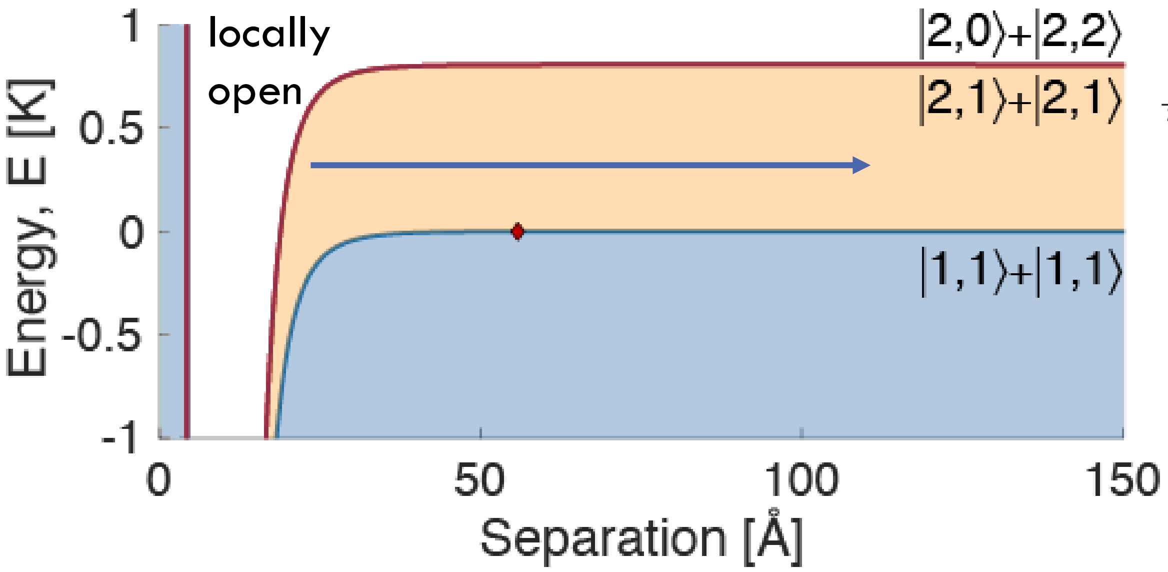
locally
open
|2,0⟩+|2,2⟩
|2,1⟩+|2,1⟩
|1,1⟩+|1,1⟩
Energy, E [K]
1
0.5
0
-0.5
-1
0
50
100
150
Separation [Å]

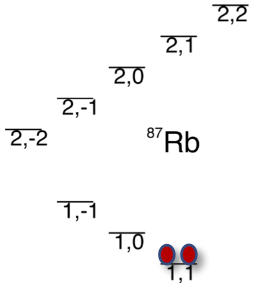
2,2
2,1
2,0
2,-1
2,-2
87Rb
1,-1
1,0
1,1

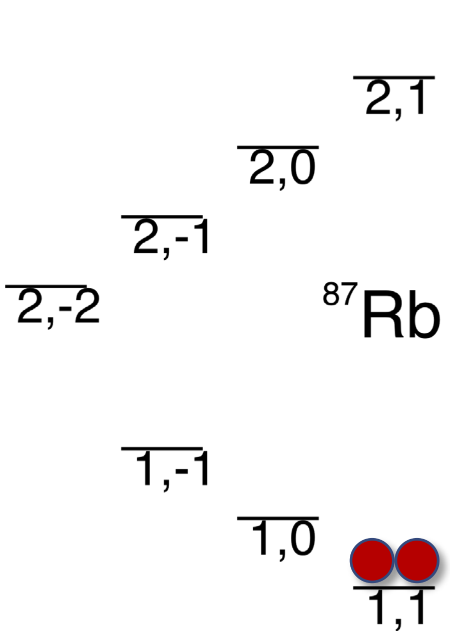
2,2
2,1
2,0
2,-1
2,-2
87Rb
1,-1
1,0
1,1

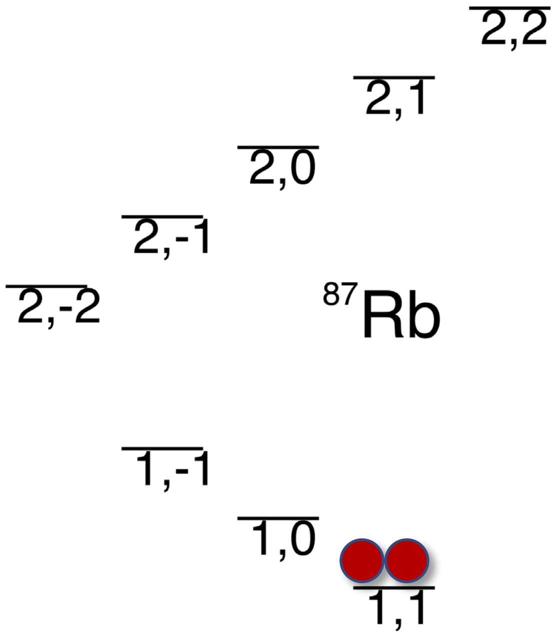
2,2
2,1
2,0
2,-1
2,-2
87Rb
1,-1
1,0
1,1

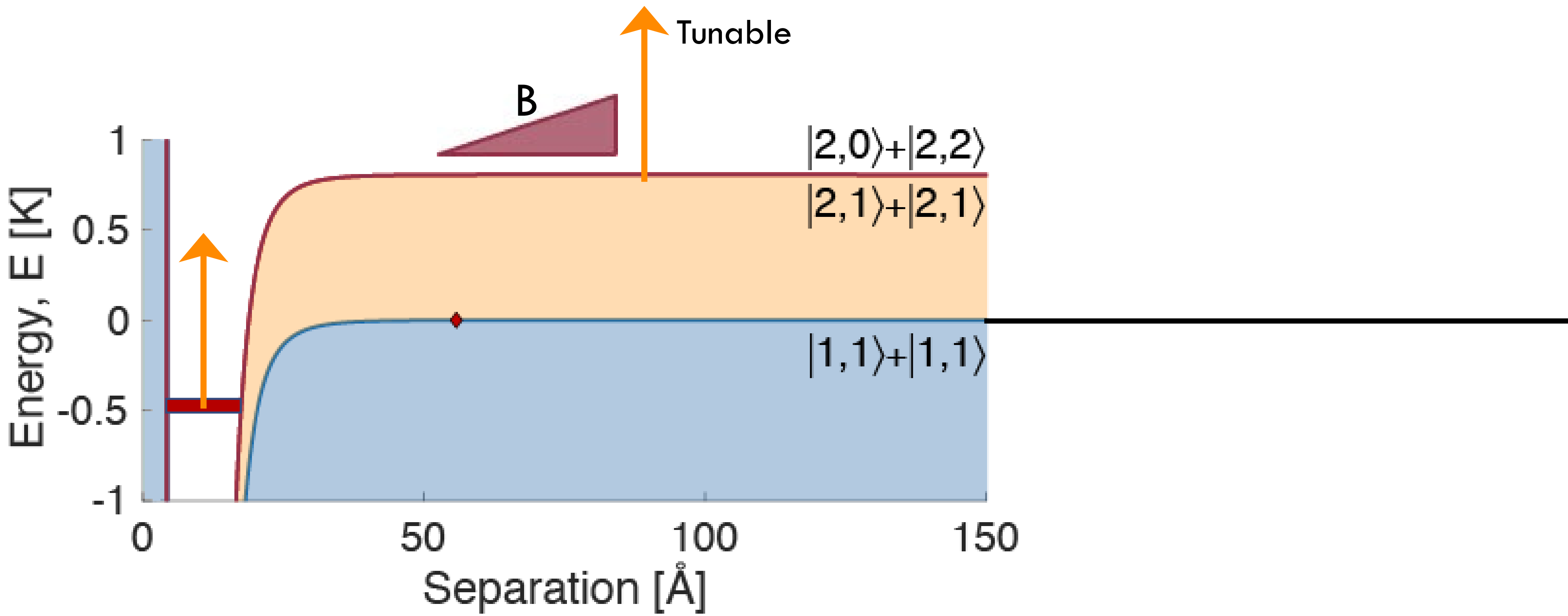

Tunable
B
|2,0⟩+|2,2⟩
|2,1⟩+|2,1⟩
|1,1⟩+|1,1⟩
1
0.5
0
-0.5
-1
Energy, E [K]
0
50
100
150
Separation [Å]

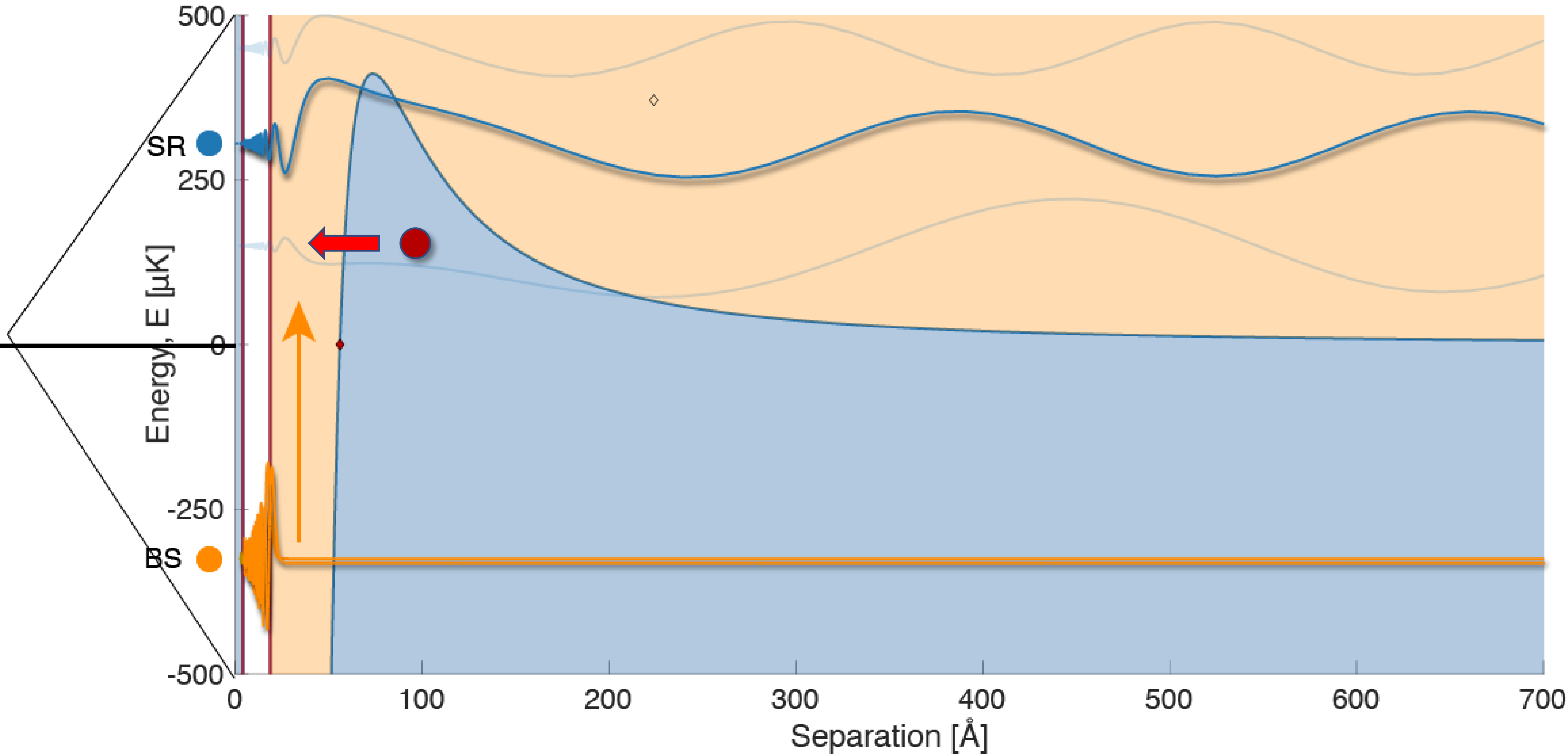

500
250
0
-250
-500
SR
BS
Energy, E [μK]
0
100
200
300
400
500
600
700
Separation [Å]

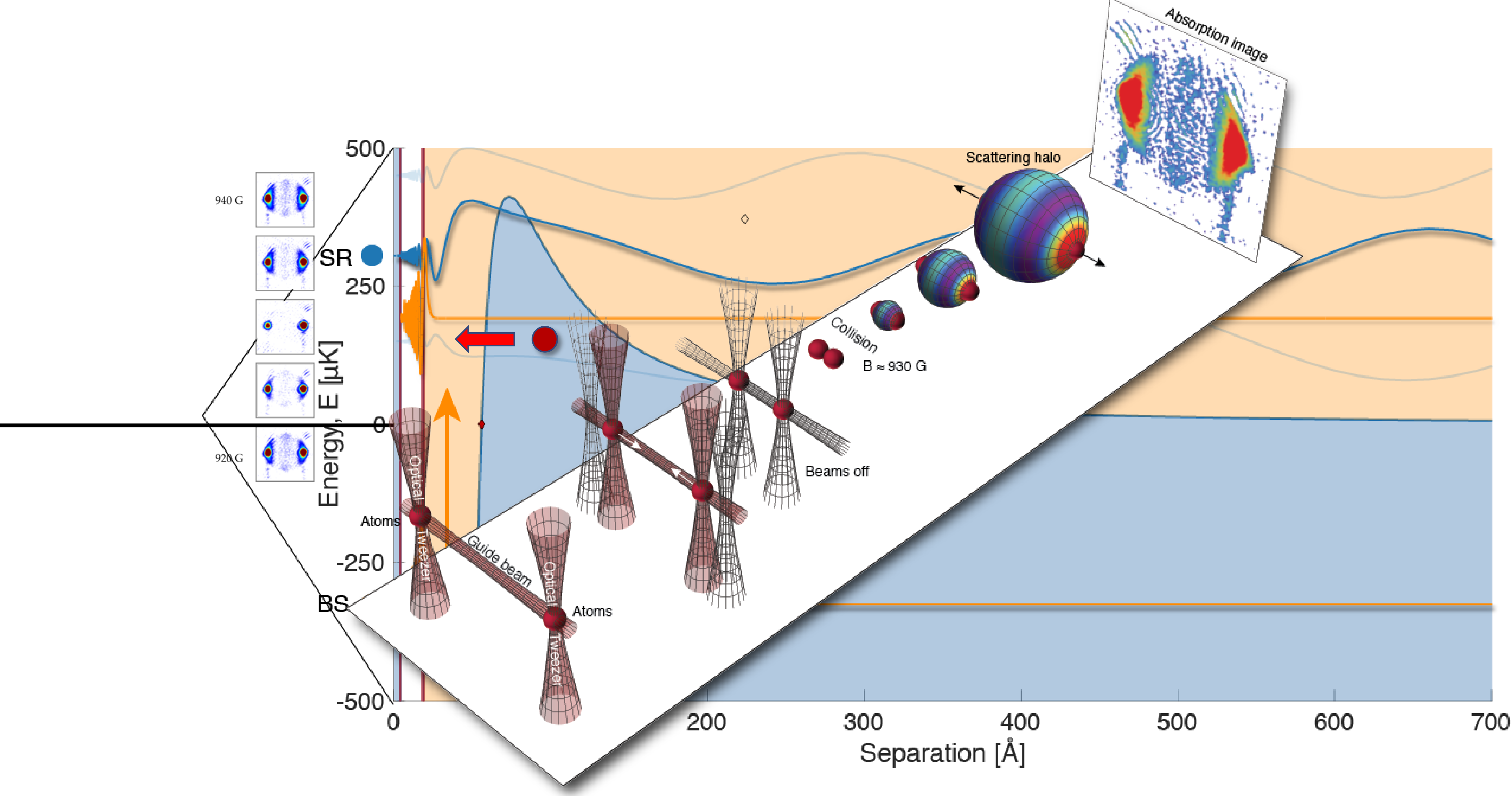

Absorption image
Scattering halo
940 G
920 G
SR
BS
500
250
0
-250
-500
Energy, E [μK]
0
200
300
400
500
600
700
Separation [Å]
Collision
B ≈ 930 G
Beams off
Atoms
Optical Tweezer
Guide beam
Atoms
Optical Tweezer

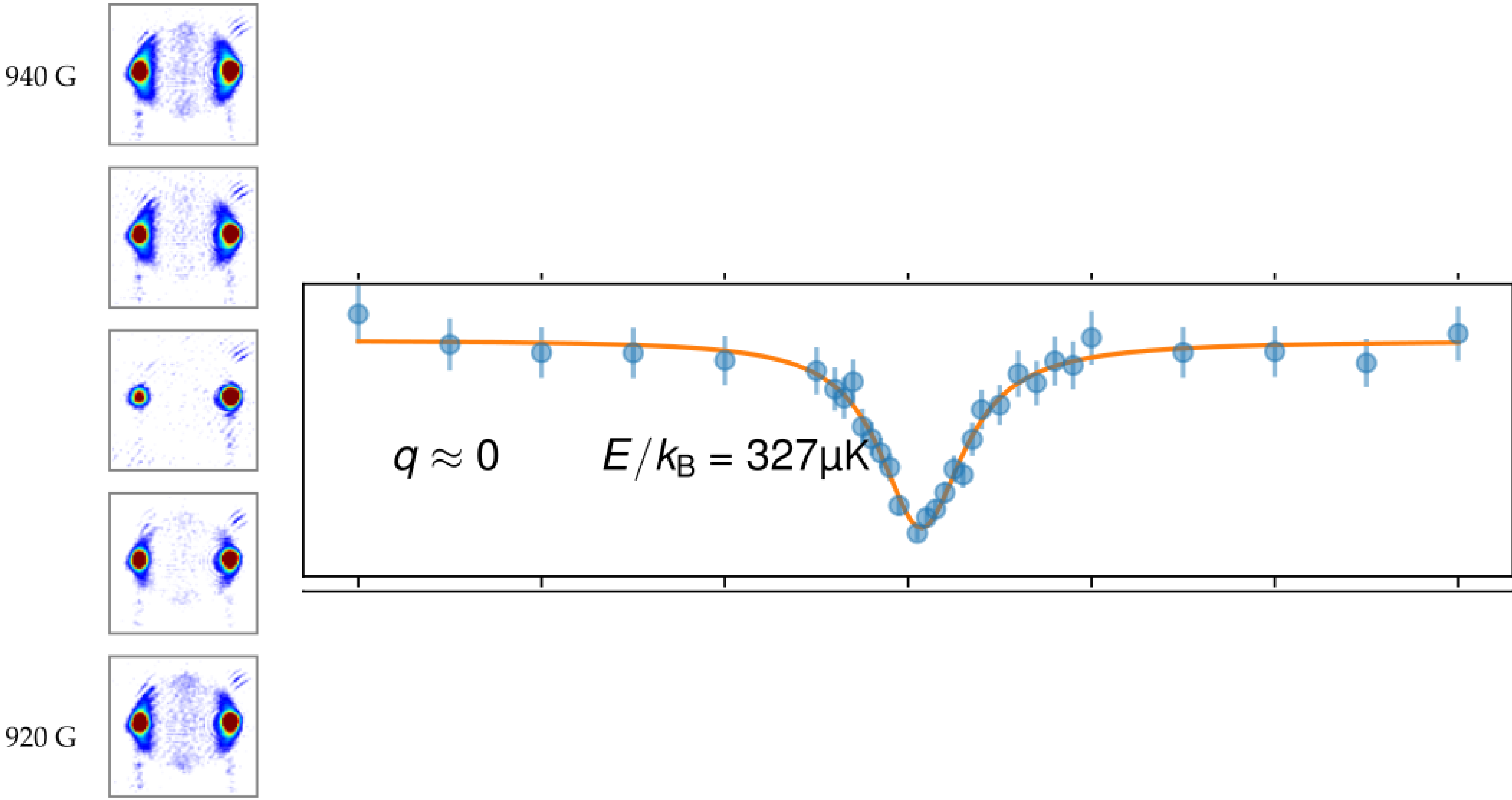

940 G
920 G
$q \approx 0$
$E/k_B = 327\mu K$

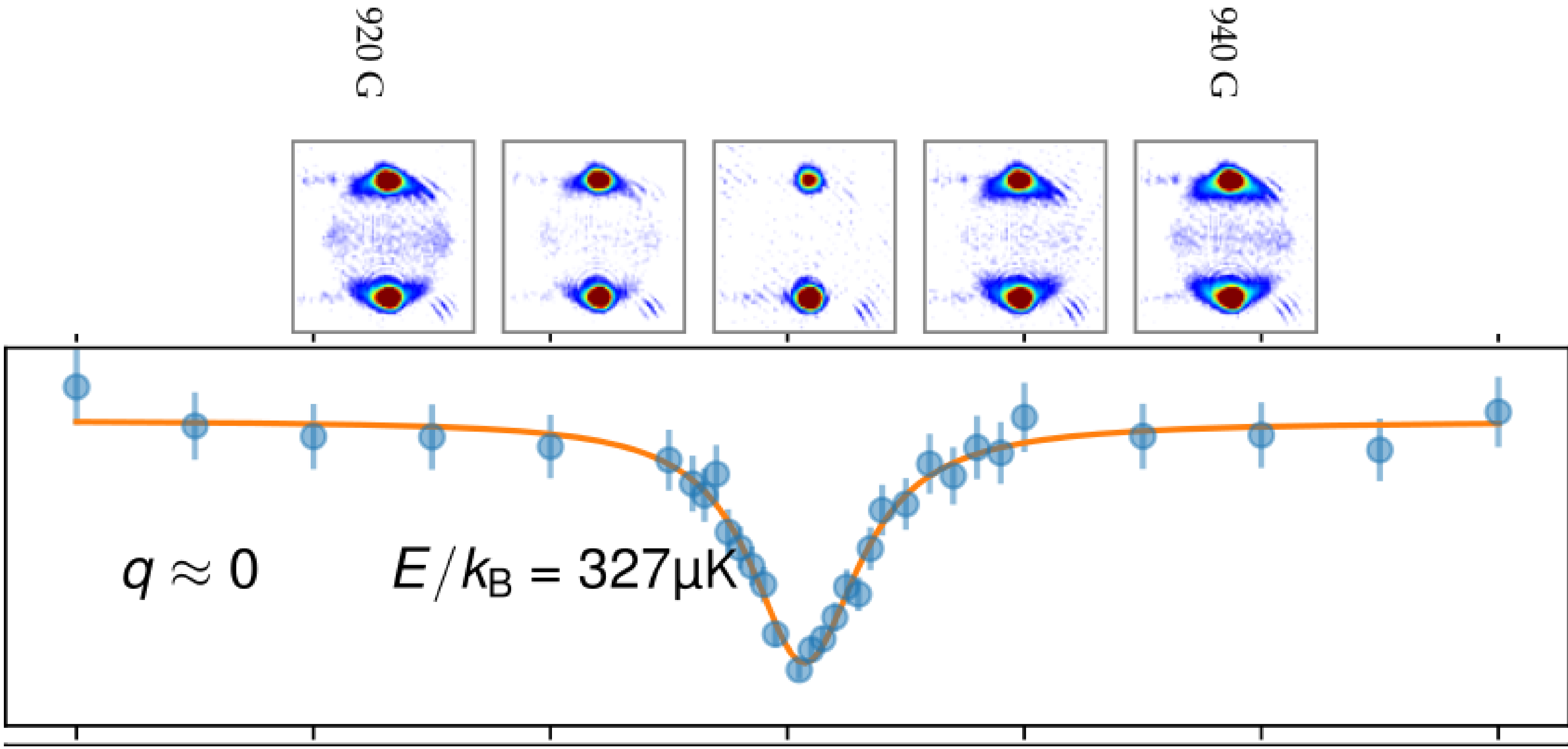

920 G
940 G
$q \approx 0$
$E/k_B = 327\mu K$

Fano profiles

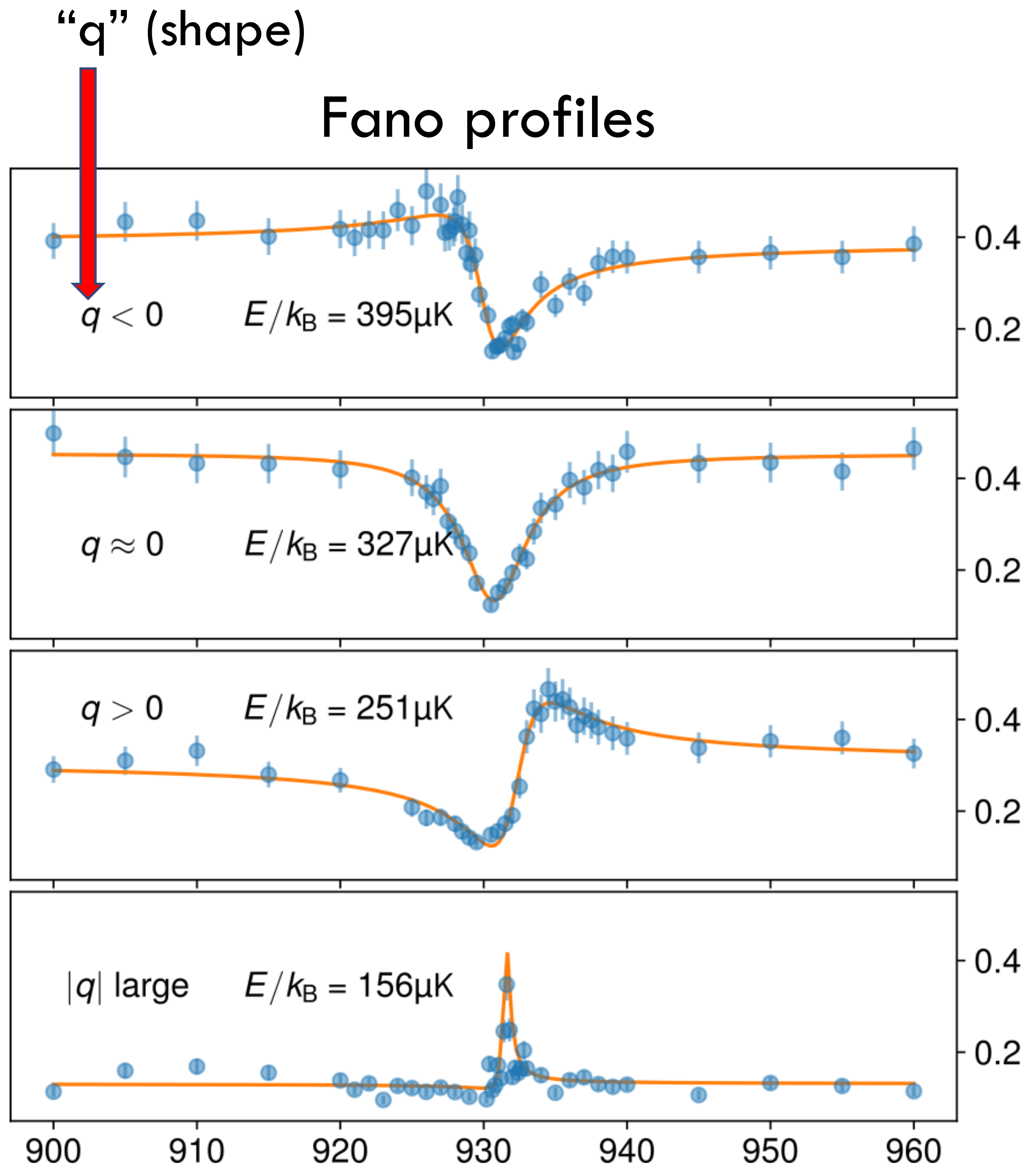

E-B map

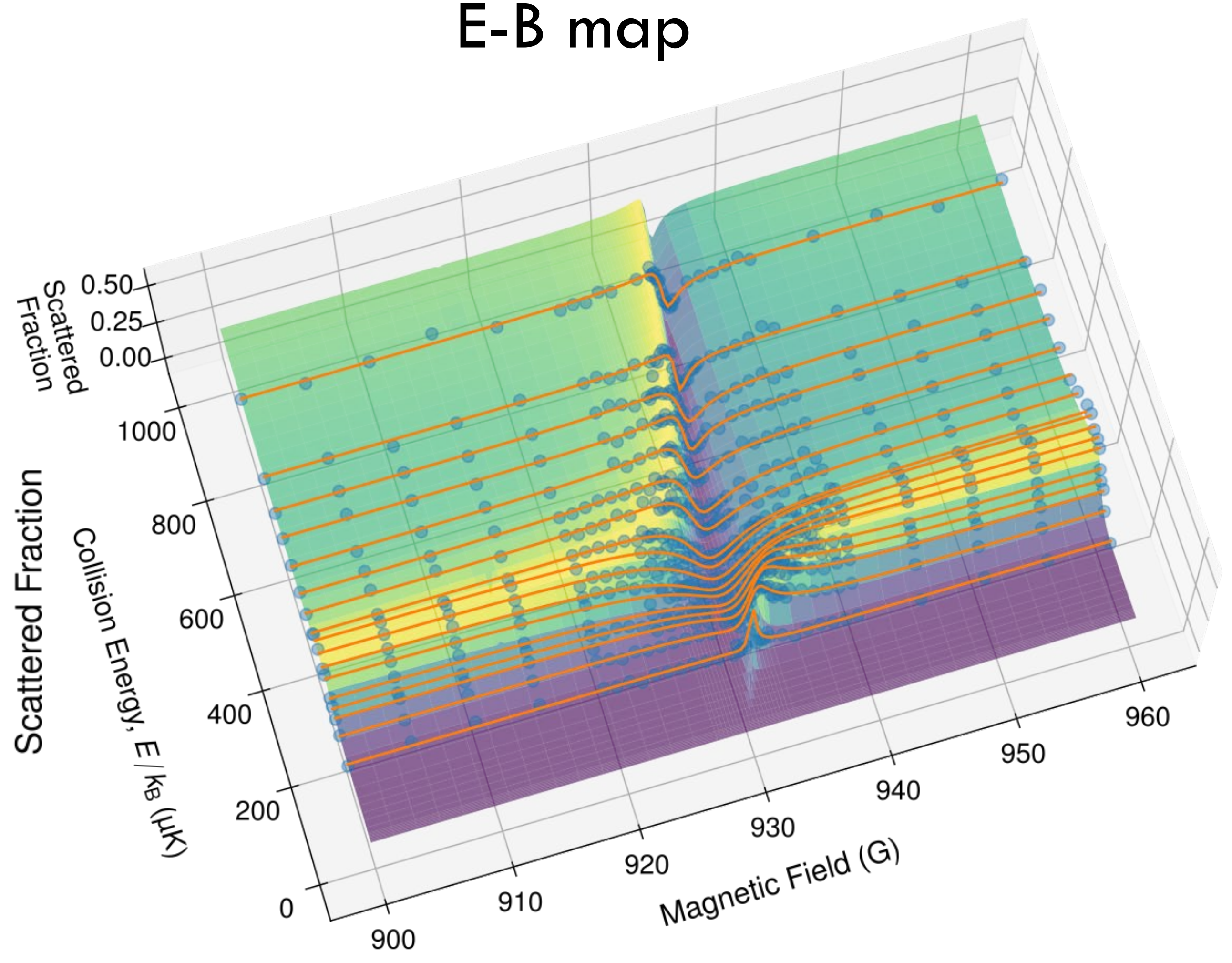

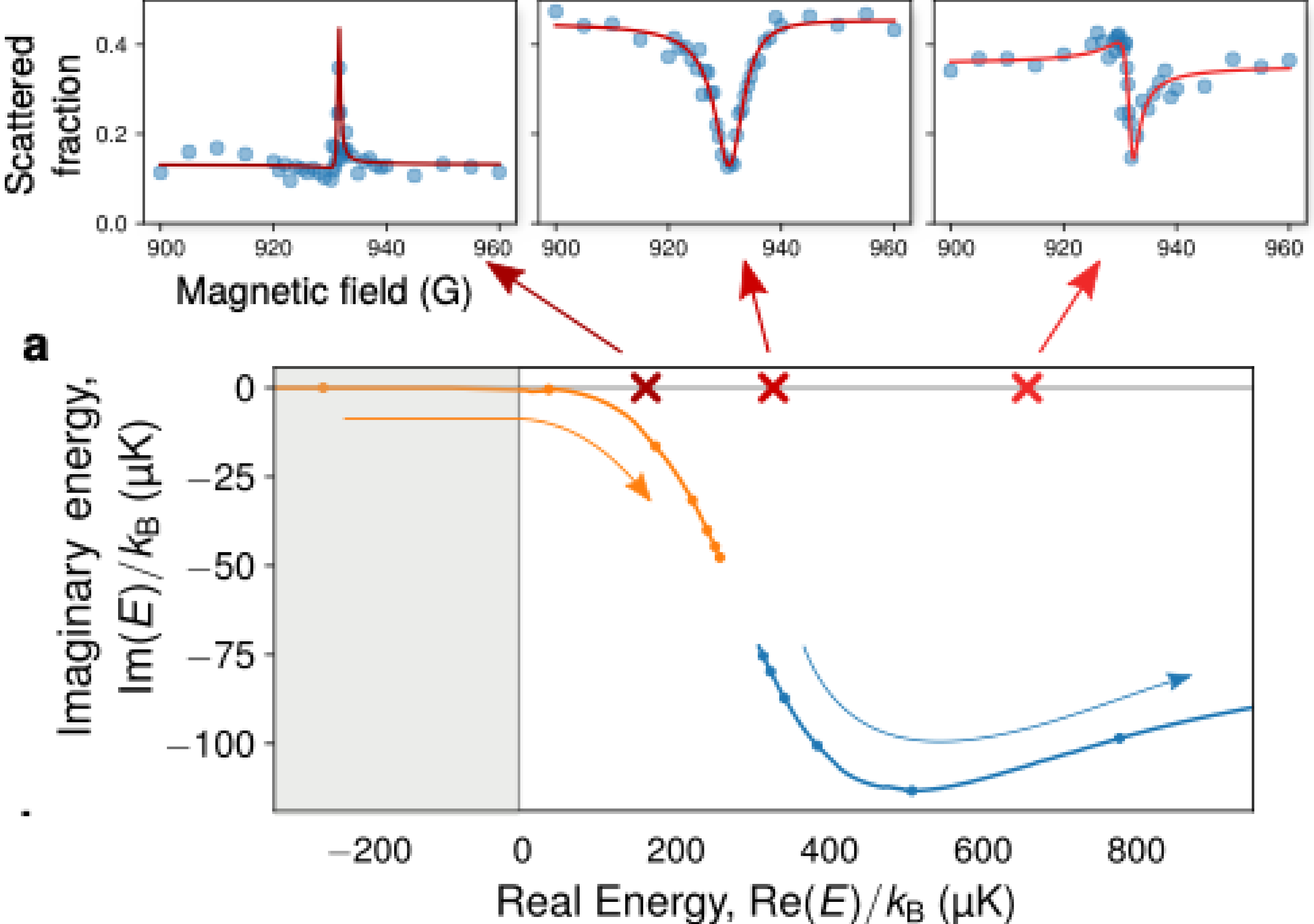

Scattered fraction
0.0
0.2
0.4
900
920
940
960
Magnetic field (G)
a
Imaginary energy, Im(E)/k_B (μK)
0
−25
−50
−75
−100
−200
200
400
600
800
Real Energy, Re(E)/k_B (μK)

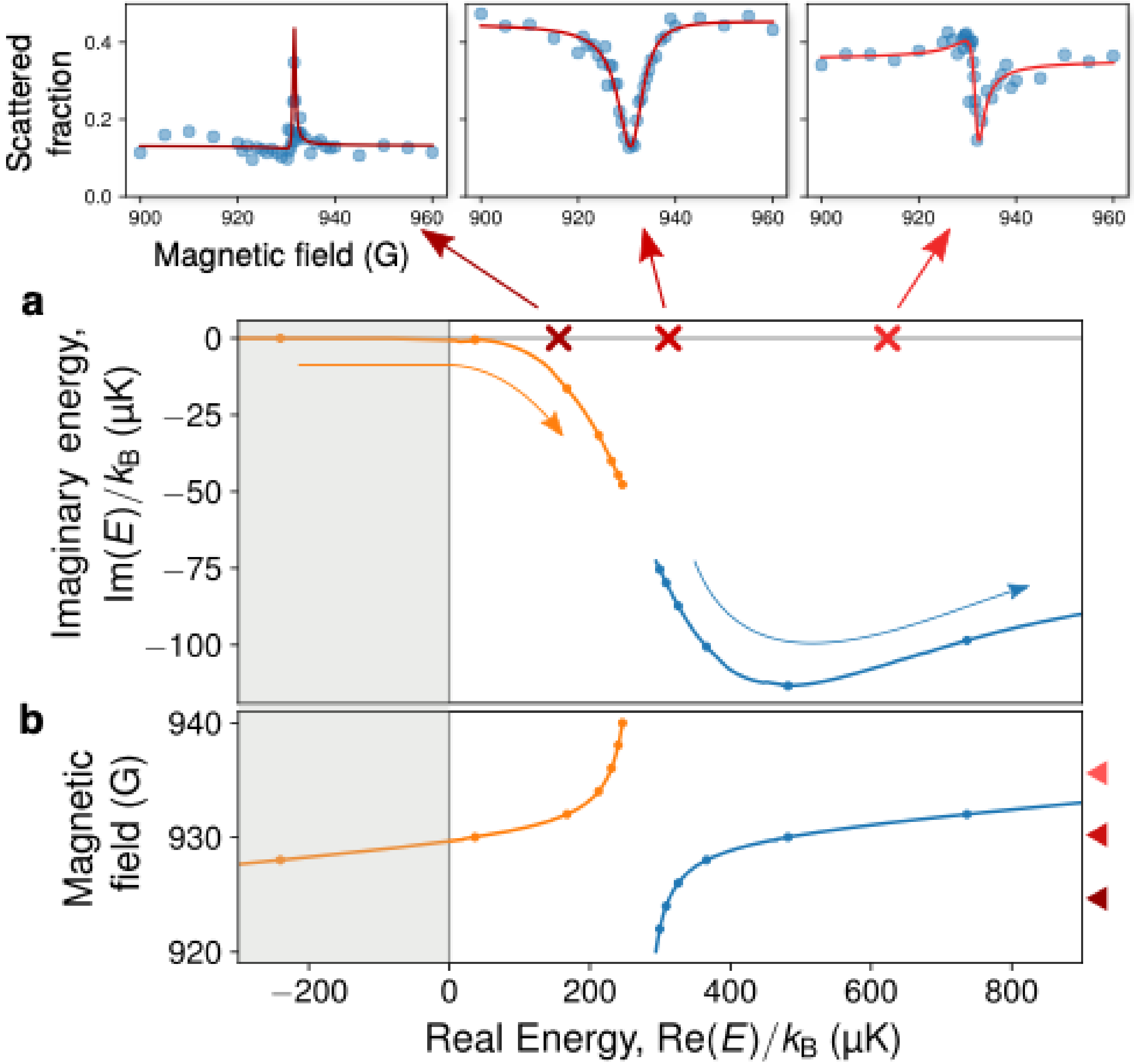

Scattered fraction
0.0
0.2
0.4
900
920
940
960
Magnetic field (G)
a
Imaginary energy, Im(E)/k_B (μK)
0
−25
−50
−75
−100
b
Magnetic field (G)
940
930
920
−200
0
200
400
600
800
Real Energy, Re(E)/k_B (μK)

Round up the usual suspects

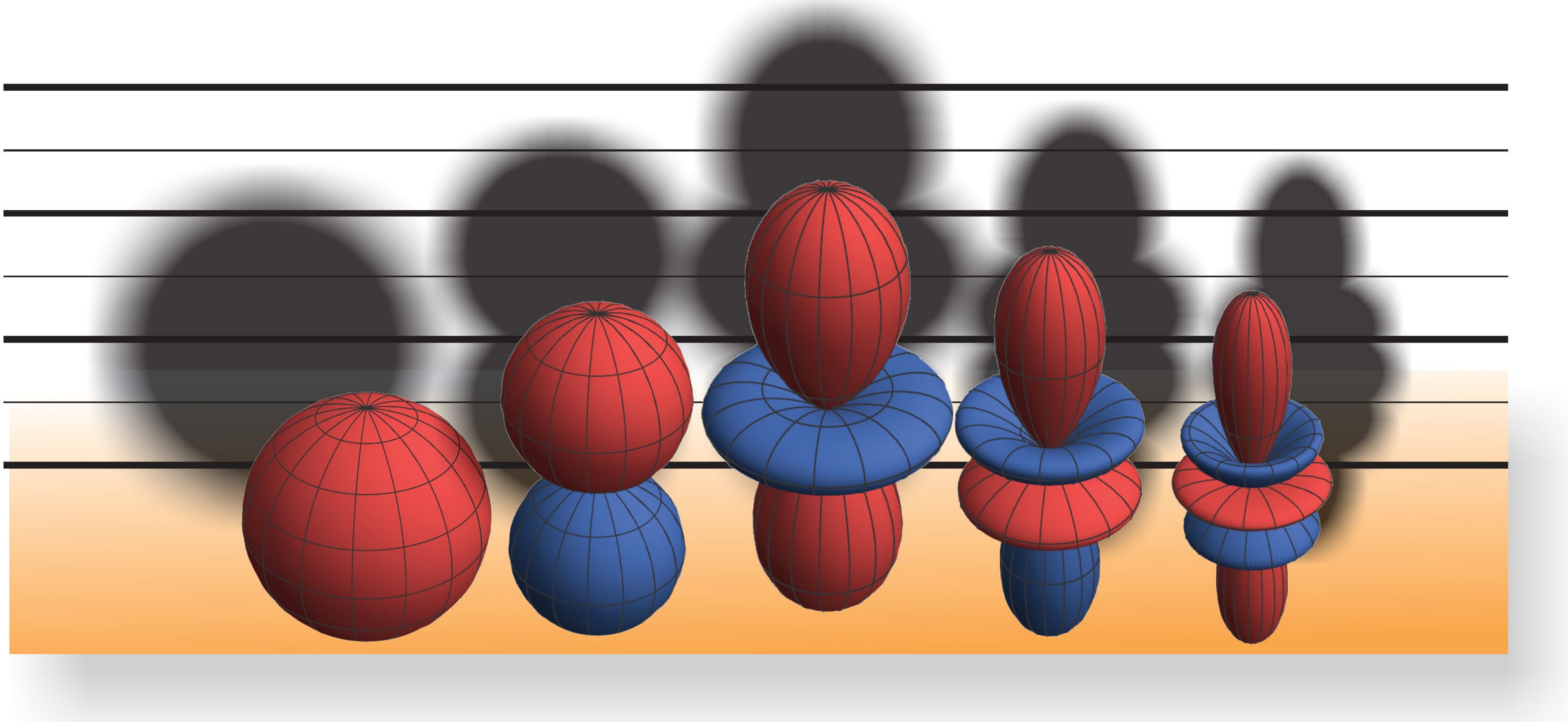

K-Rb: broad elastic s-wave Feshbach resonance

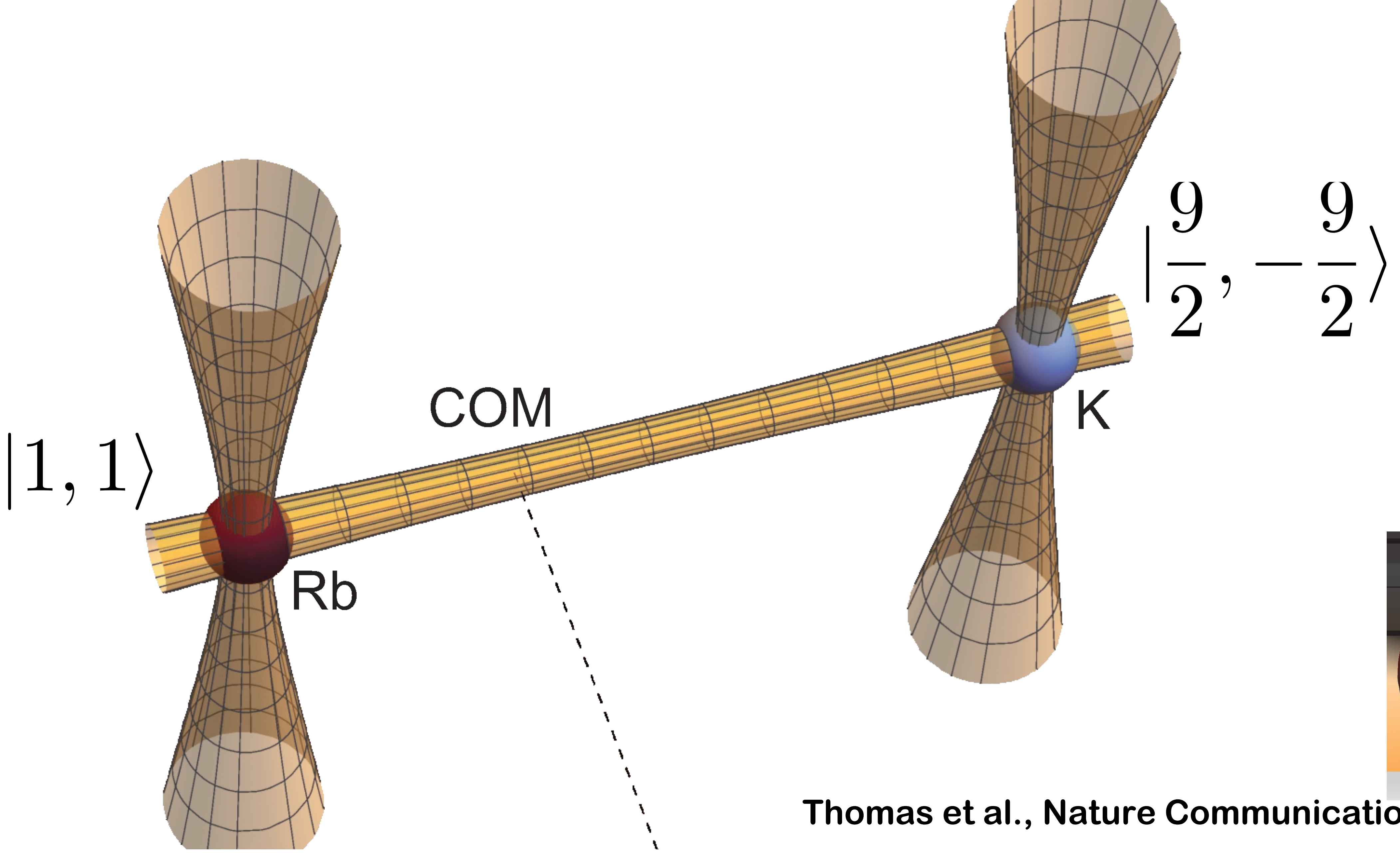

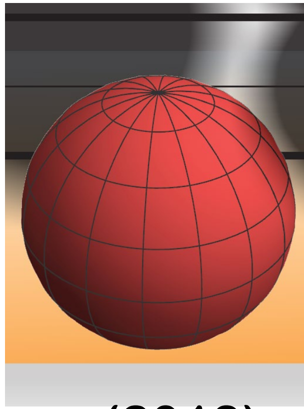

Thomas et al., Nature Communications (2018)

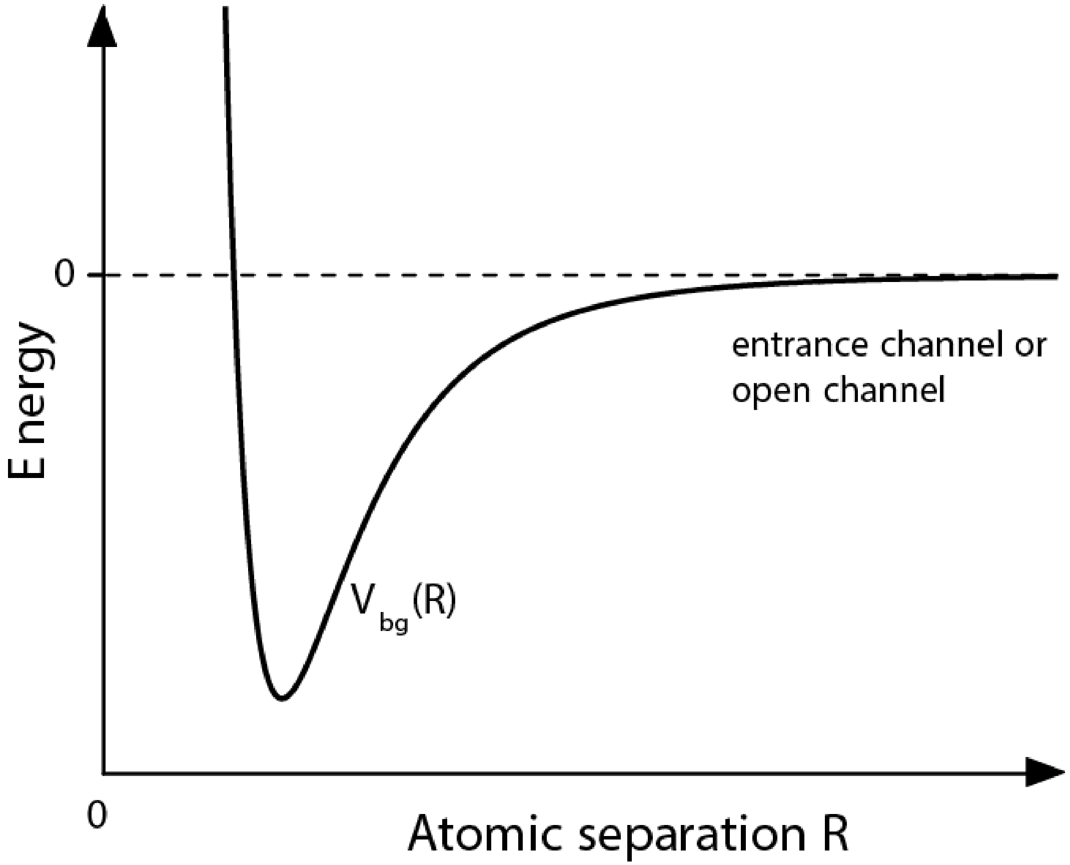

0
Energy
entrance channel or
open channel
V bg(R)
0
Atomic separation R

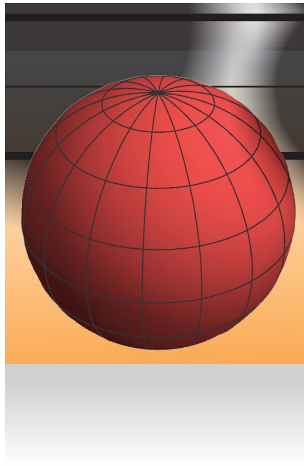

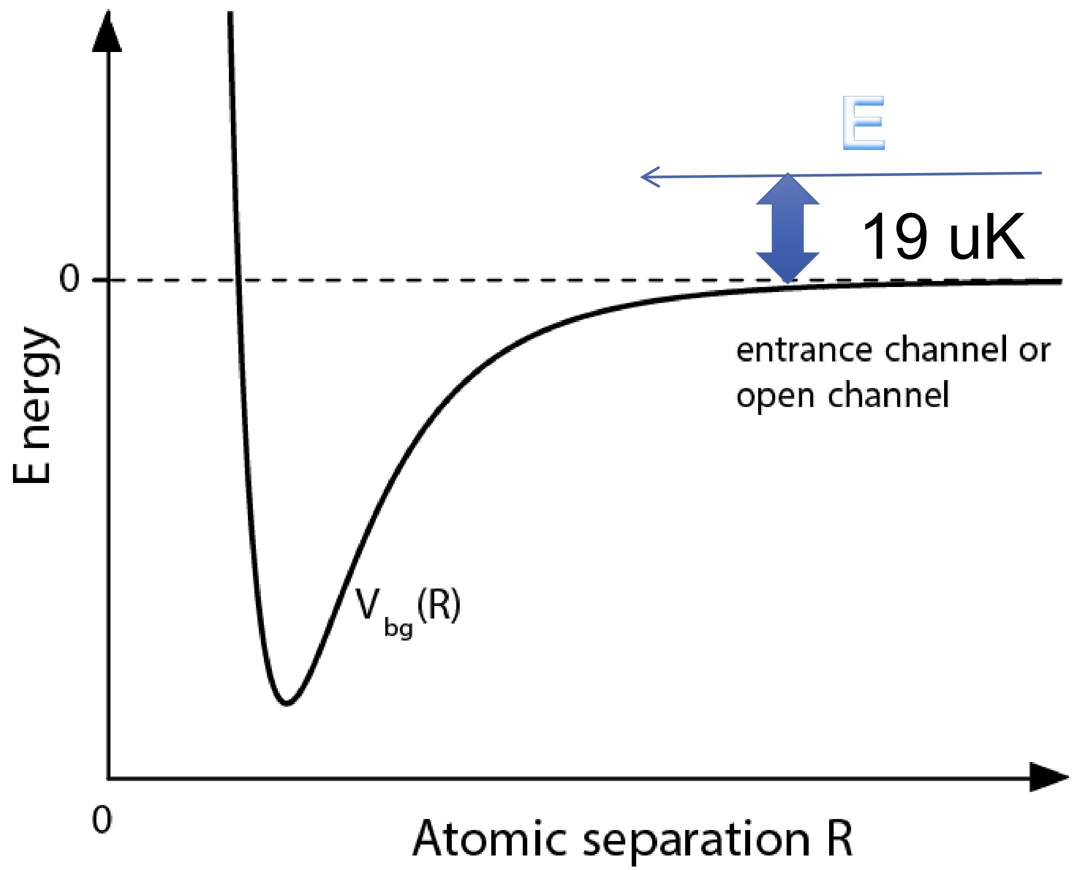
E
19 uK
0
E nergy
entrance channel or
open channel
$V_{bg}(R)$
0
Atomic separation R

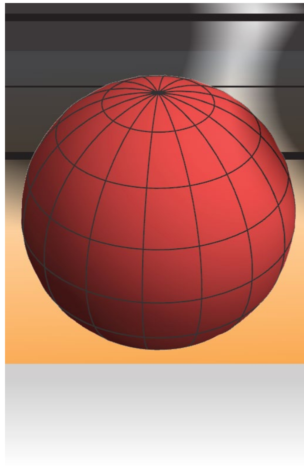

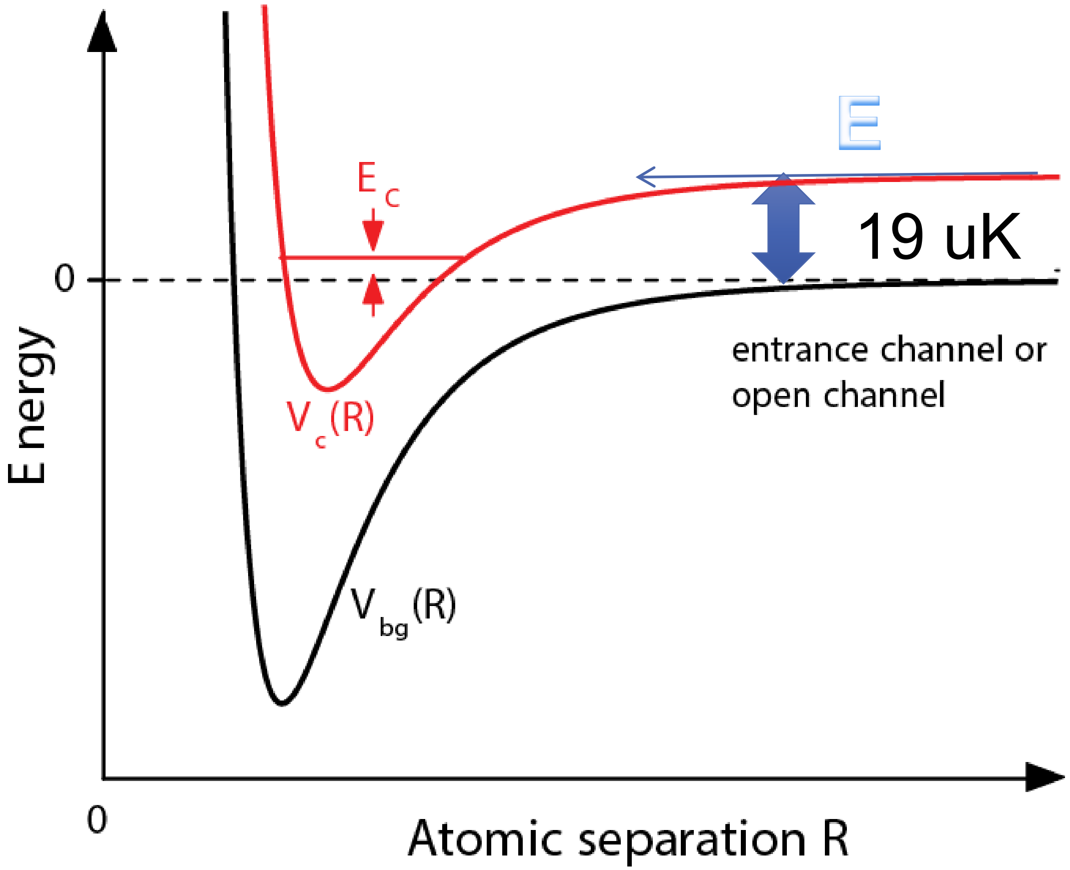

E
E c
19 uK
0
Energy
V c (R)
V bg (R)
entrance channel or
open channel
0
Atomic separation R

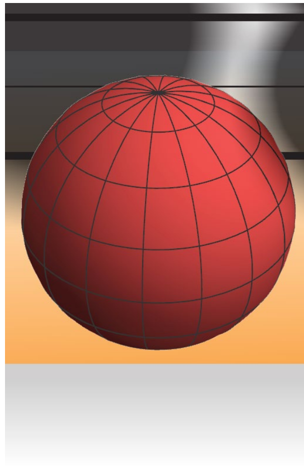

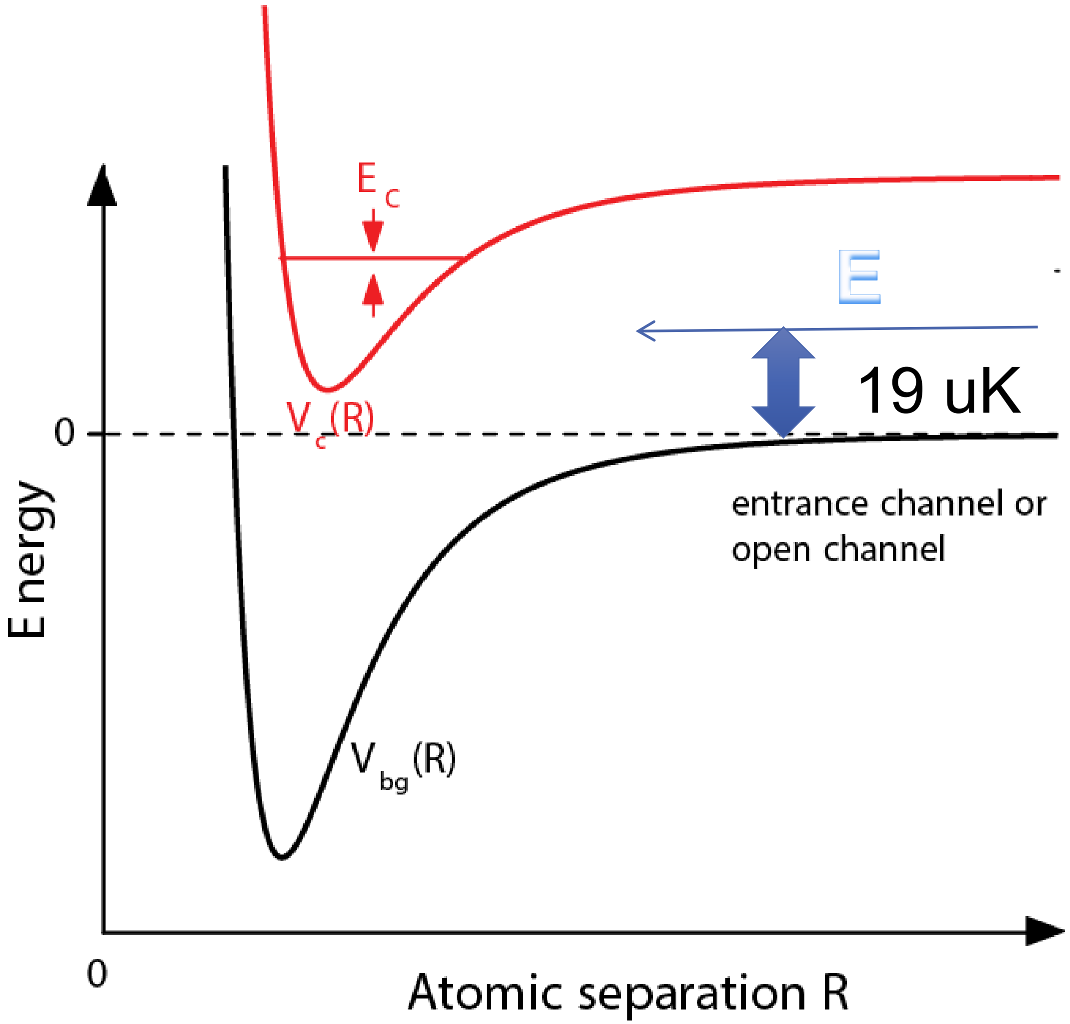
E c
E
19 uK
0
V c (R)
entrance channel or
open channel
E nergy
V bg (R)
0
Atomic separation R

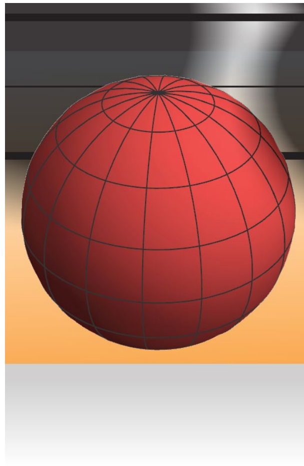

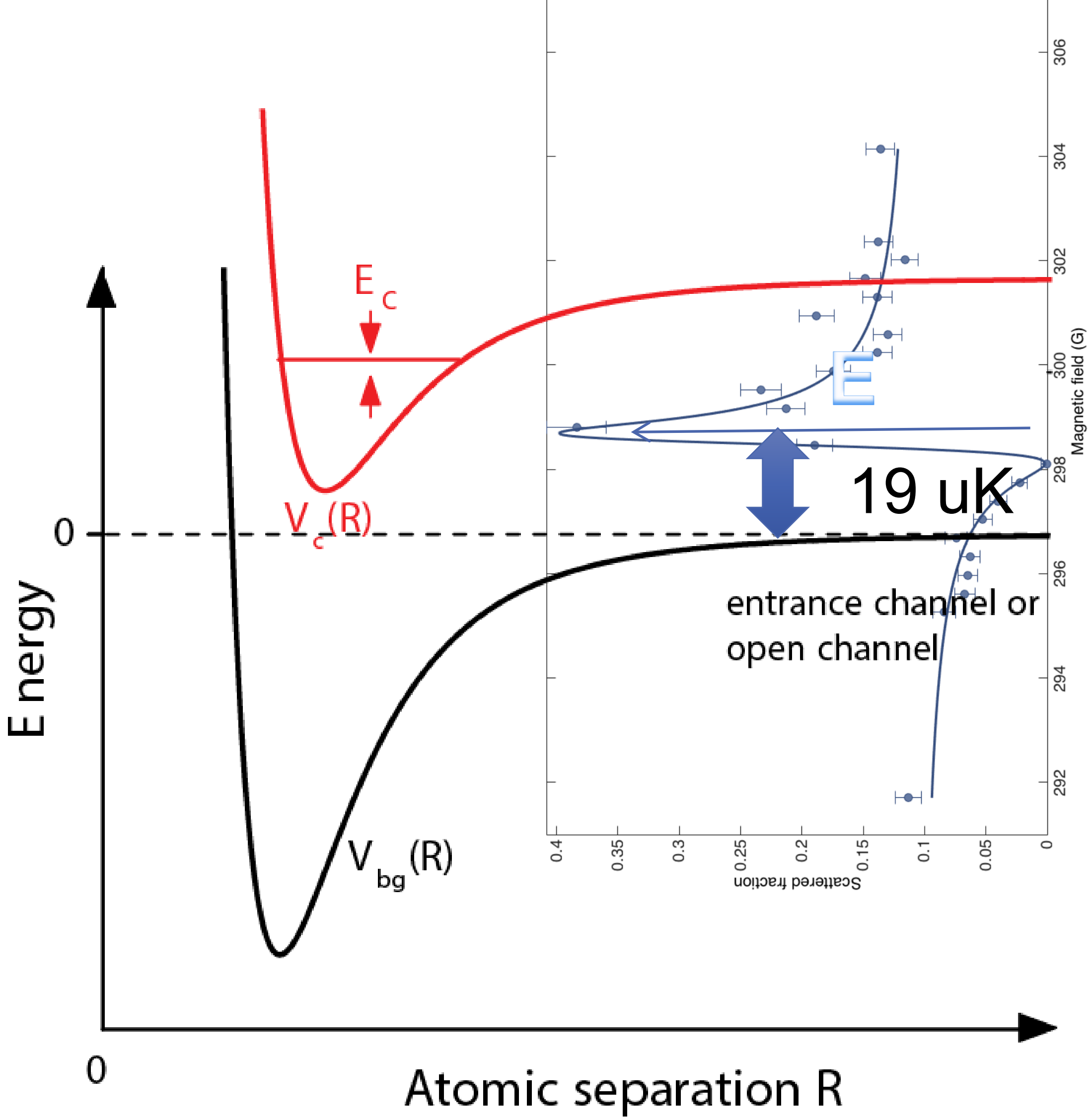
E nergy
0
E c
V c (R)
V bg (R)
19 uK
entrance channel or
open channel
Magnetic field (G)
Scattered fraction
0
Atomic separation R

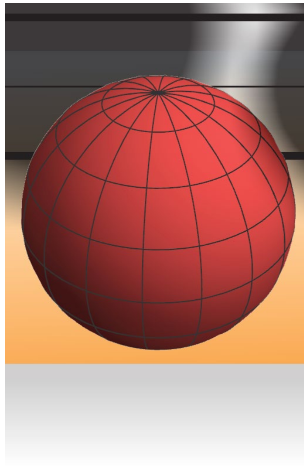

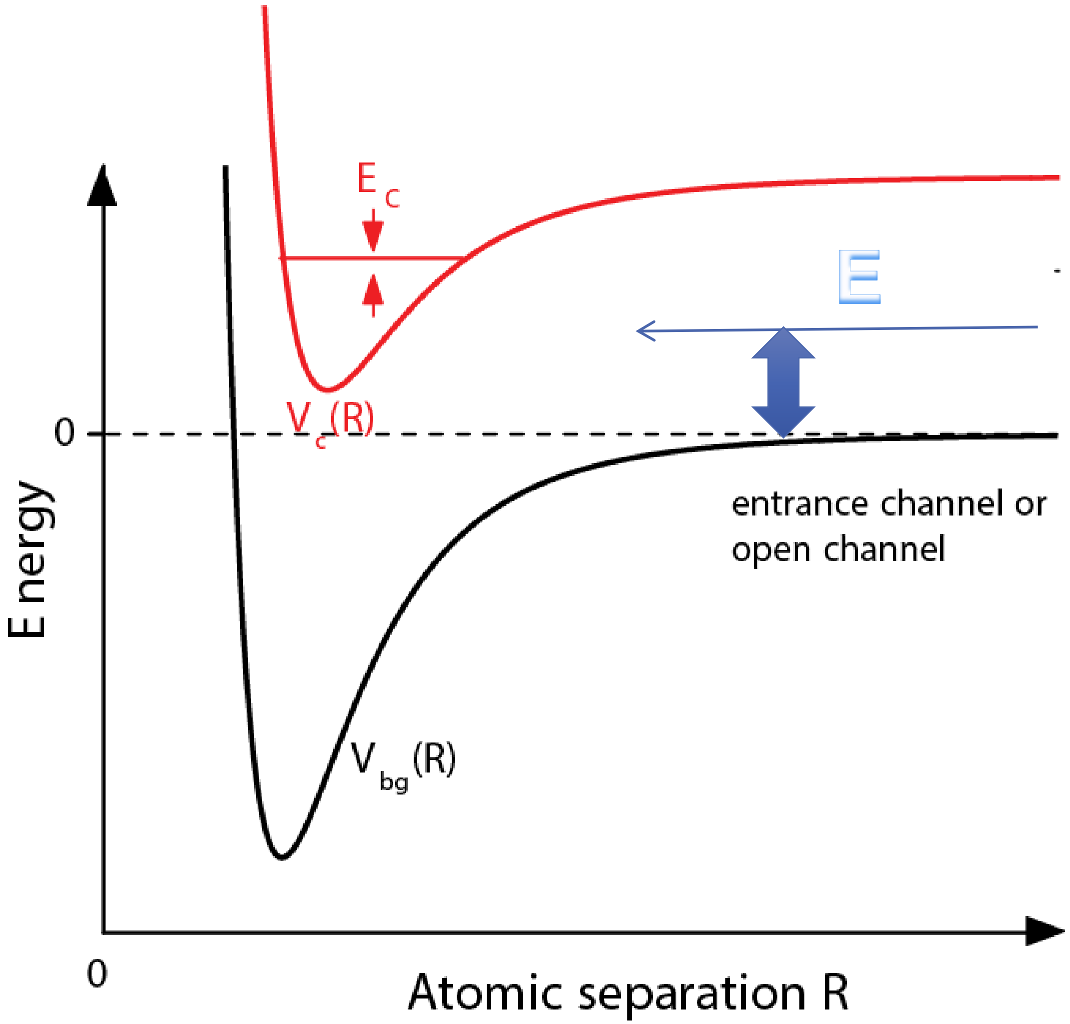
E c
E
0
V c (R)
entrance channel or
open channel
V bg (R)
E nergy
0
Atomic separation R

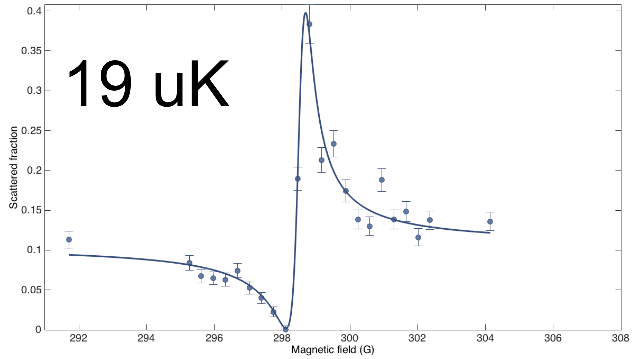
19 uK
Scattered fraction
Magnetic field (G)

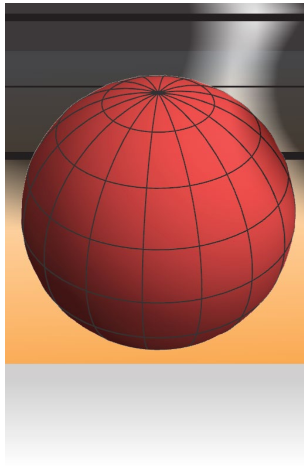

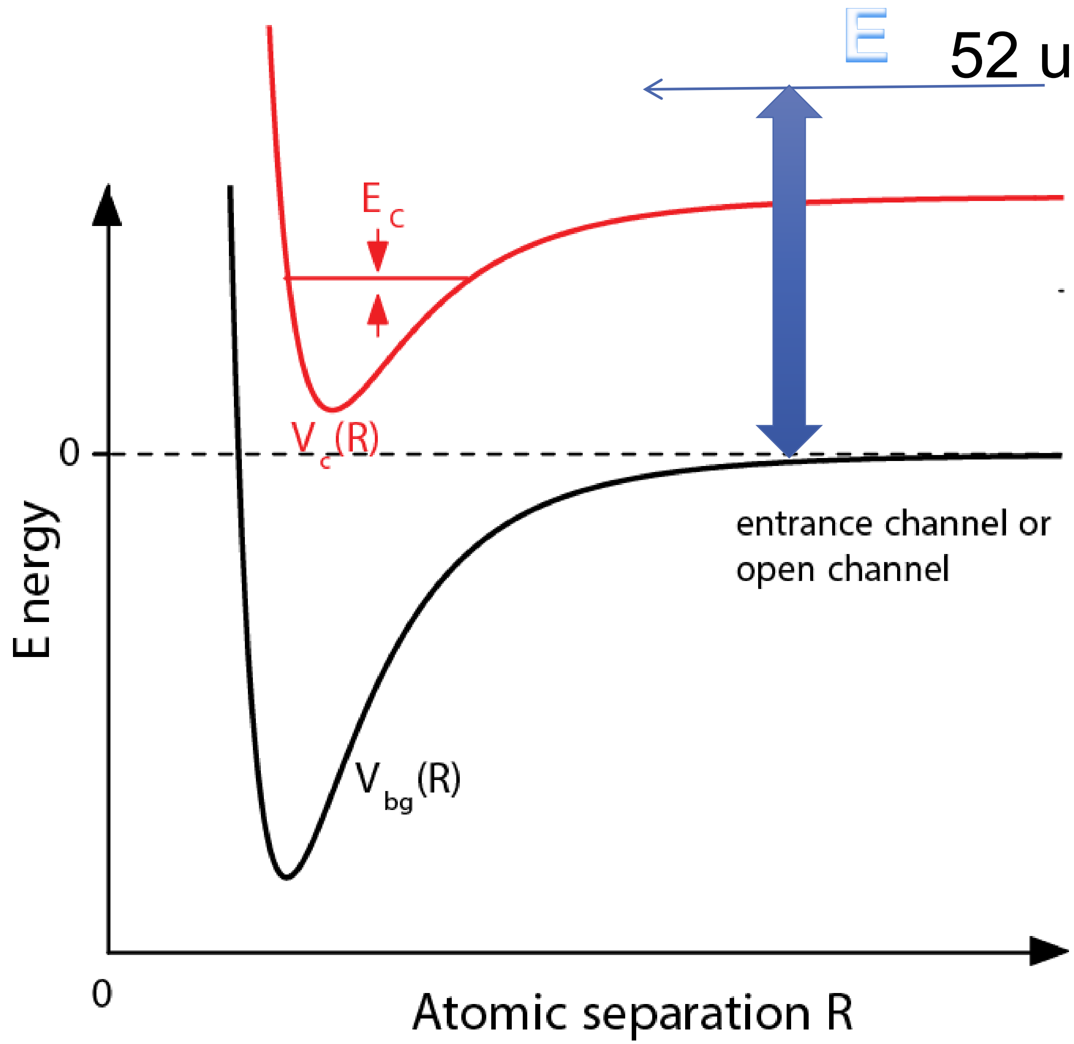
E
E c
V c (R)
0
E nergy
V bg (R)
entrance channel or
open channel
0
Atomic separation R

52 uK

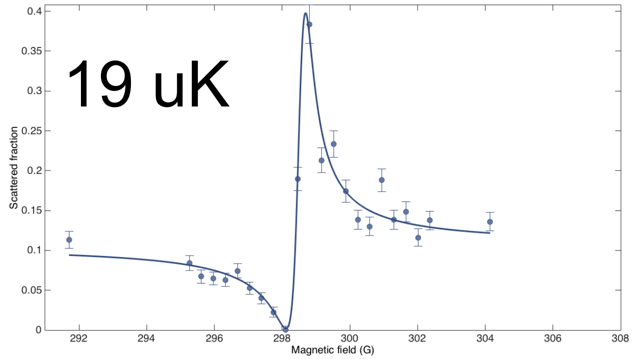
19 uK
Scattered fraction
Magnetic field (G)

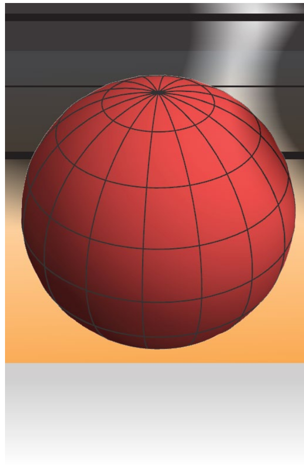

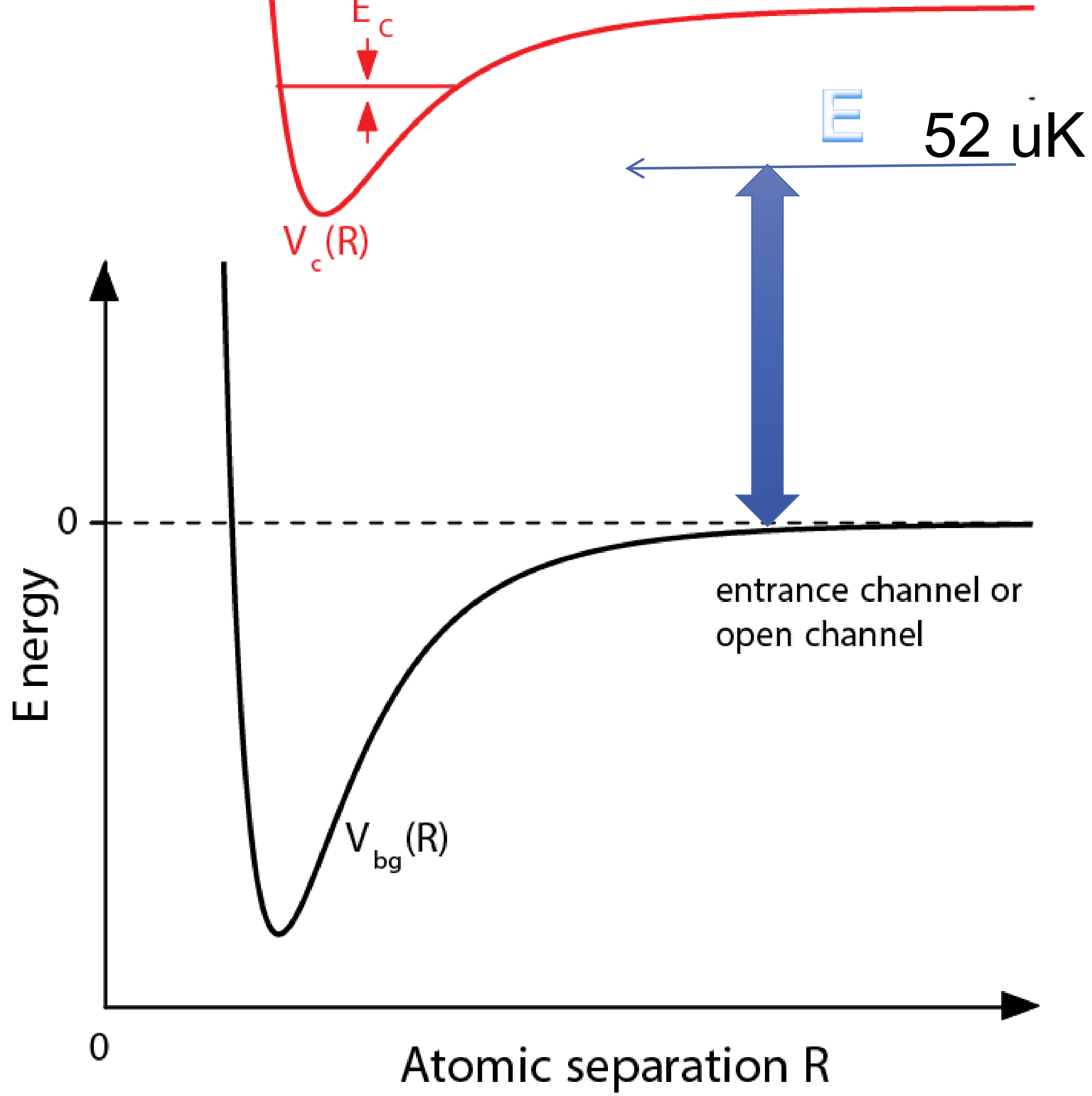
E C
V c (R)
E
52 uK
0
E nergy
entrance channel or
open channel
V bg (R)
0
Atomic separation R

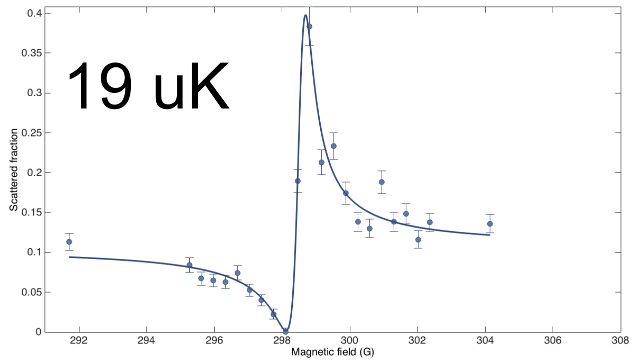
19 uK
Scattered fraction
Magnetic field (G)
0.4
0.35
0.3
0.25
0.2
0.15
0.1
0.05
0
292
294
296
298
300
302
304
306
308

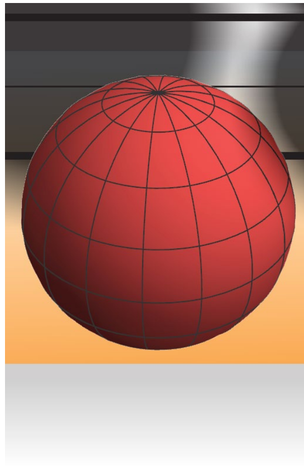

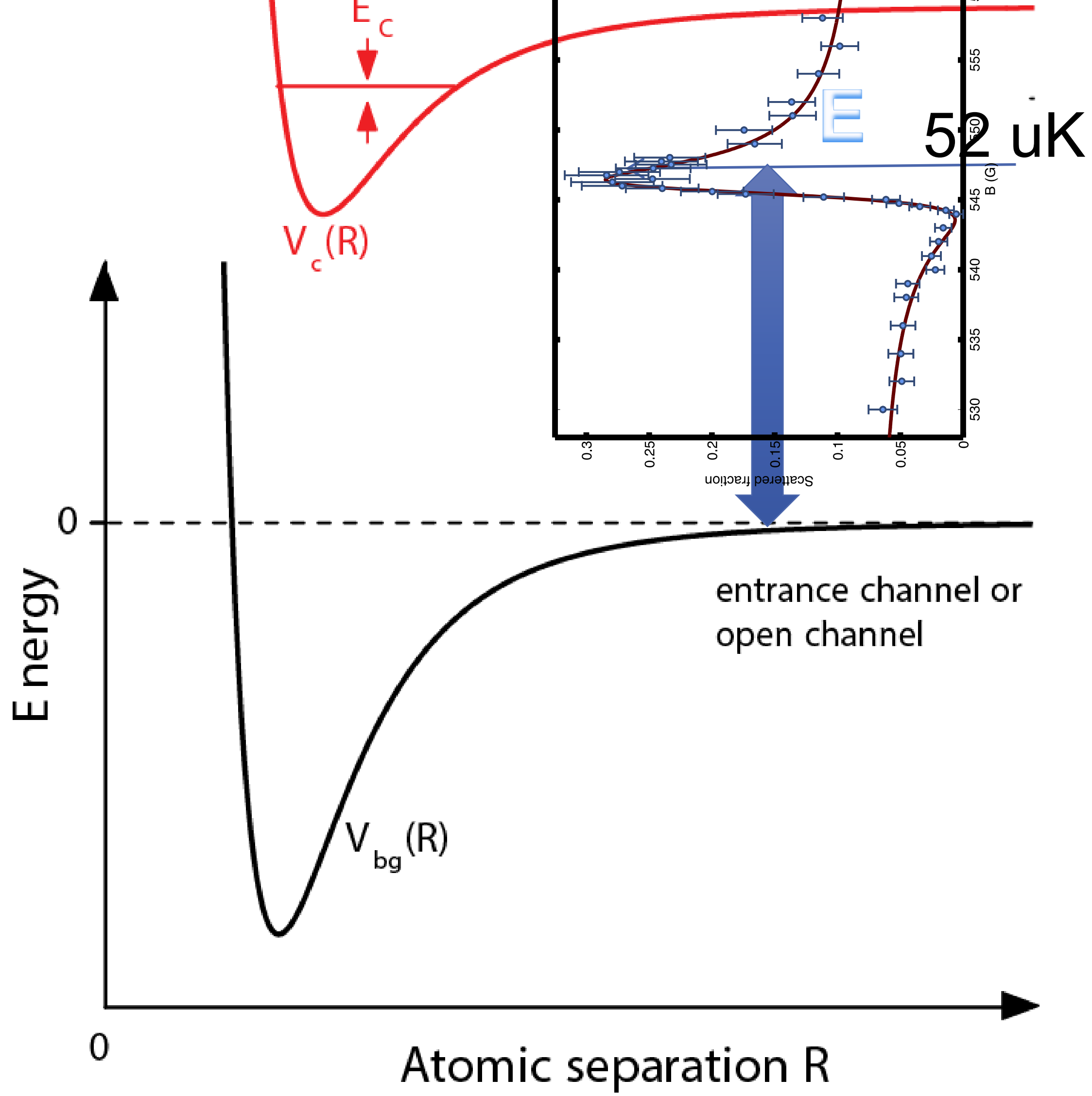
E c
V c (R)
52 uK
B (G)
Scattered fraction
0
Energy
entrance channel or
open channel
V bg (R)
0
Atomic separation R

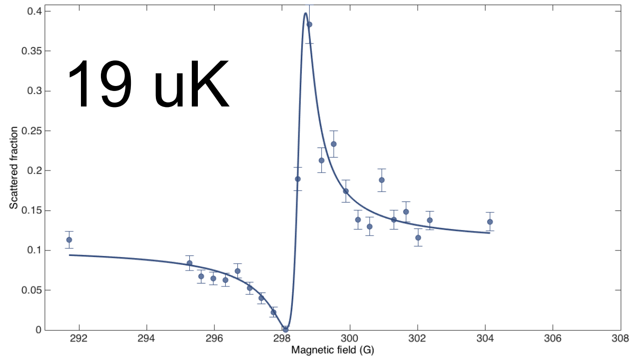
19 uK
Scattered fraction
Magnetic field (G)

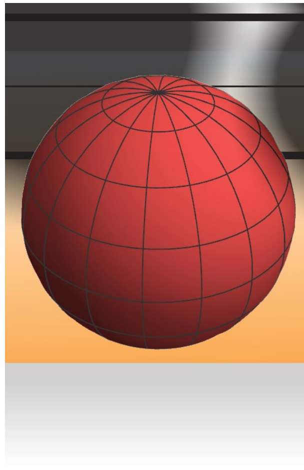

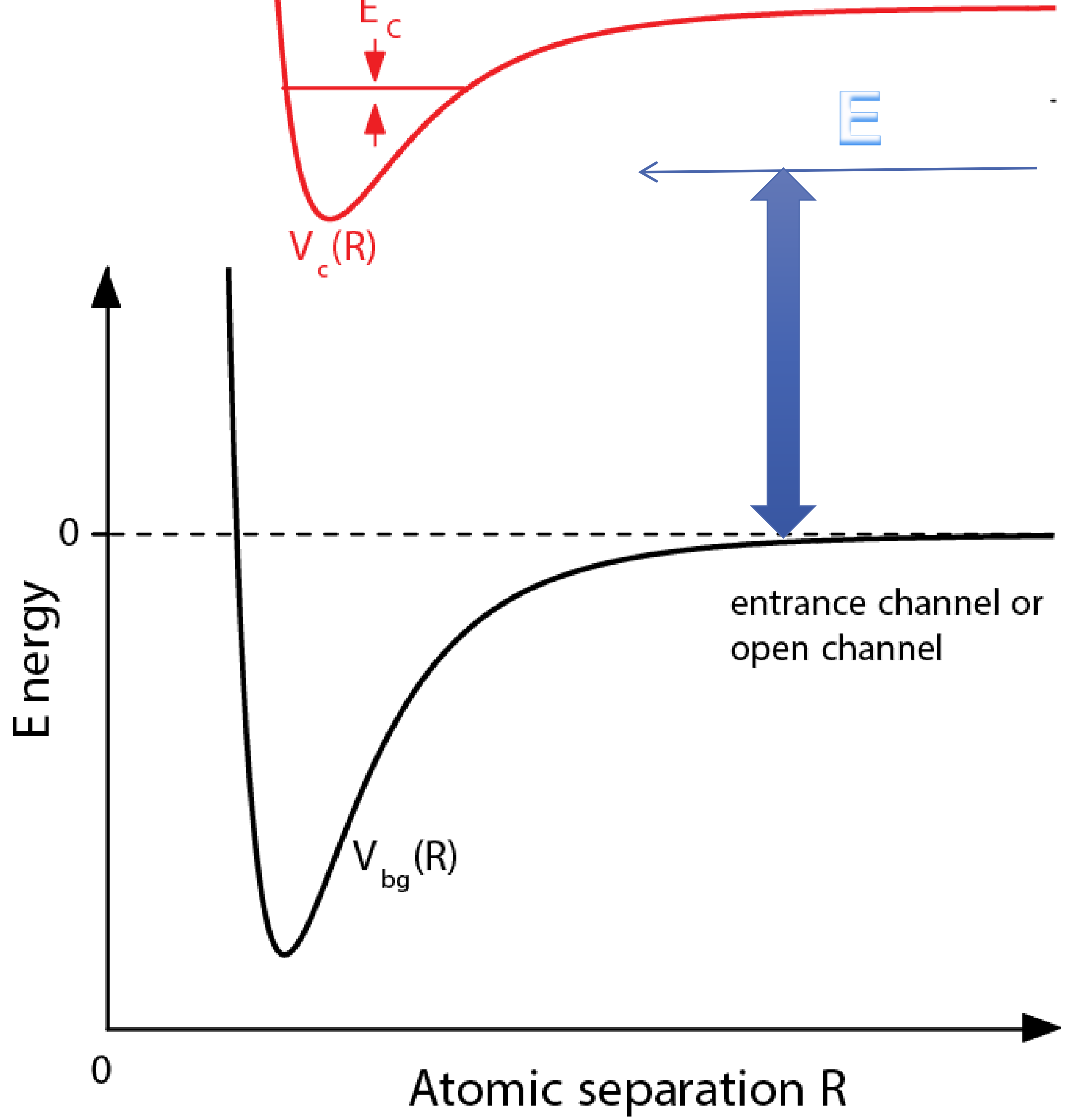

E c
V c (R)
E
0
Energy
V bg (R)
entrance channel or
open channel
0
Atomic separation R

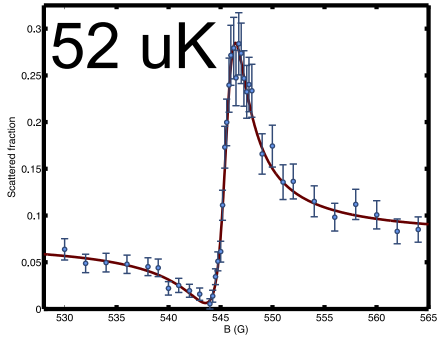

52 uK
Scattered fraction
B (G)

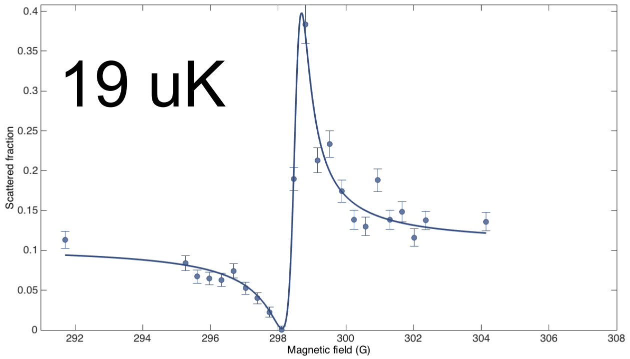

19 uK
Scattered fraction
Magnetic field (G)

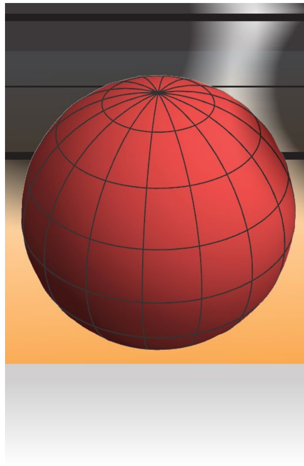

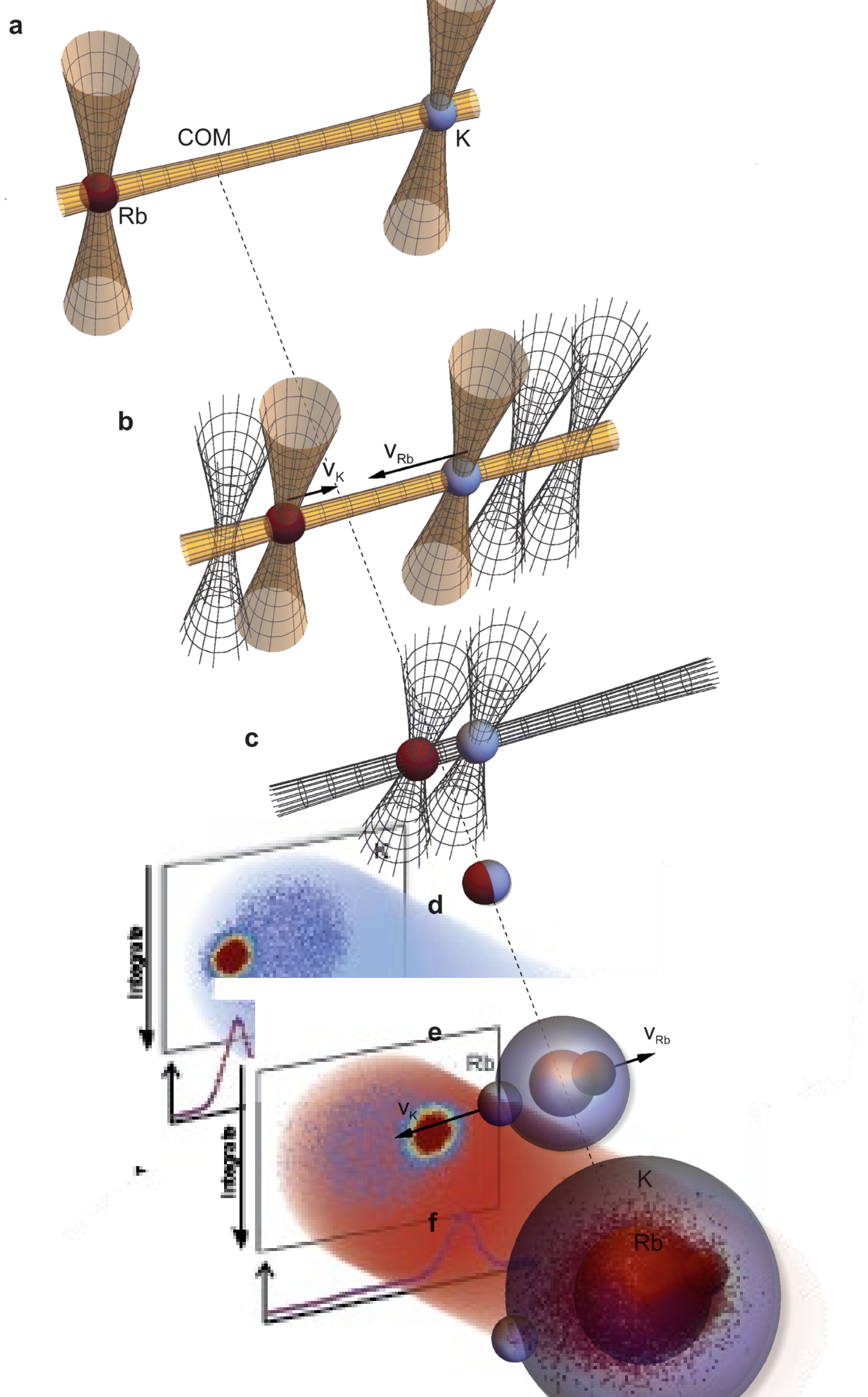
a
COM
K
Rb
b
v_K
v_{Rb}
c
d
e
v_{Rb}
Rb
v_K
K
Rb
f

$E/k_B = 52\ \mu K$

Beutler-Fano Line shape

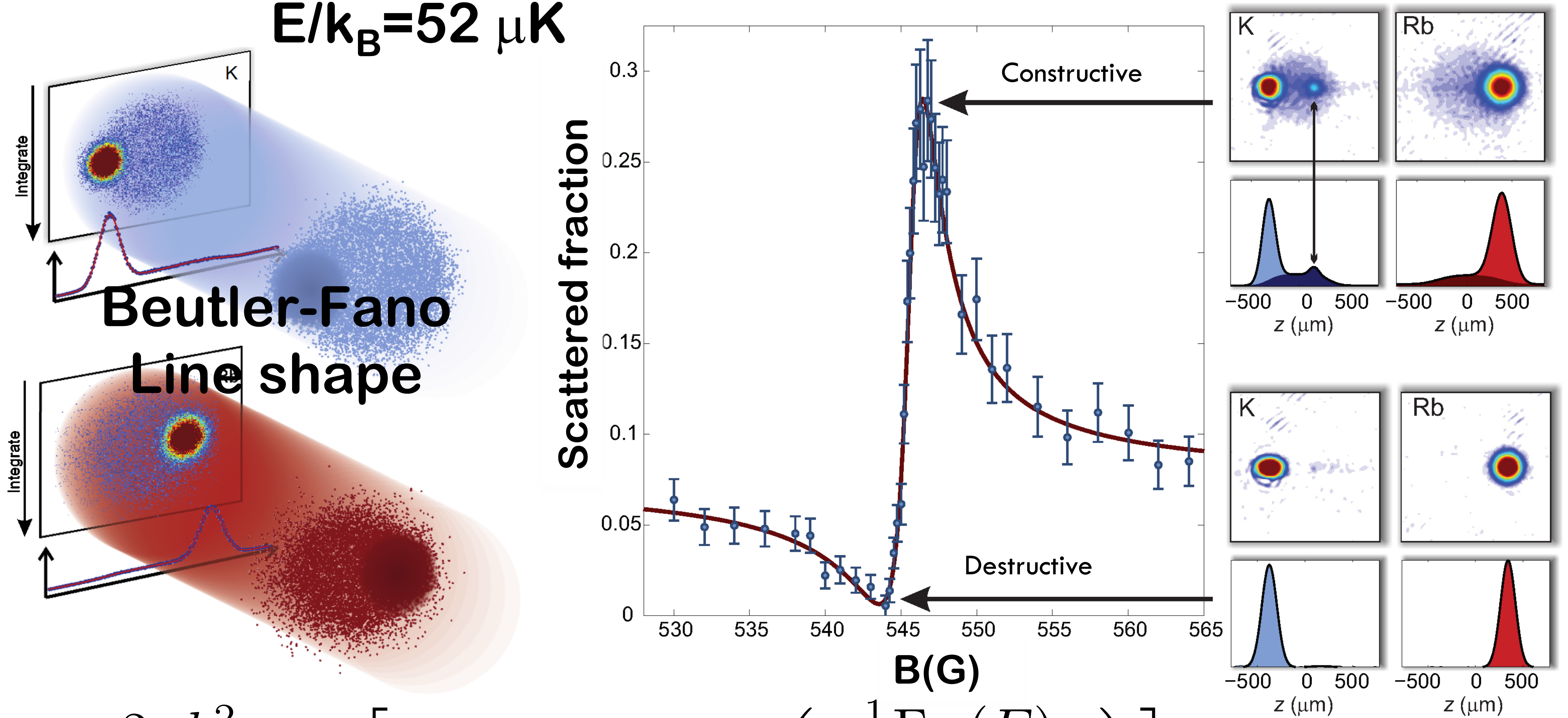

$$\sigma = \frac{2\pi\hbar^2}{mE}\sin^2\left[\delta_{\text{bg}}(E) + \tan^{-1}\left(\frac{\frac{1}{2}\Gamma_B(E)}{B - B_0(E)}\right)\right]$$

Record resonant B-field vs energy

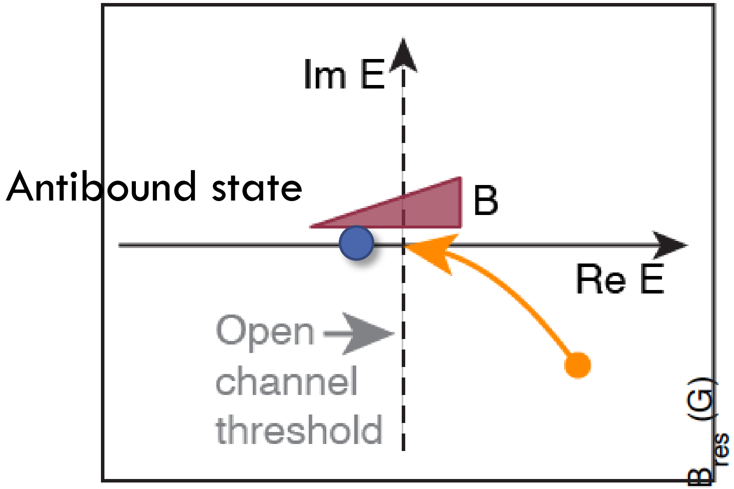

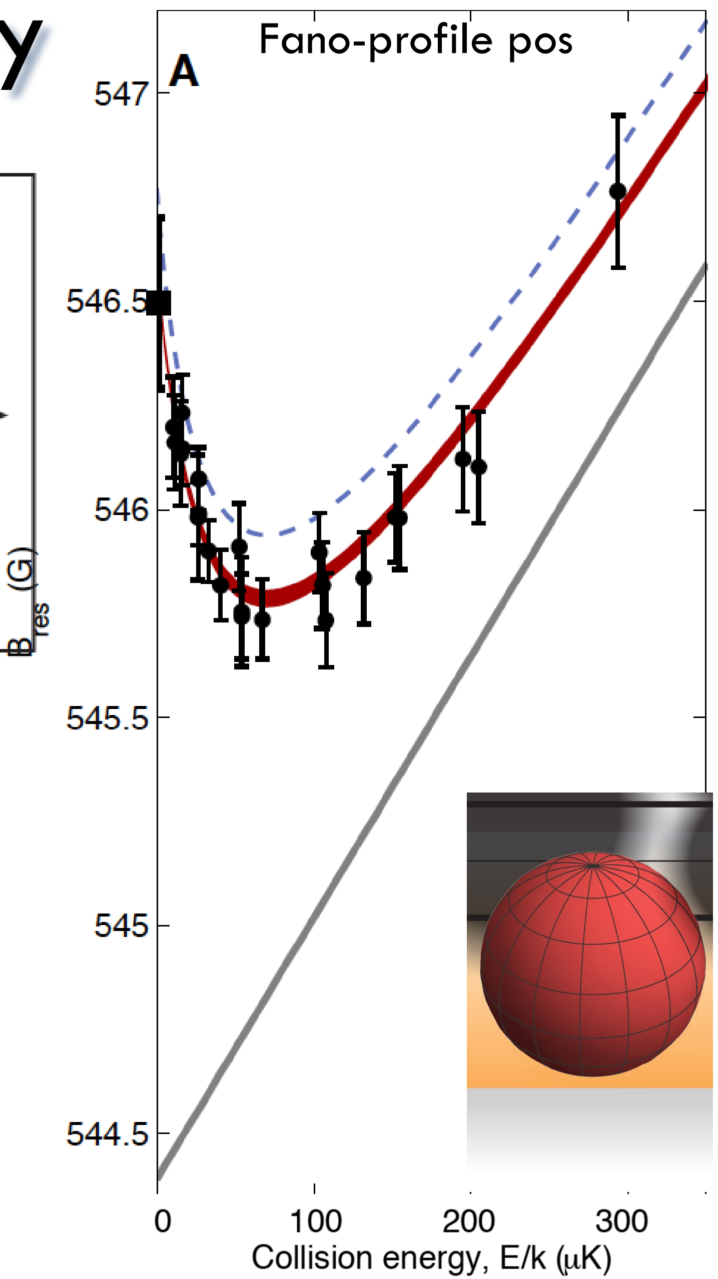

Record resonant B-field vs energy

Feshbach resonances with large background scattering length: Interplay with open-channel resonances

B. Marcelis, E. G. M. van Kempen, B. J. Verhaar, and S. J. J. M. F. Kokkelmans
Phys. Rev. A **70**, 012701 – Published 1 July 2

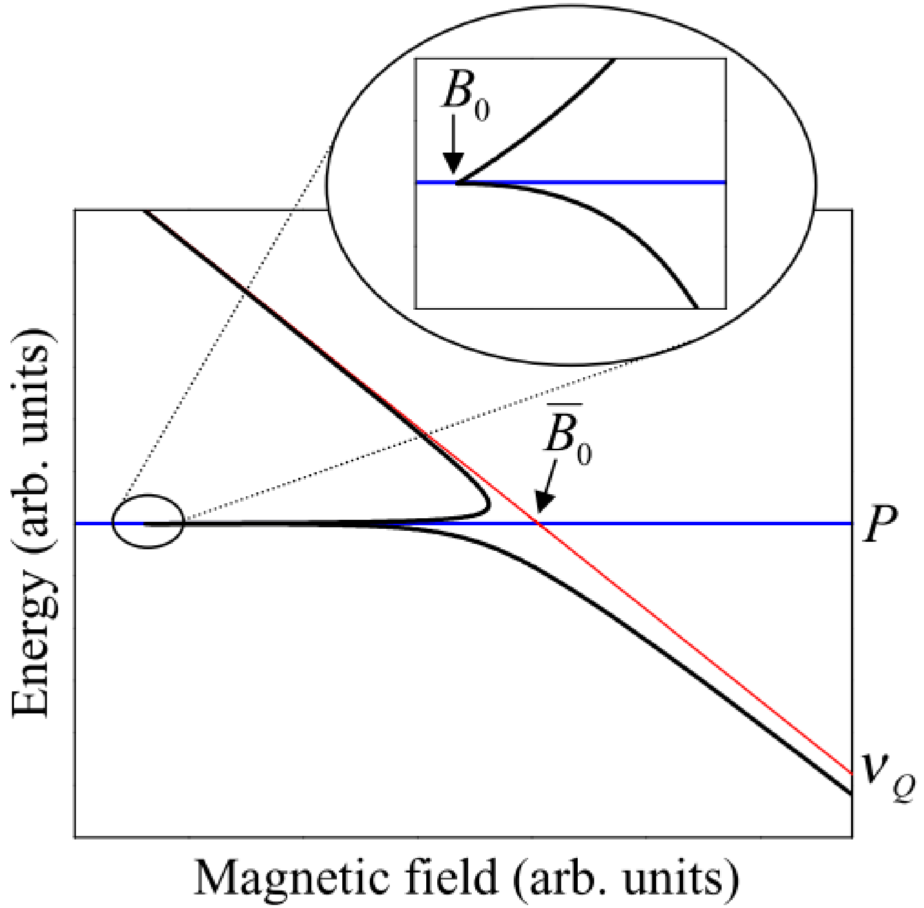

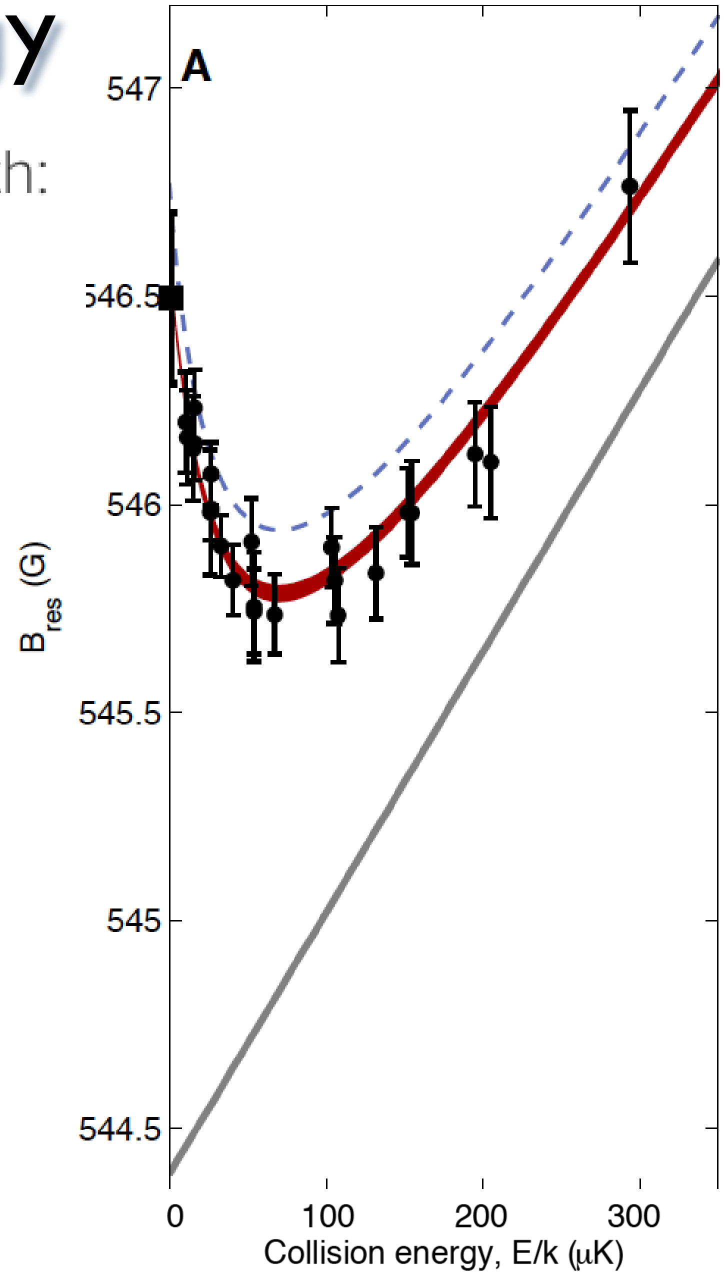

Record resonant B-field vs energy

Feshbach resonances with large background scattering lengtl
Interplay with open-channel resonances

B. Marcelis, E. G. M. van Kempen, B. J. Verhaar, and S. J. J. M. F. Kokkelmans
Phys. Rev. A **70**, 012701 – Published 1 July 2

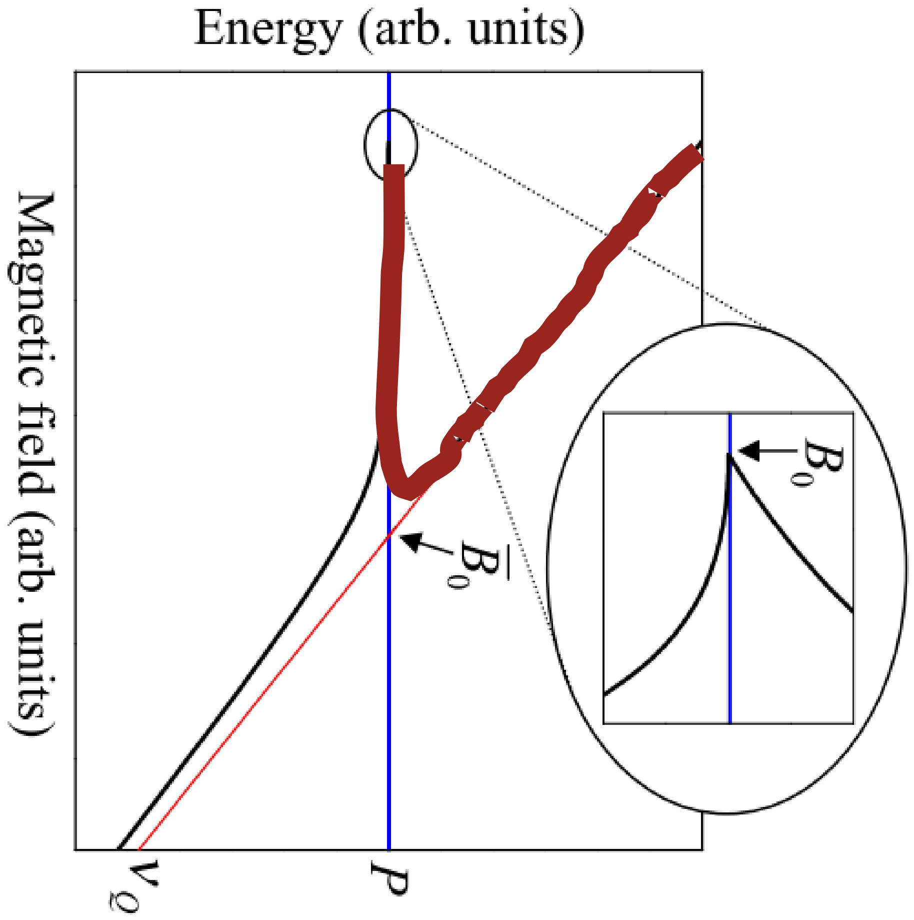

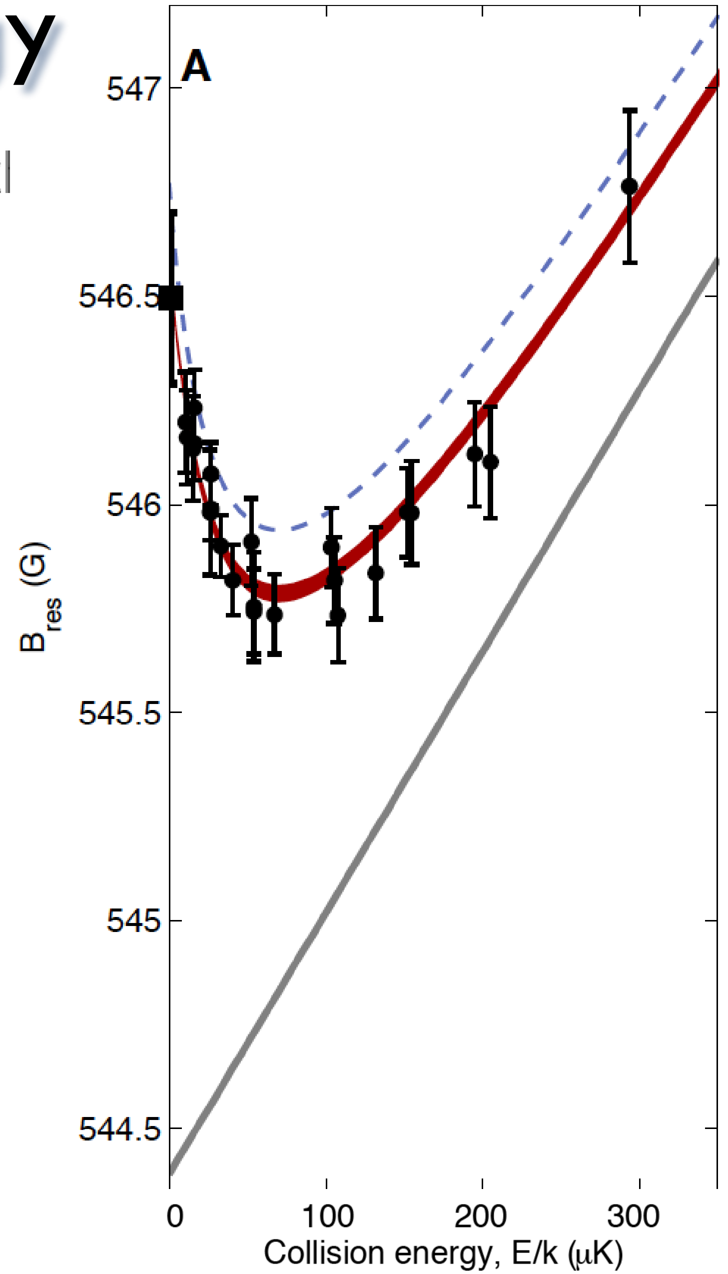

Caption: “Effect of virtual state on Feshbach resonance…”

Record resonant B-field vs energy

Antibound state (virtual state)

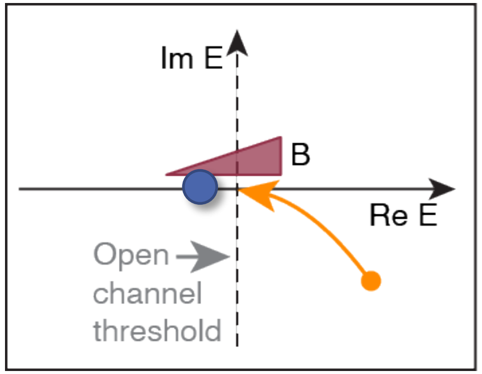

Bound state

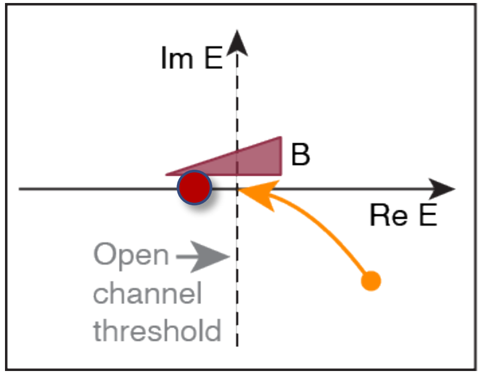

Prediction

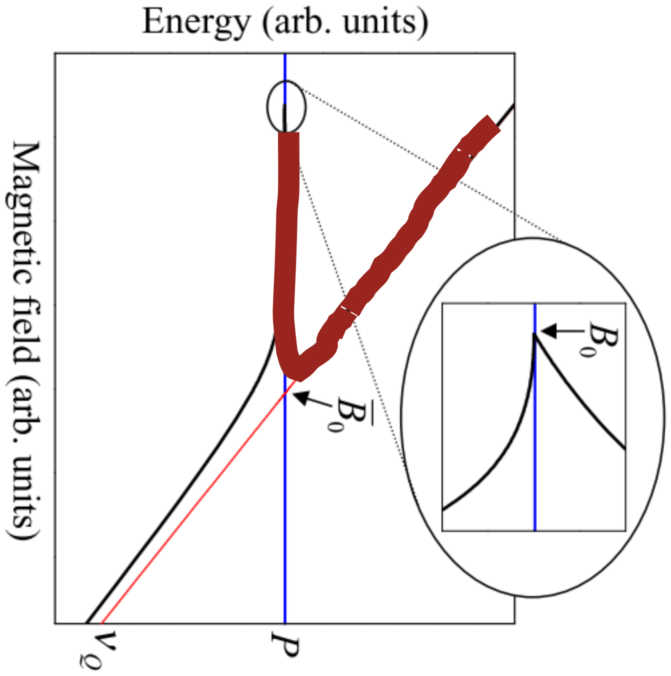

Experiment

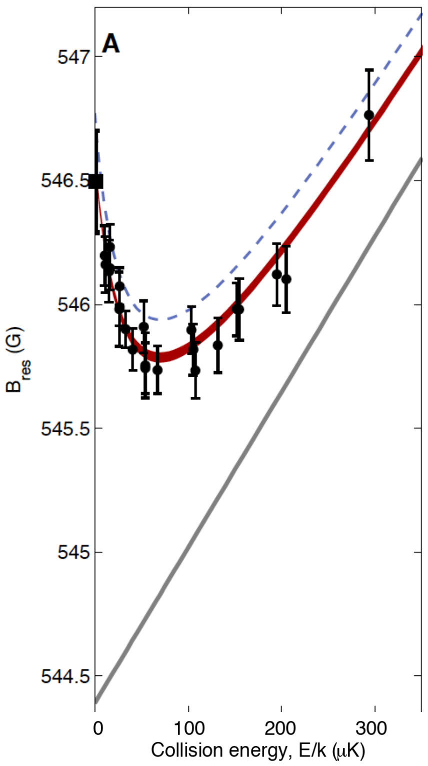

Prediction

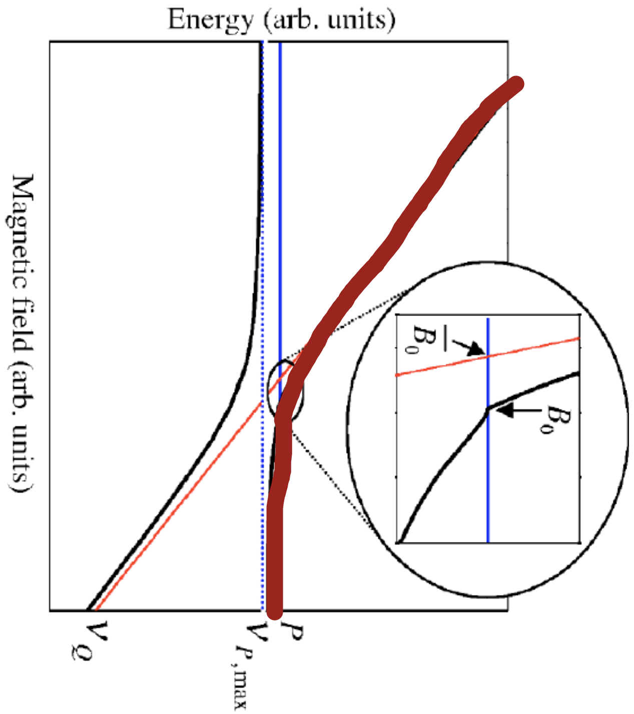

Monday Talk

Deep learning: alternative analysis tool

Benchmarked on the known nucleon-nucleon bound state
Given only the s-wave cross section, the origin of enhancement can be unambiguously identified.

DLBS, YI, TS, AH PRD 102 016024 (2020)
DLBS, YI, TS, AH Few-Body Syst. 62, 52 (2021)

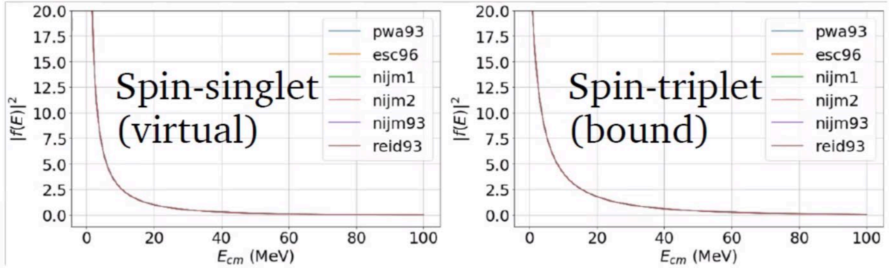

For near-threshold pole:

$$k\cot\delta \sim -1/a \text{ (constant)}$$

$$|f(k)|^{-2} = |k\cot\delta - ik|^2 \sim \frac{1}{a^2} + k^2$$

There is no way to discriminate a bound state pole enhancement with a virtual enhancement using only $|f(k)|^2$ on the scattering region.

In addition to the near-threshold pole, the S-matrix can have distant singularities on the unphysical sheet.

Use different (unitary, analytic) backgrounds to help DNN distinguish bound and virtual enhancements.

$$S(k) = \exp\left[2i\delta_{bg}(k)\right]\frac{k+i\gamma}{k-i\gamma}$$

$$(k)|^{-2} = |k\cot\delta - ik|^{2} \sim \frac{1}{a^2} + k^2$$

There is no way to discriminate a bound state pole enhancement with a virtual enhancement using only $|f(k)|^2$ on the scattering region.

Record resonant B-field vs energy

Antibound state
(virtual state)

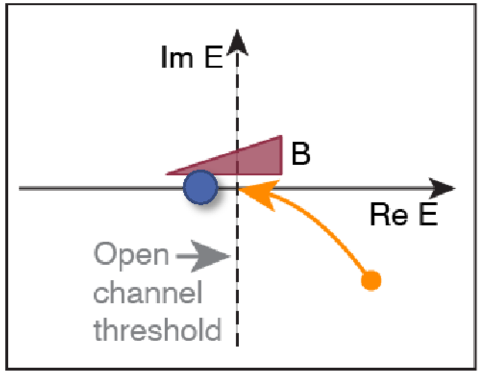

Bound state

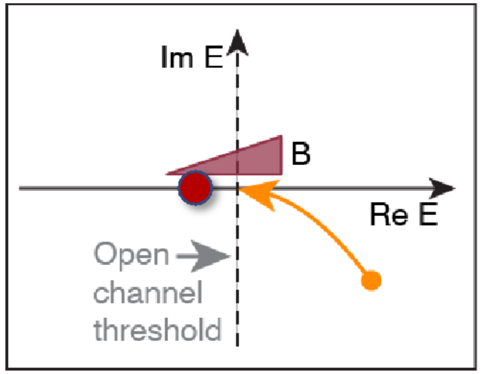

Prediction

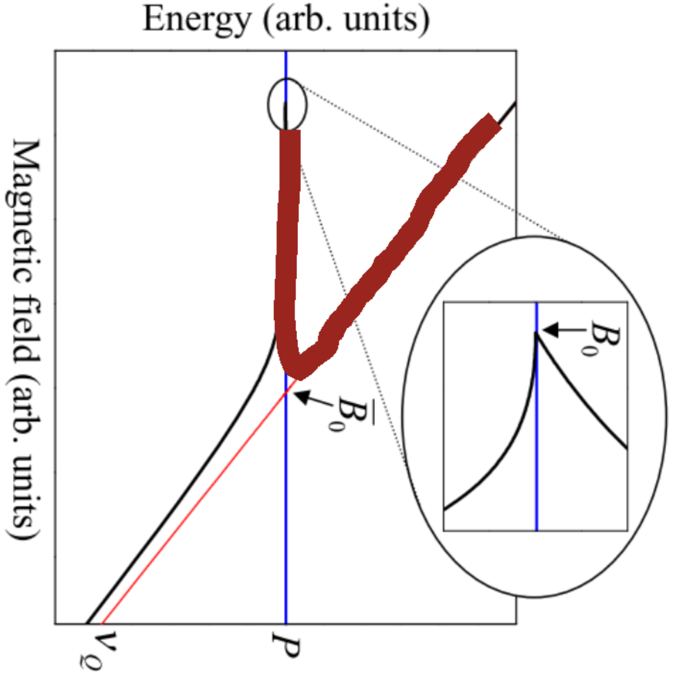

Experiment

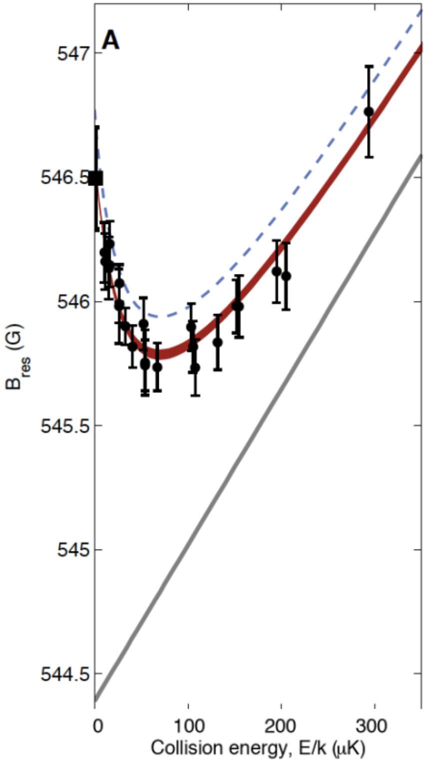

Prediction

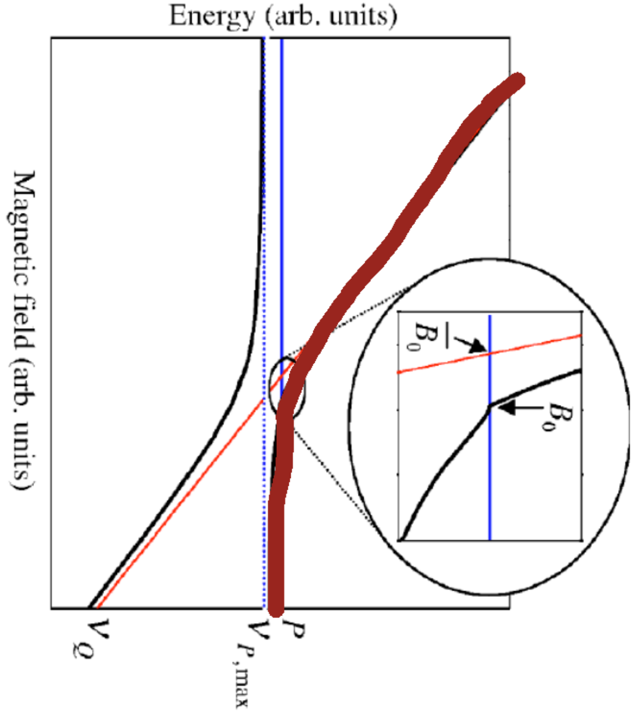

PHYSICAL REVIEW A 106, 023303 (2022)

Microscopy of an ultranarrow Feshbach resonance using a laser-based atom collider: A quantum defect theory analysis

Matthew Chilcott,[1] James F. E. Croft,[1] Ryan Thomas,[1,2] and Niels Kjærgaard[1,*]

[1]*Department of Physics, Quantum Science Otago, and Dodd-Walls Centre for Photonic and Quantum Technologies, University of Otago, Dunedin 9016, New Zealand*

[2]*Department of Quantum Science and Technology, Research School of Physics, The Australian National University, Canberra 2601, Australia*

(Received 7 February 2022; accepted 9 June 2022; published 4 August 2022)

We employ a quantum defect theory framework to provide a detailed analysis of the interplay between a magnetic Feshbach resonance and a shape resonance in cold collisions of ultracold ^{87}Rb atoms as captured in recent experiments using a laser-based collider [M. Chilcott *et al.*, Phys. Rev. Research 3, 033209 (2021)]. By exerting control over a parameter space spanned by both collision energy and magnetic field, the width of a Feshbach resonance can be tuned over several orders of magnitude. We apply a quantum defect theory specialized for ultracold atomic collisions to fully describe of the experimental observations. While the width of a Feshbach resonance generally increases with collision energy, its coincidence with a shape resonance leads to a significant additional boost. By conducting experiments at a collision energy matching the shape resonance and using the shape resonance as a magnifying lens, we demonstrate a feature broadening to a magnetic width of 8 G compared to a predicted Feshbach resonance width much less than 0.1 mG.

DOI: 10.1103/PhysRevA.106.023303

Revisit 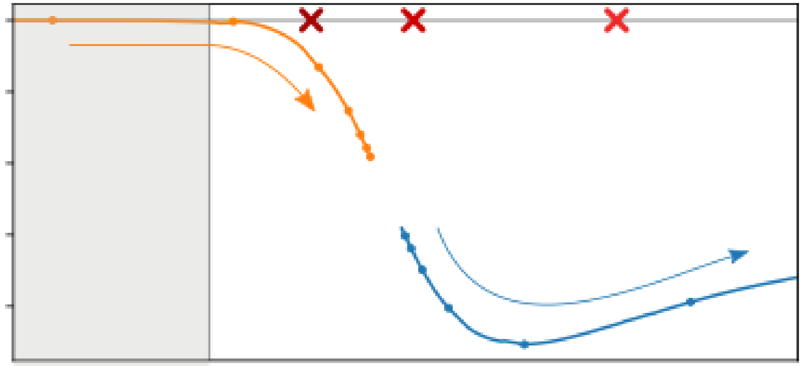 in MQDT framework

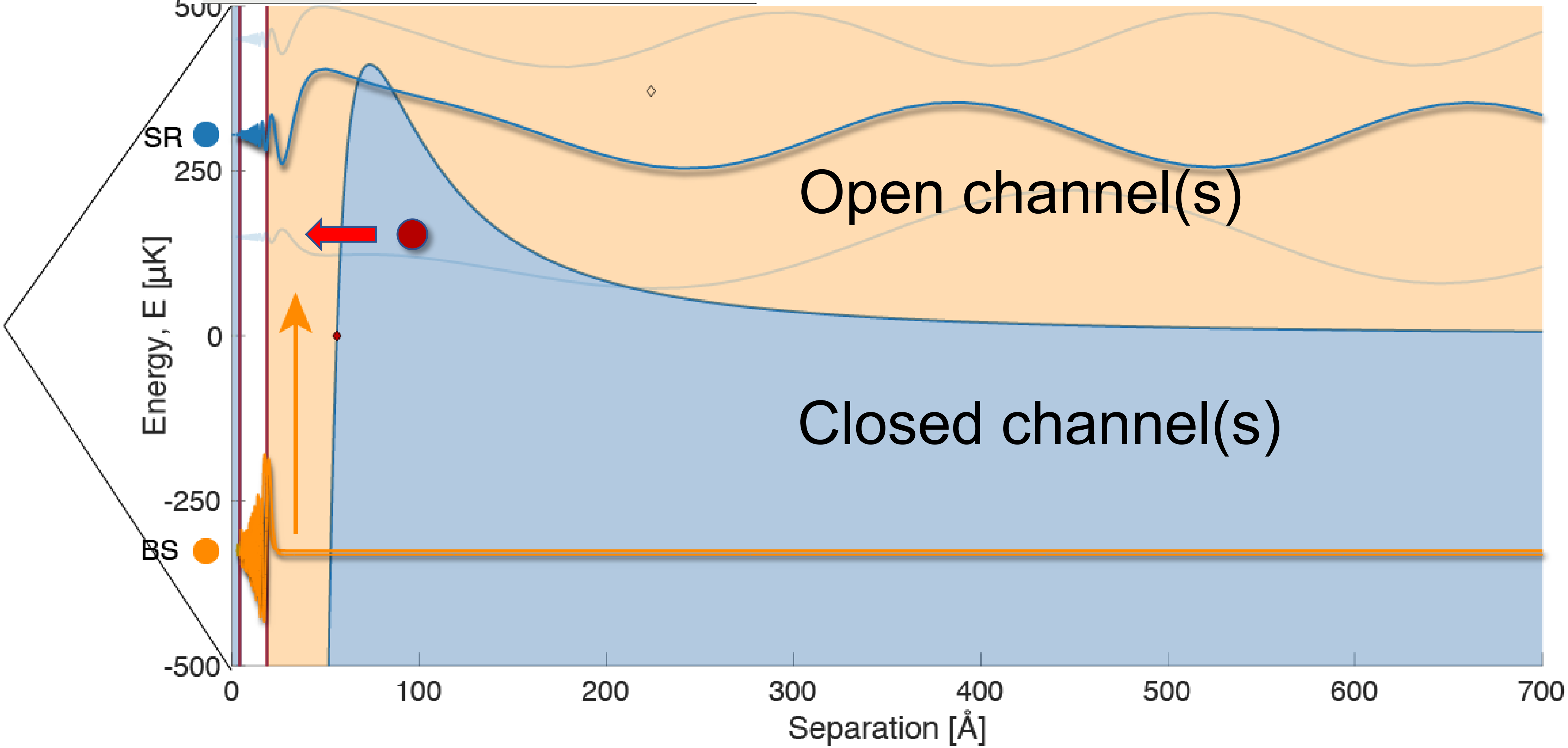

Revisit 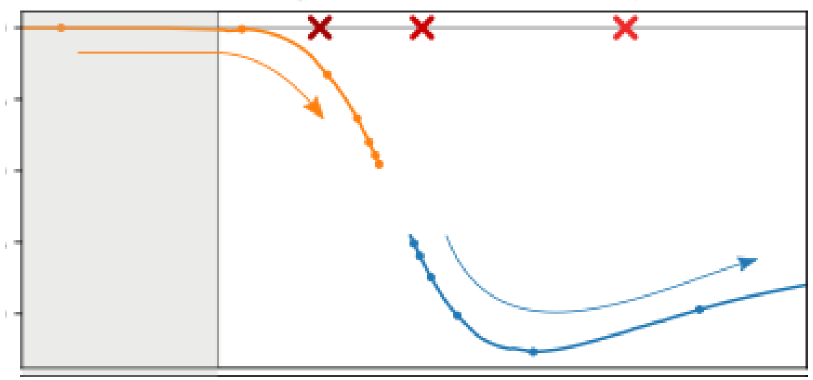 in MQDT framework

- Things only get complicated at short range
- Complicated coupled multichannel short-range interaction can be captured by a single **energy-independent** quantity

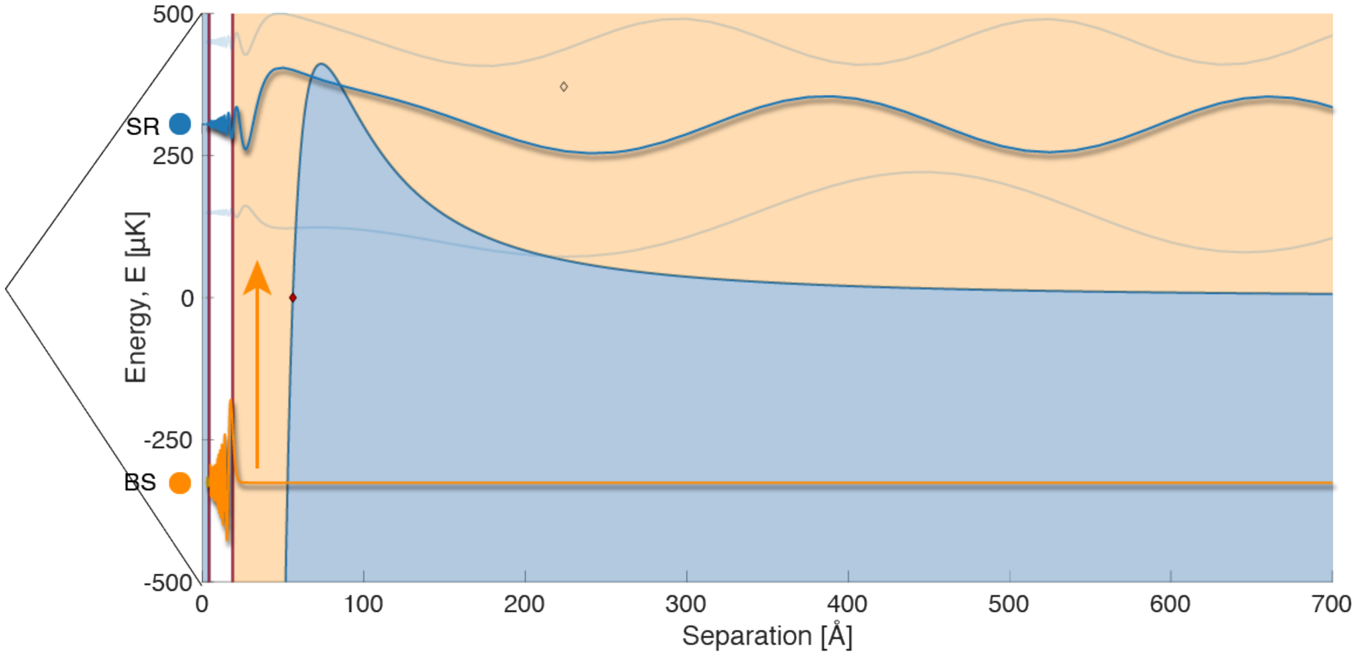

unlocks QDT's use of only the long-range vdW potential

Quantum defect theory framework

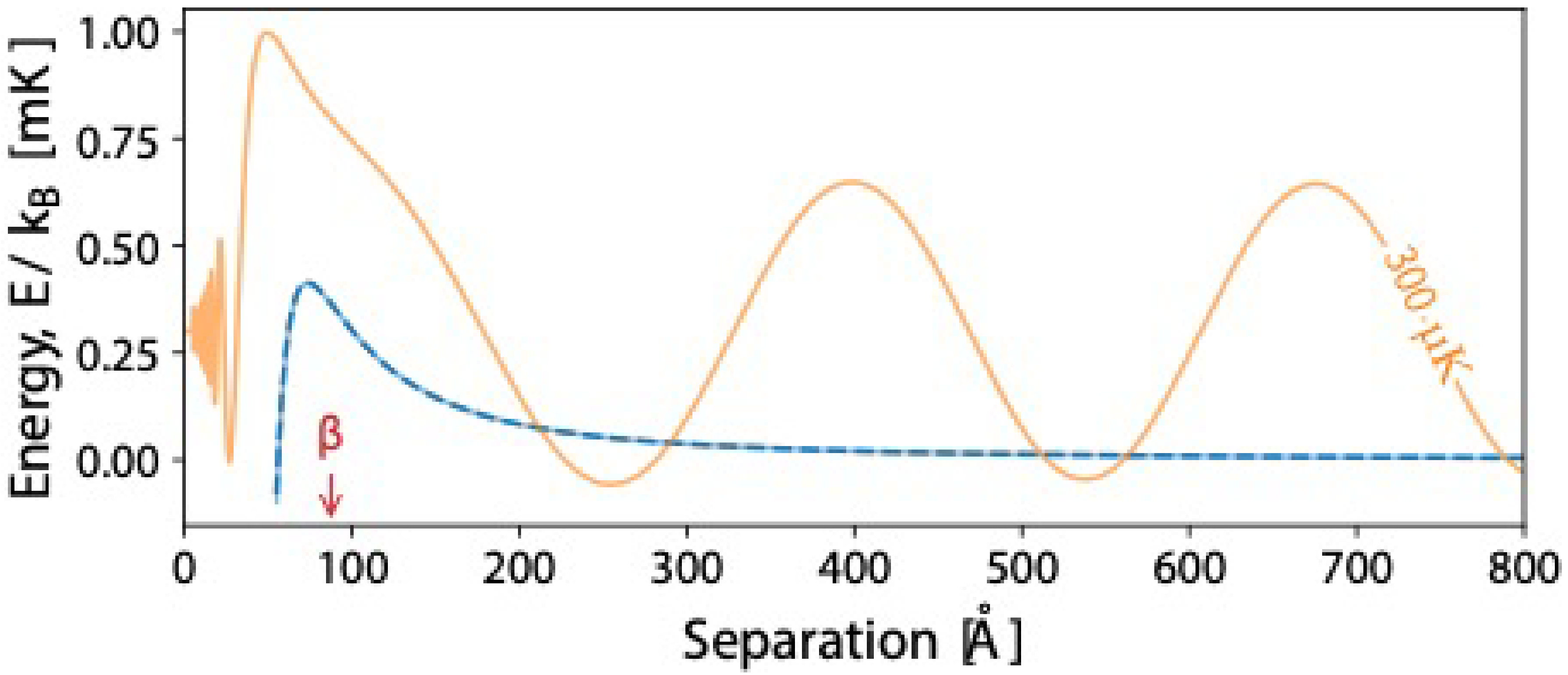

Sine at long range (phase shifted)

Phase shift with respect to free space

$$S_0(k) = e^{2i\delta_0(k)}$$

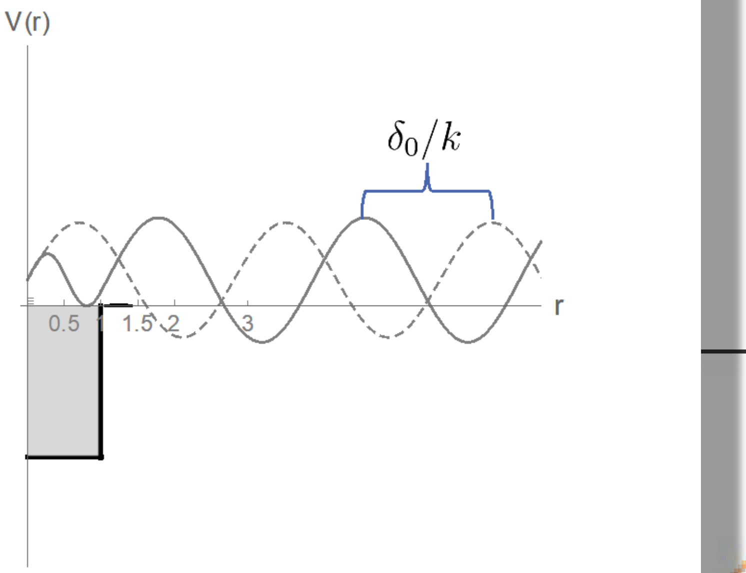

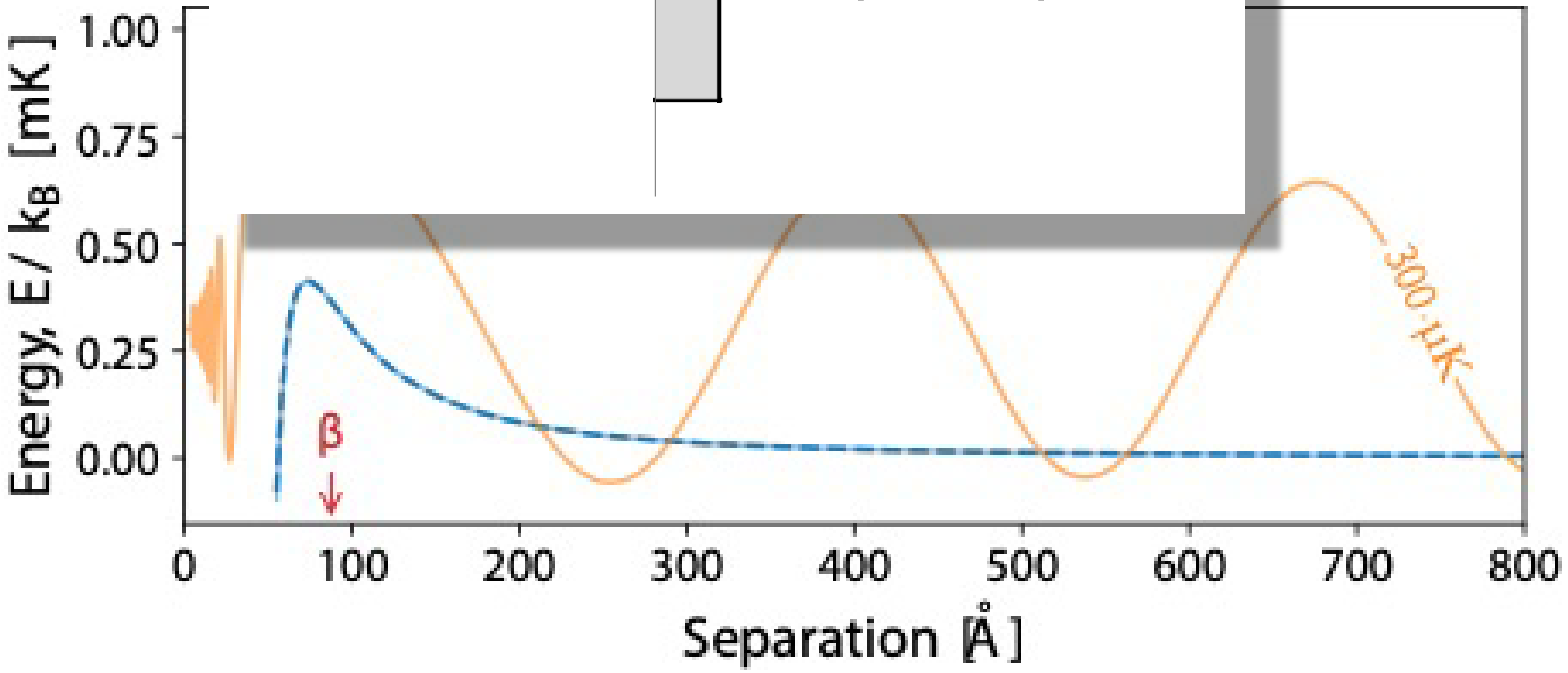

Increasing energy: faster sine at long range

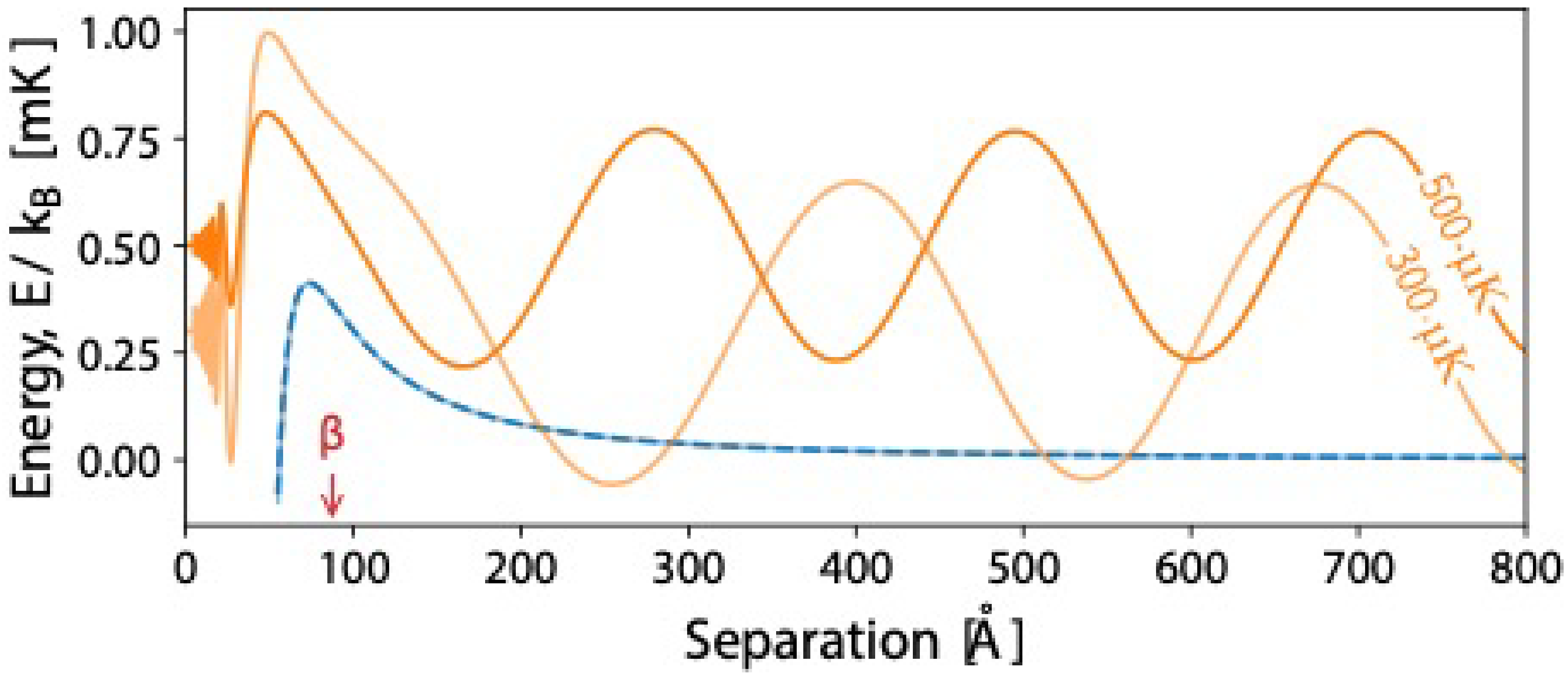

Increasing energy: faster sine at long range

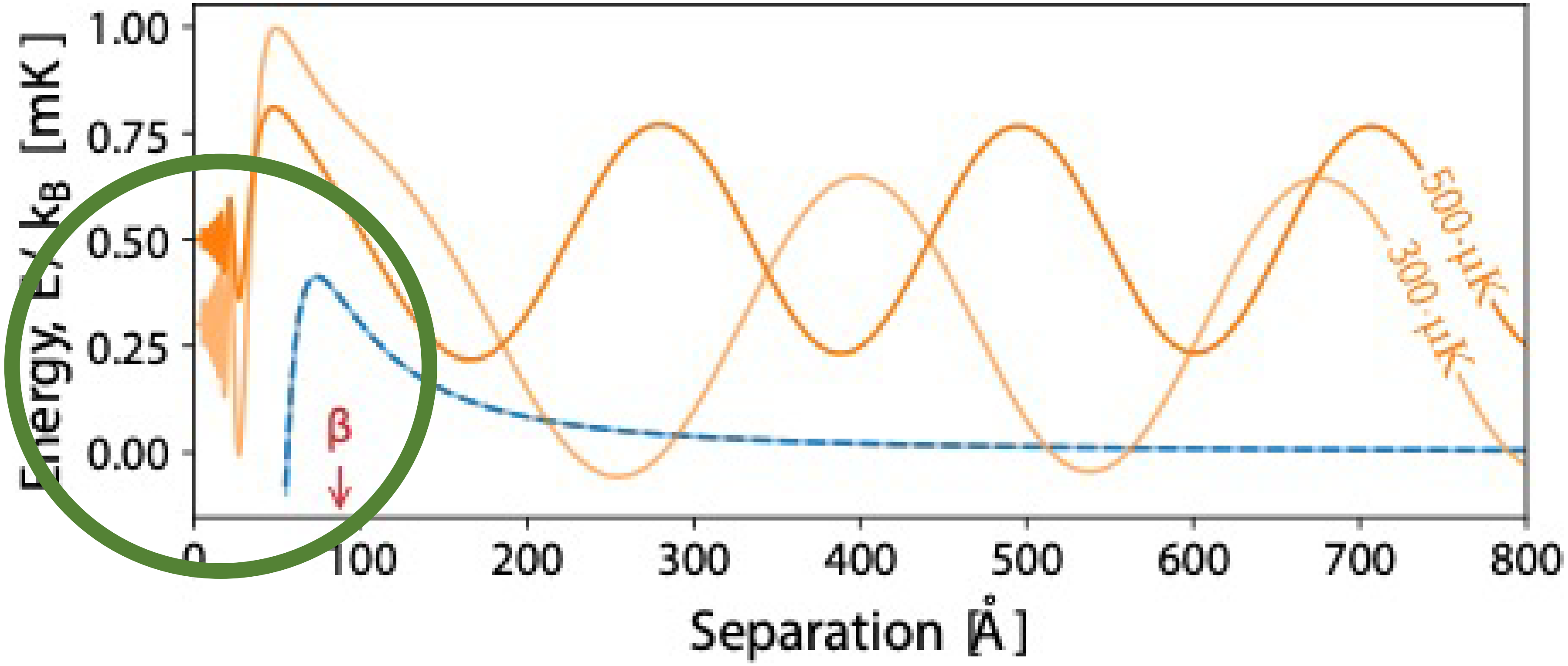

What about short range where well is VERY deep?

Short range where well is VERY deep: Wave function looks the same!

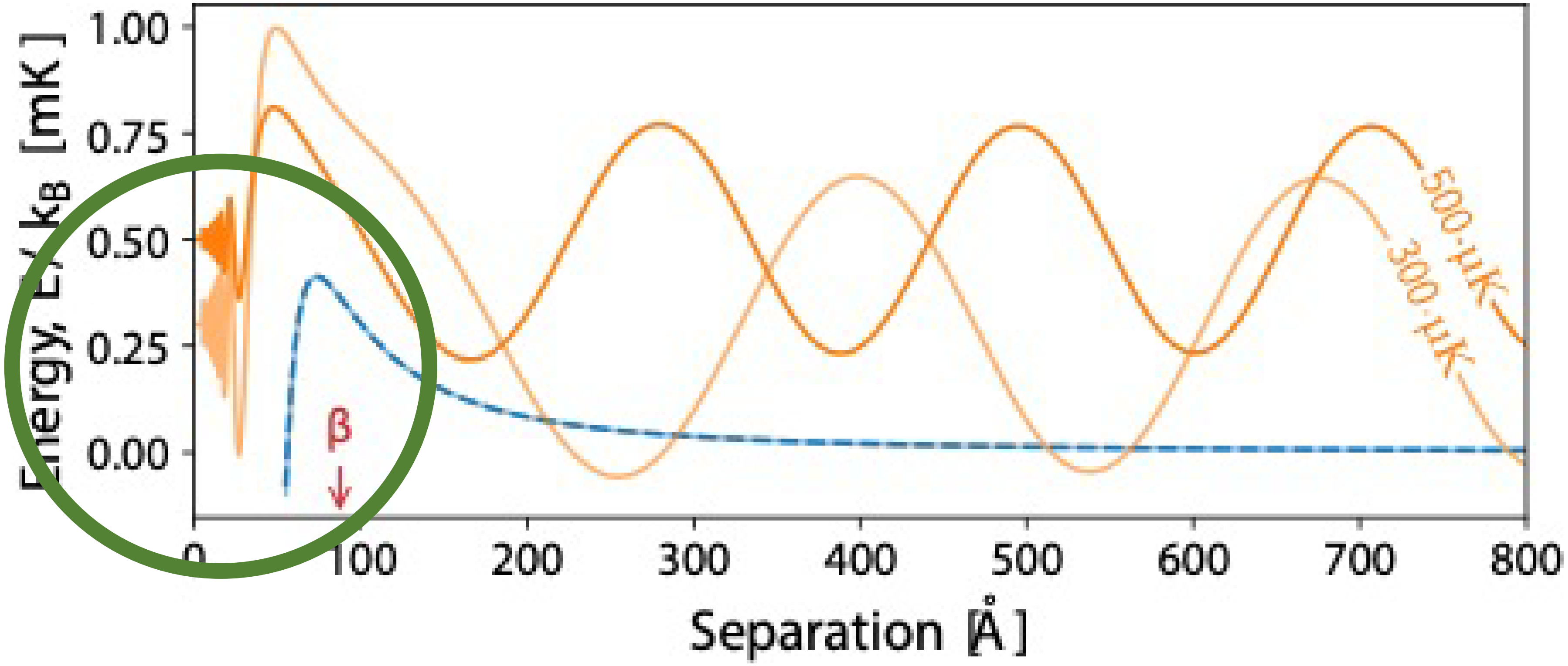

Short range where well VERY deep: Wave function looks the same!

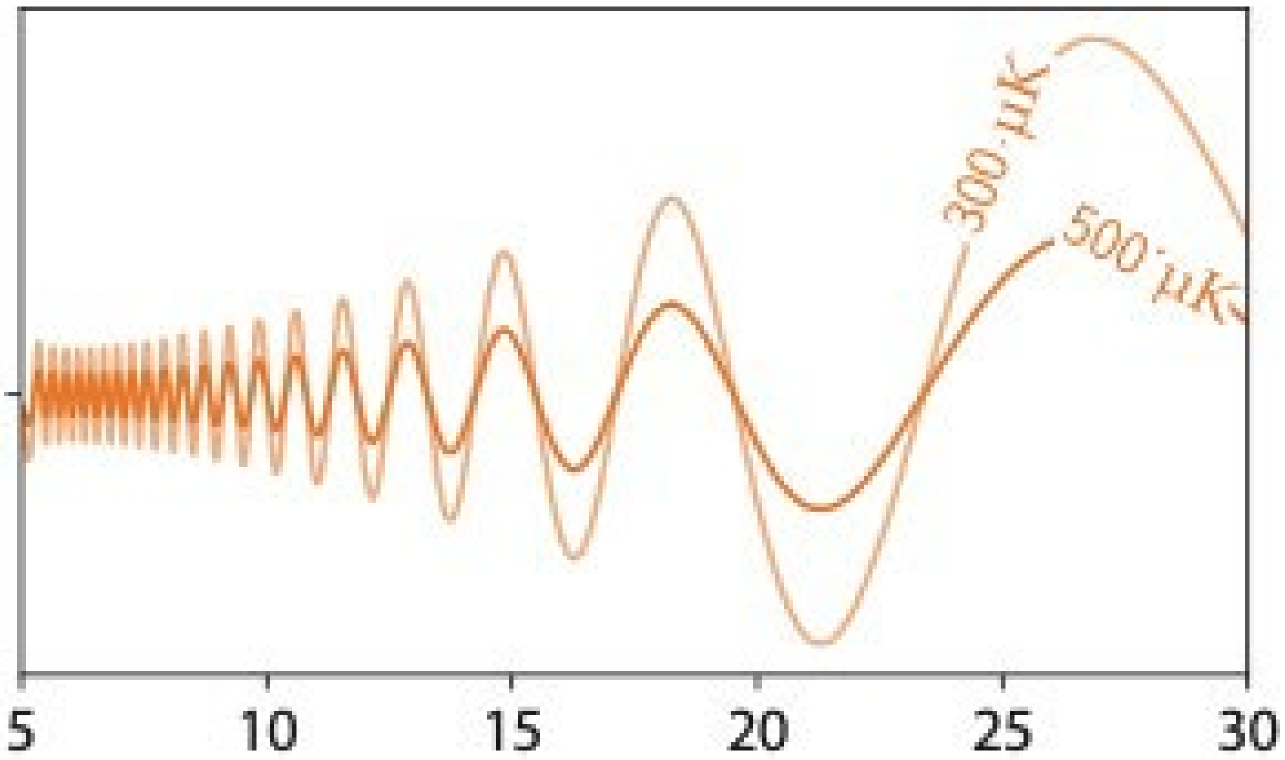

Quantum defect theory framework

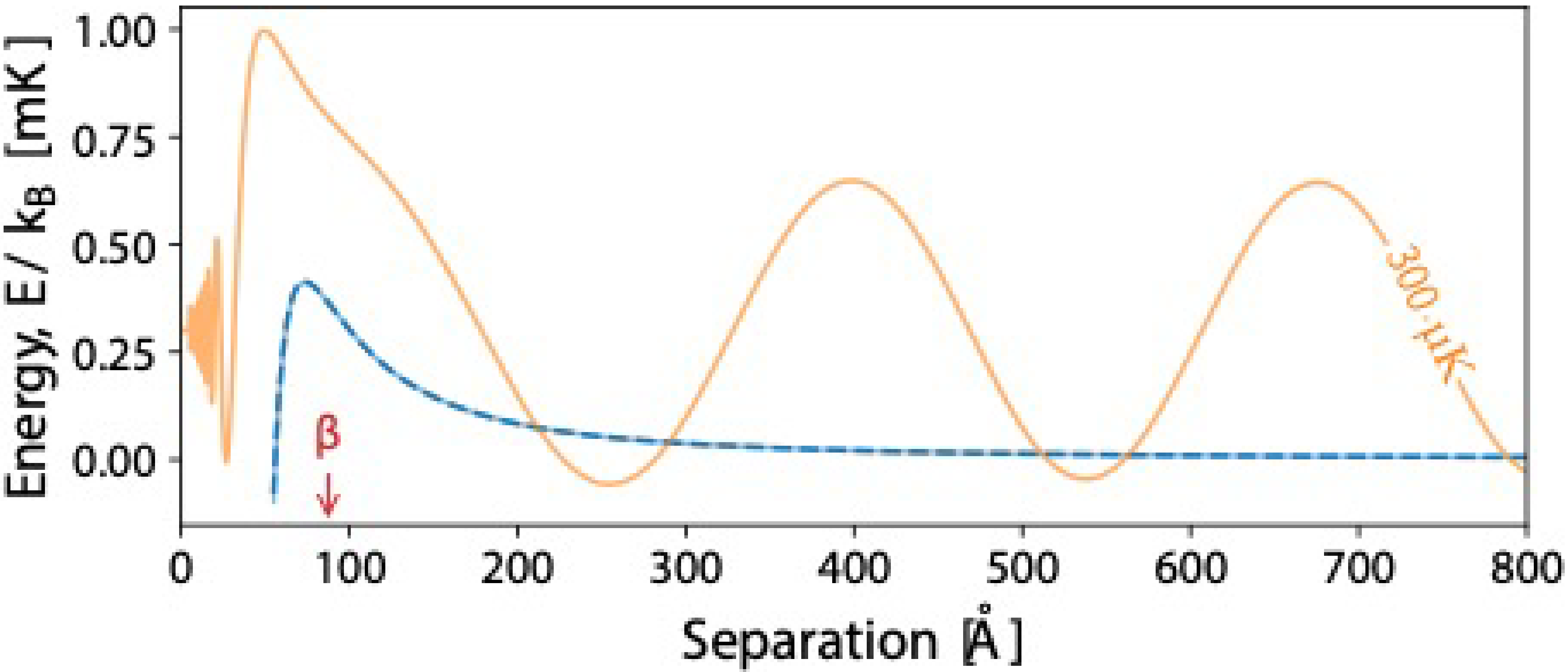

Solution linear combination

$$u_1(R) = c_1 f_1(R) + c_2 g_1(R)$$

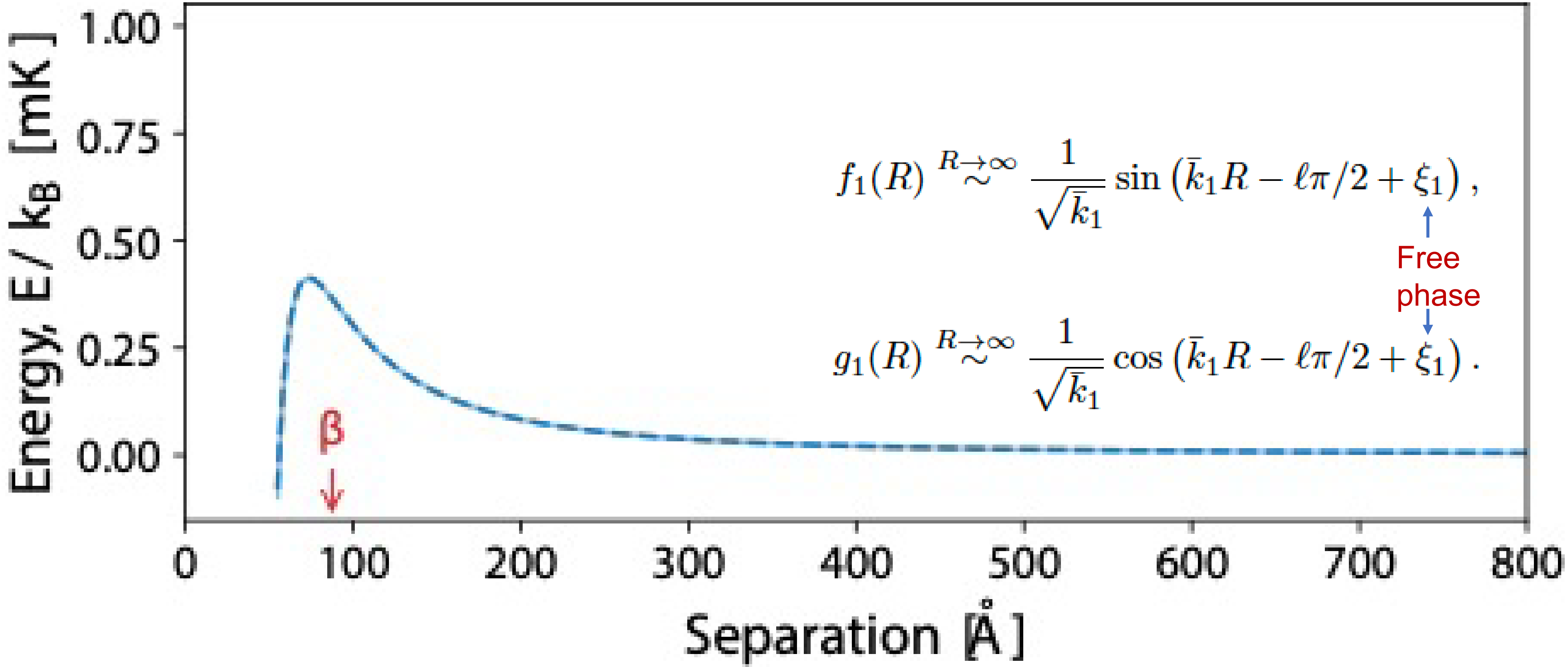

$$f_1(R) \overset{R\to\infty}{\sim} \frac{1}{\sqrt{\bar{k}_1}} \sin\left(\bar{k}_1 R - \ell\pi/2 + \xi_1\right),$$

$$g_1(R) \overset{R\to\infty}{\sim} \frac{1}{\sqrt{\bar{k}_1}} \cos\left(\bar{k}_1 R - \ell\pi/2 + \xi_1\right).$$

Solution linear combination

$$u_1(R) = c_1 f_1(R) + c_2 g_1(R)$$

$$u_1(R) = \hat{c}_1 \hat{f}_1(R) + \hat{c}_2 \hat{g}_1(R)$$

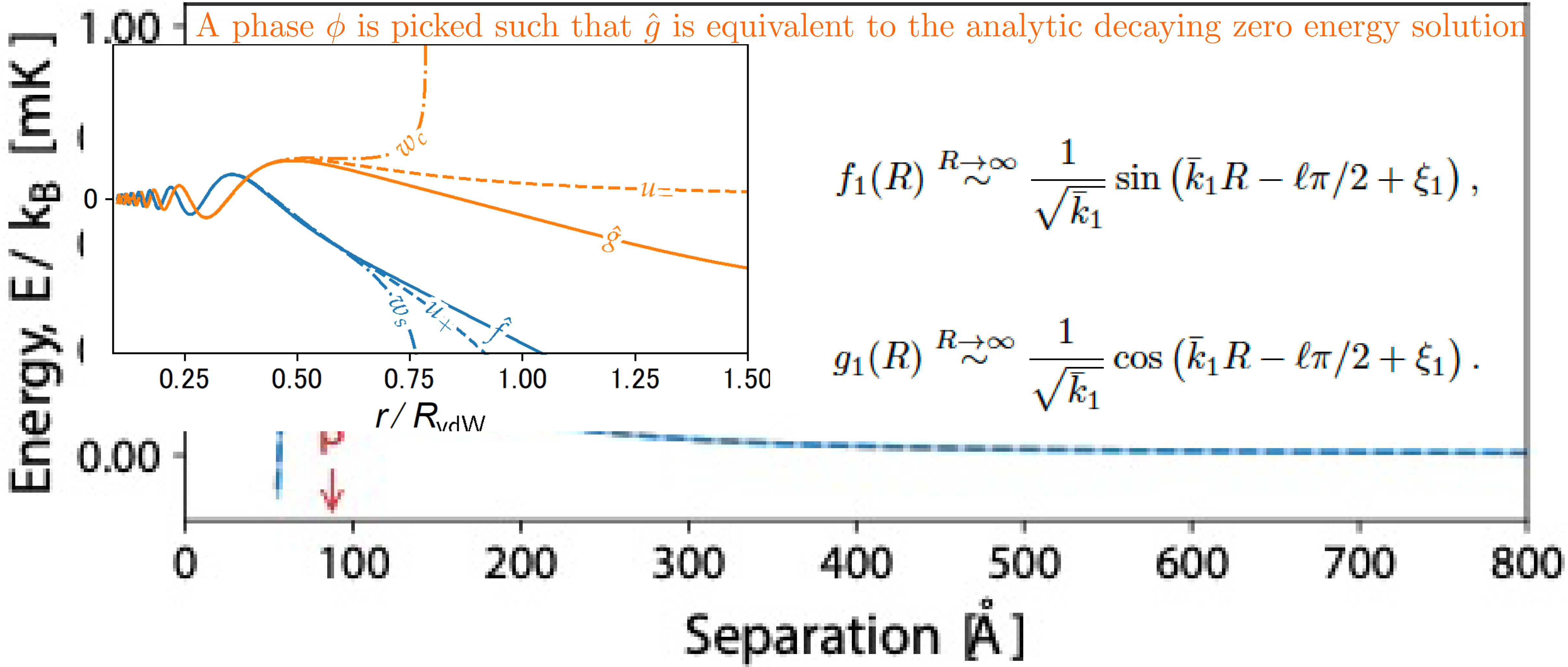

$$f_1(R) \overset{R\to\infty}{\sim} \frac{1}{\sqrt{\bar{k}_1}} \sin\left(\bar{k}_1 R - \ell\pi/2 + \xi_1\right),$$

$$g_1(R) \overset{R\to\infty}{\sim} \frac{1}{\sqrt{\bar{k}_1}} \cos\left(\bar{k}_1 R - \ell\pi/2 + \xi_1\right).$$

Solution linear combination

$$u_1(R) = c_1 f_1(R) + c_2 g_1(R)$$

$$u_1(R) = \hat{c}_1 \hat{f}_1(R) + \hat{c}_2 \hat{g}_1(R)$$

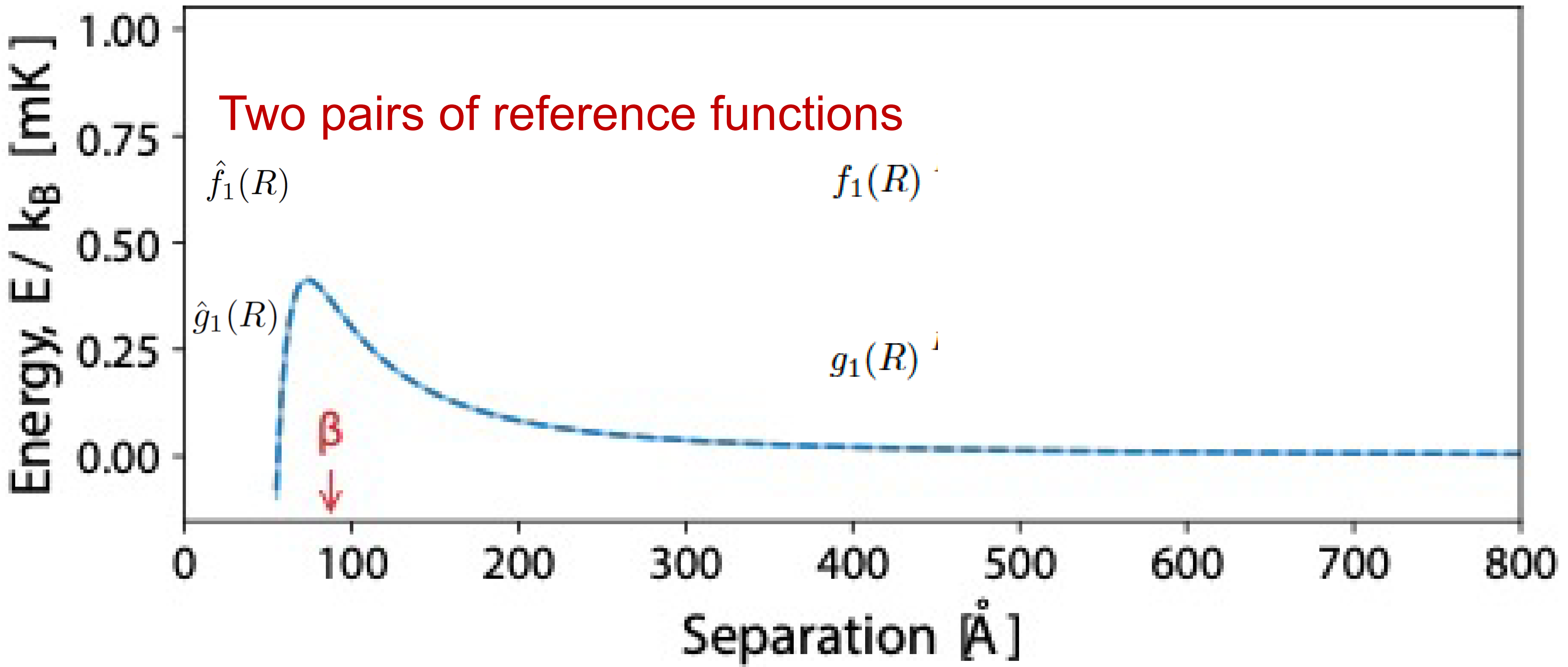

Solution linear combination

$$u_1(R) = c_1 f_1(R) + c_2 g_1(R)$$

$$u_1(R) = \hat{c}_1 \hat{f}_1(R) + \hat{c}_2 \hat{g}_1(R)$$

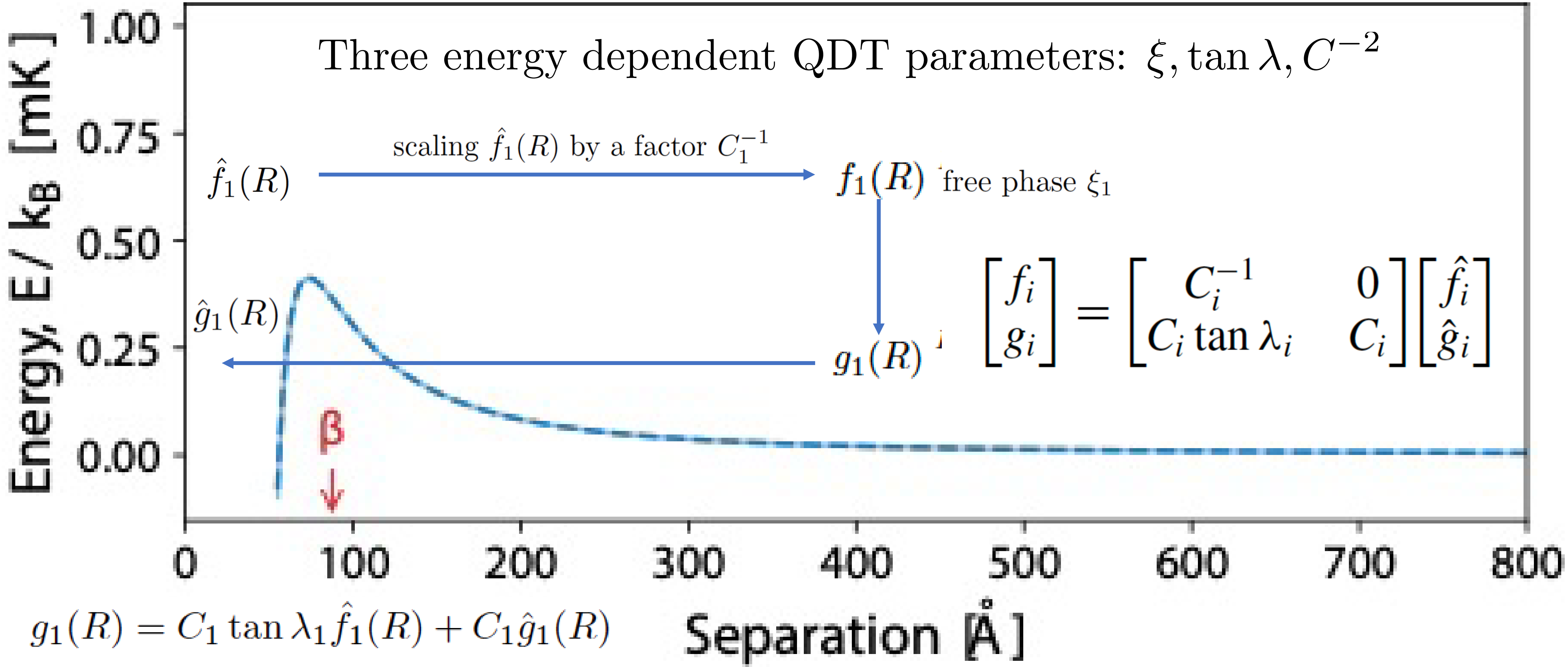

$$g_1(R) = C_1 \tan\lambda_1 \hat{f}_1(R) + C_1 \hat{g}_1(R)$$

Three energy dependent QDT parameters: $\xi, \tan\lambda, C^{-2}$

A phase ϕ is picked such that $\hat{g}$ is equivalent to the analytic decaying zero energy solution

Choice advantageous for numerics

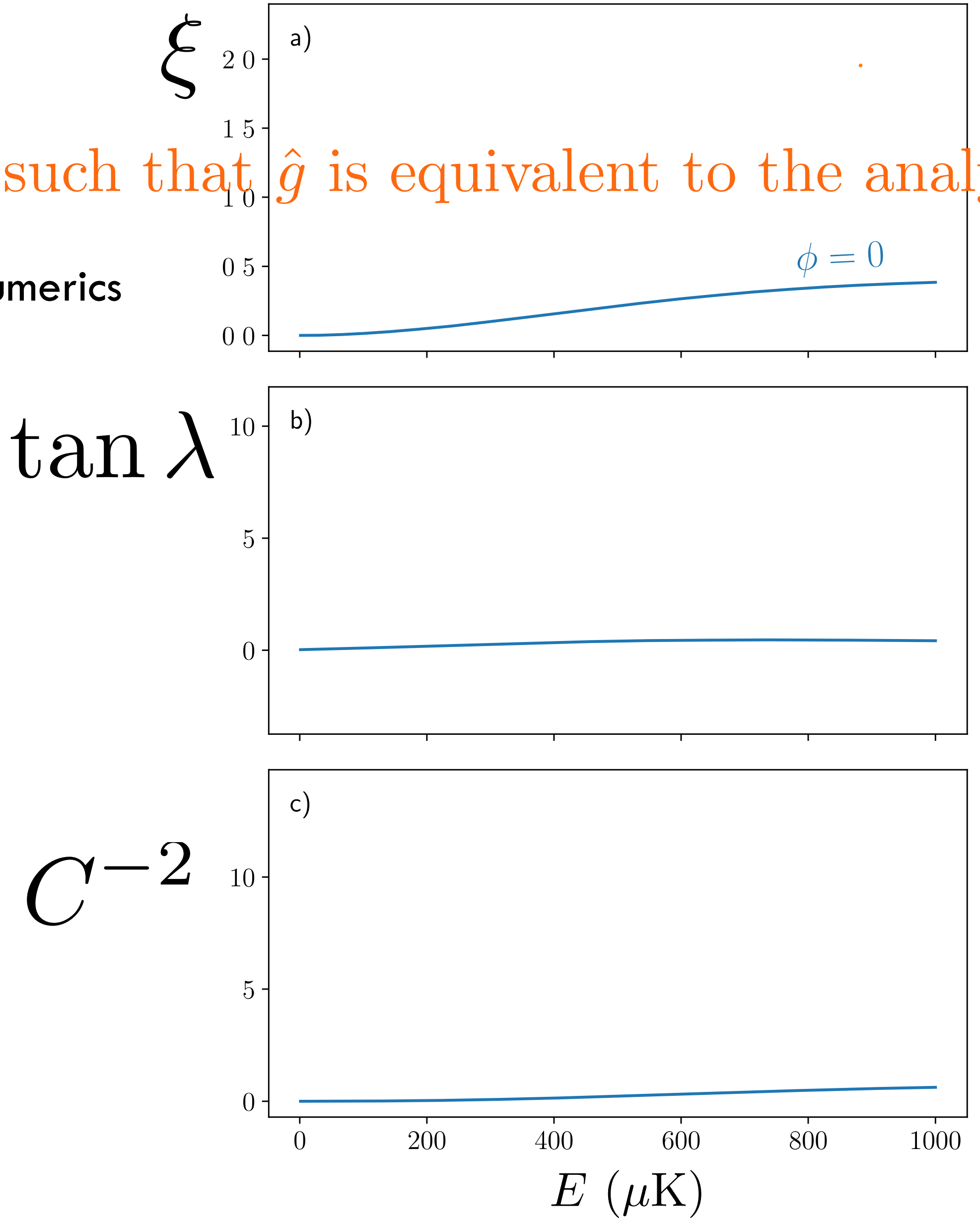

Analytic rotation of QDT parameters

? Why pick $\phi = 0.590 \times \pi$

Because this choice reproduces ξ as the background phase shift in

$$\delta_d(E,B) = \delta_{\mathrm{bg}}(E) + \arctan\left(\frac{\Gamma_B(E)/2}{B - B_{\mathrm{res}}(E)}\right)$$

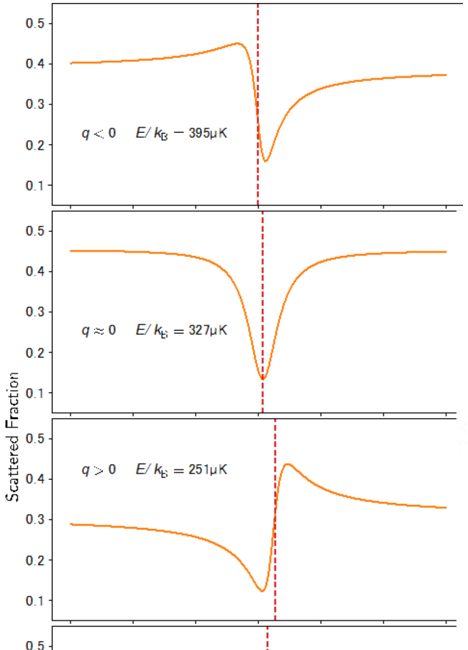

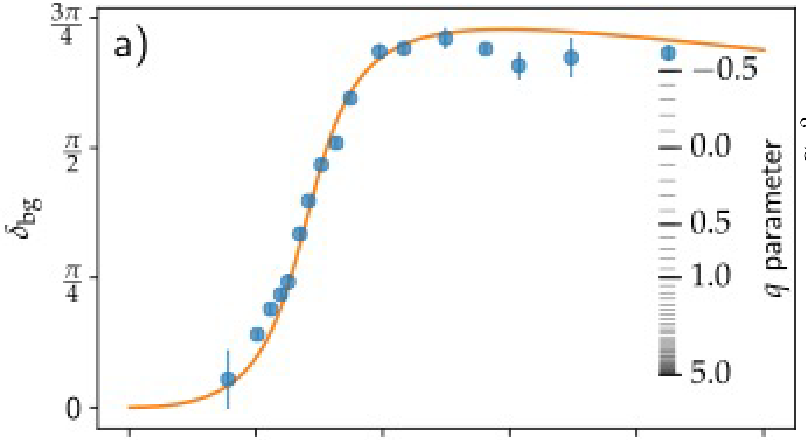

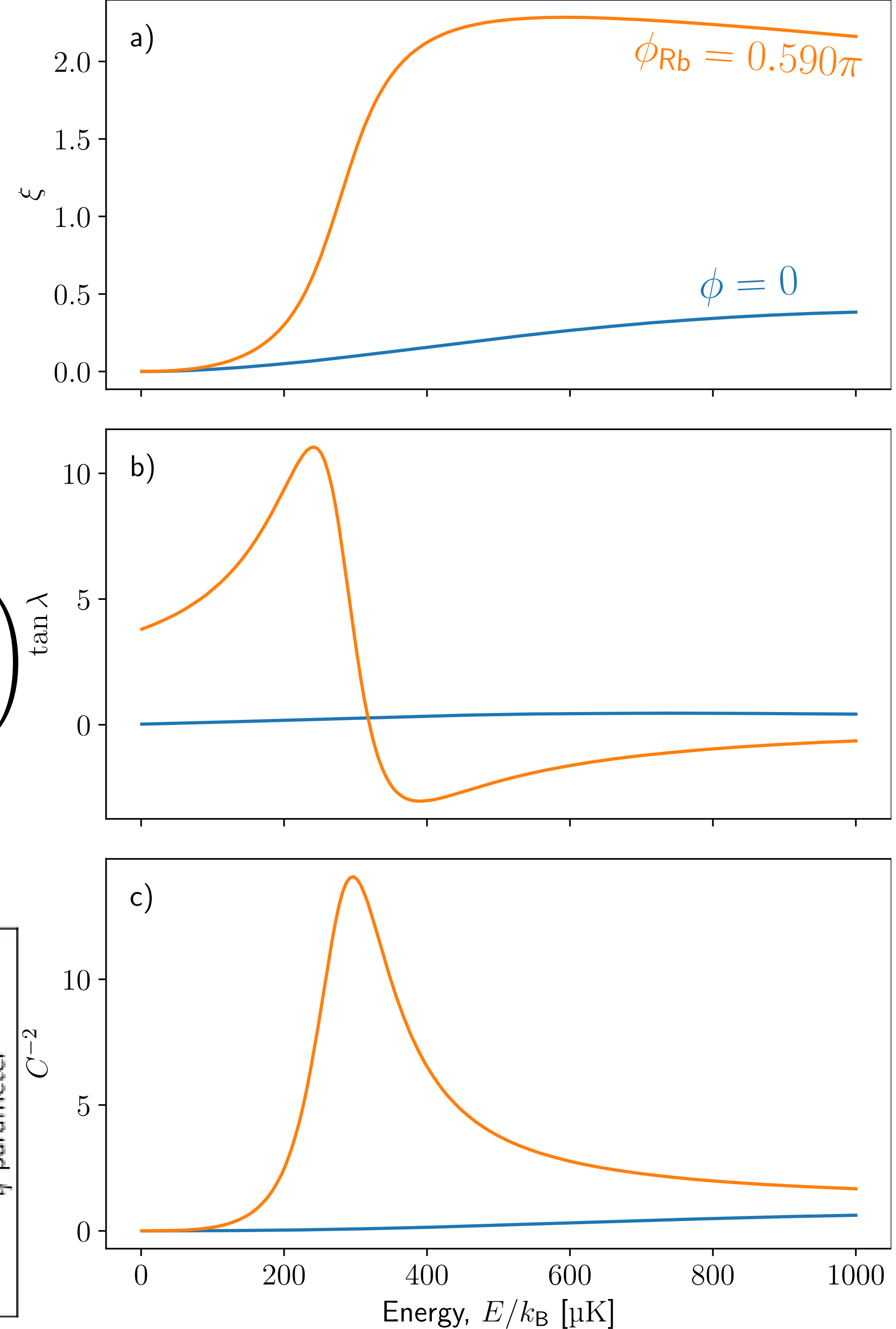

Closed channel QDT parameter

$$\cos\nu_i \hat{f}_i - \sin\nu_i \hat{g}_i \overset{r\to\infty}{\sim} \frac{e^{-|k_i|R}}{2\sqrt{|k_i|}}$$

We do not determine $\tan\nu$, but assume that at some energy E_0 it becomes zero

$$\tan\nu \approx \left.\frac{\partial\nu}{\partial E}\right|_{E=E_0} (E - E_0)$$

The above can be shown to lead to a parametrization of the resonance position

$$B_{\rm res}(E) = B_0 + \frac{E}{\delta\mu} + \frac{\bar{\Gamma}_B}{2}\tan\lambda$$

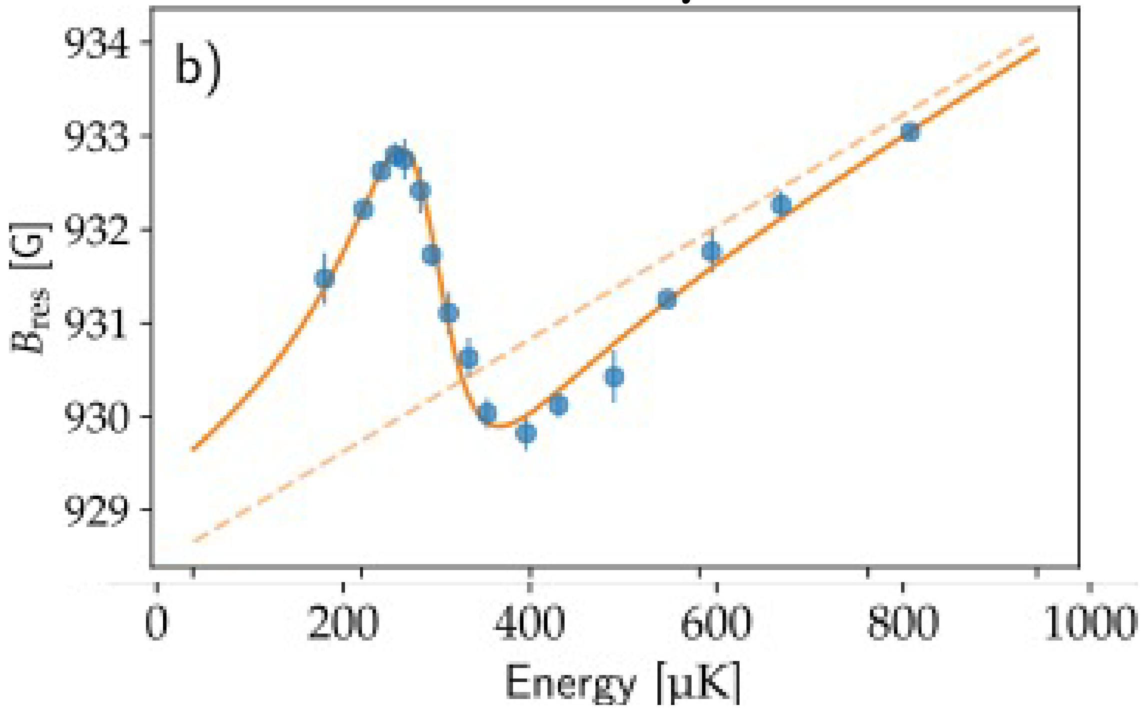

$$\Gamma = 96\ \mu K,\ \delta\mu = 184\ \mu{\rm K/G},\ B_0 = 928.7\ {\rm G}$$

Prediction for widths of Fano profiles

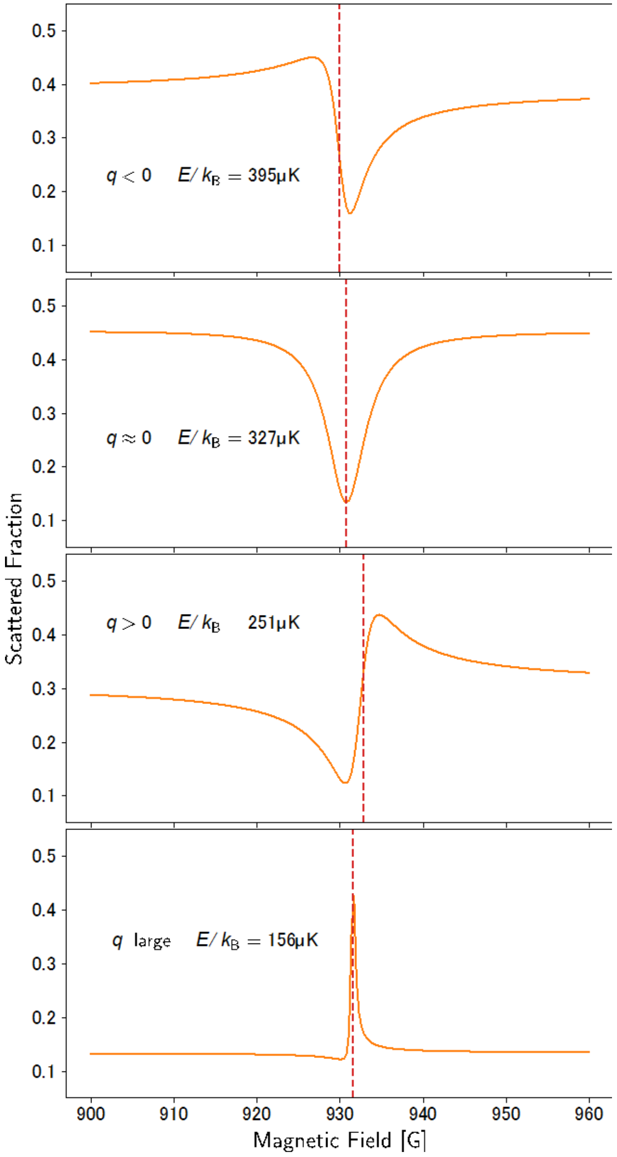

$$\Gamma_B(E) = C^{-2}(E)\bar{\Gamma}_B$$

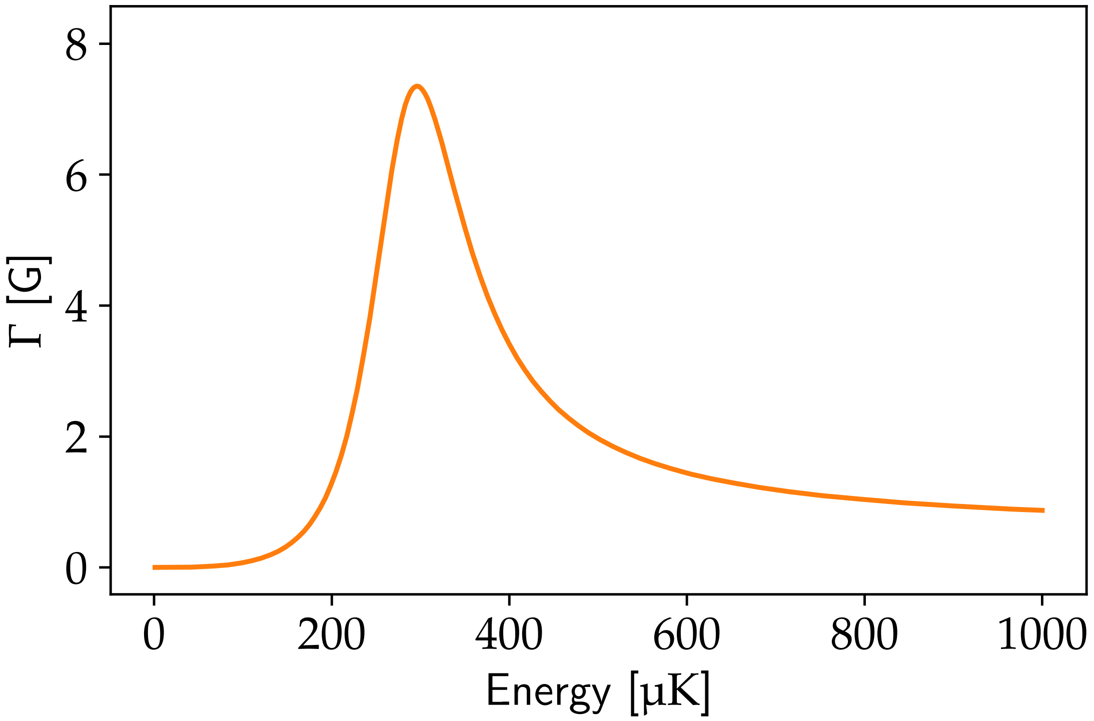

ıance

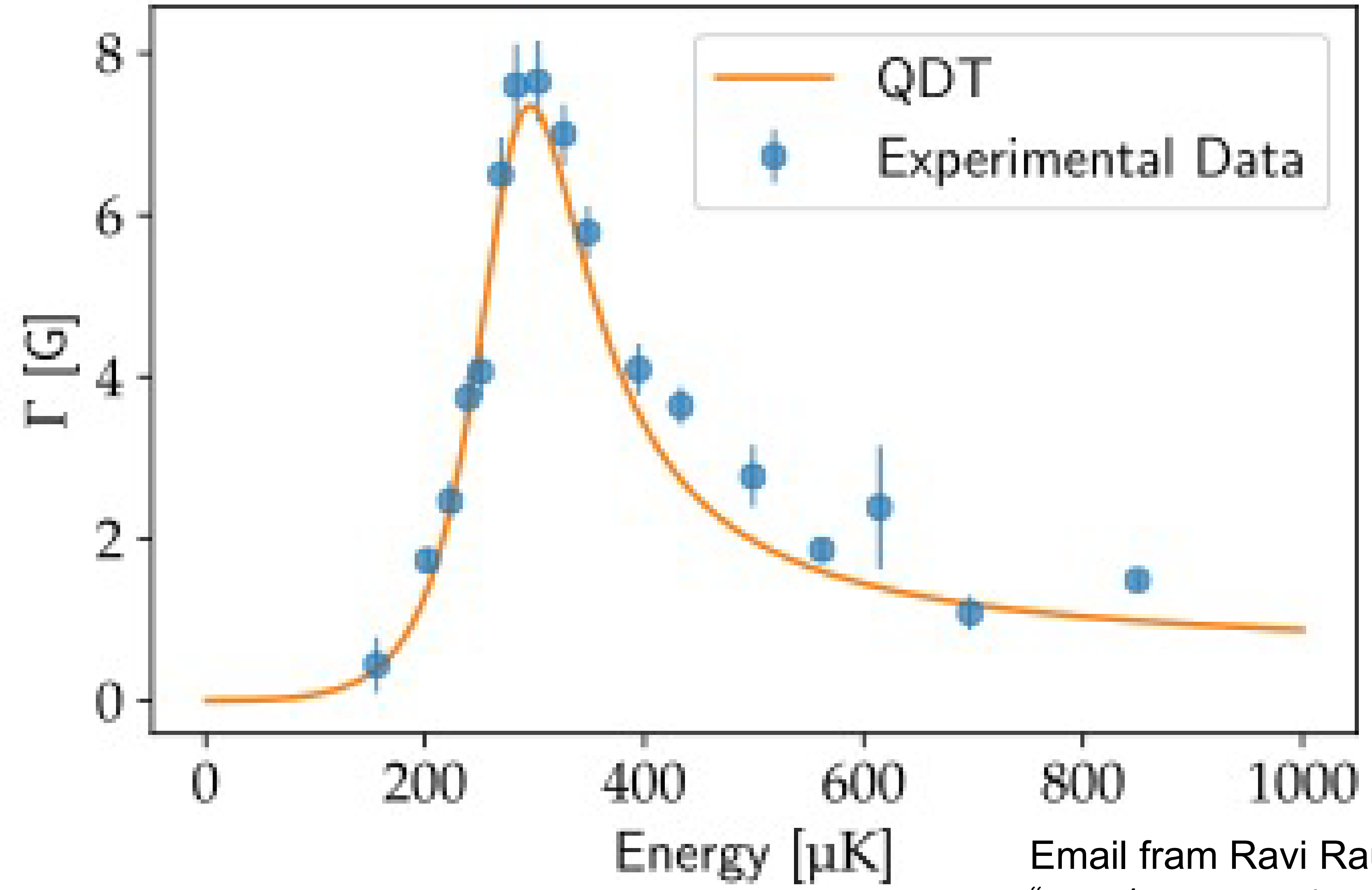

Email fram Ravi Rau:

“I read you very nice posting on shape and Feshbach resonances in a QDT analysis.

It is a very rich paper and Fig.7 impressive.”


Team
Amita Deb
Ryan Thomas
Bianca Sawyer
Craig Chisholm
Milena Horvath
Matthew Chilcott
James Croft

Contributions

- Pristine system for elucidating paradigms of quantum scattering

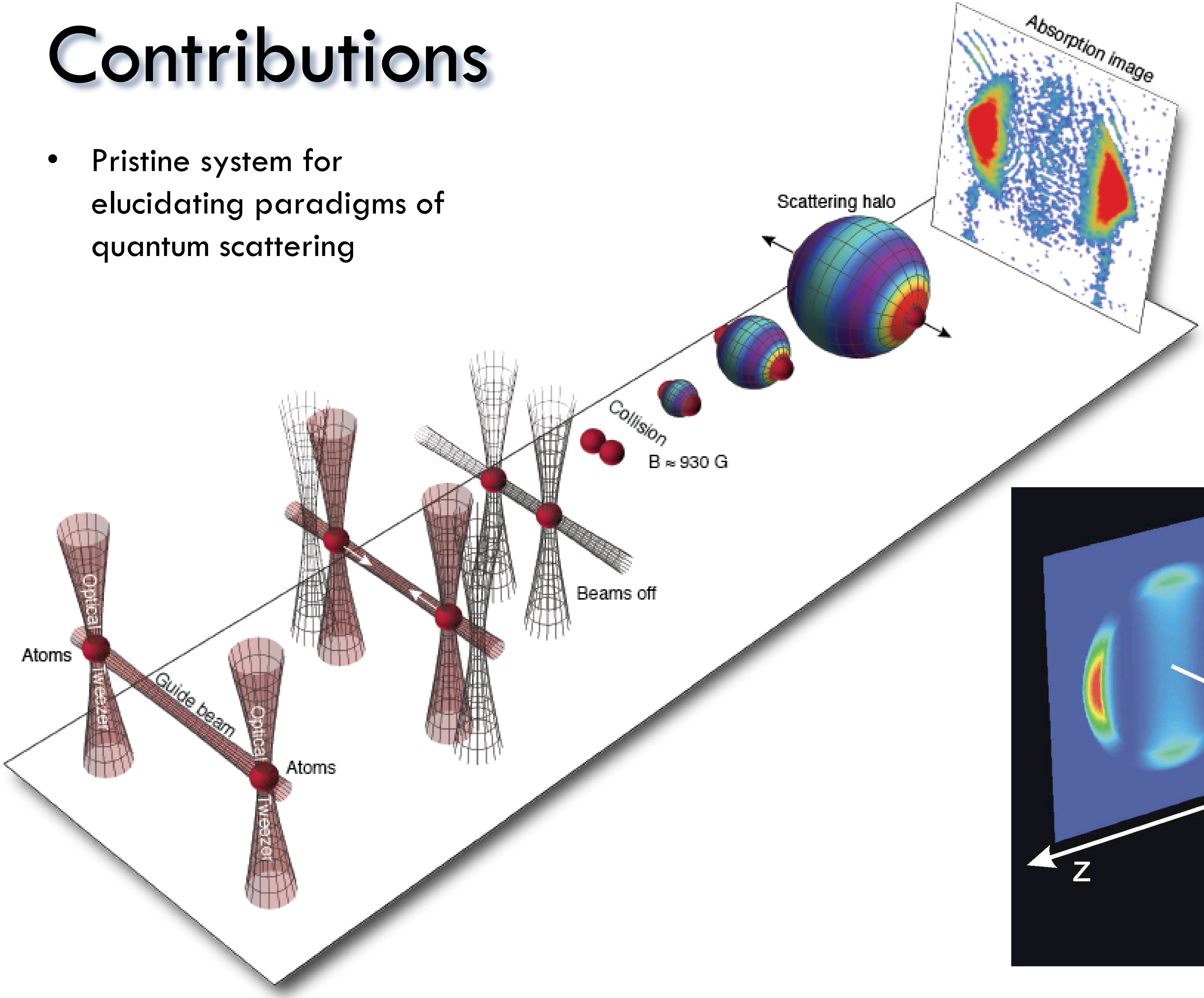

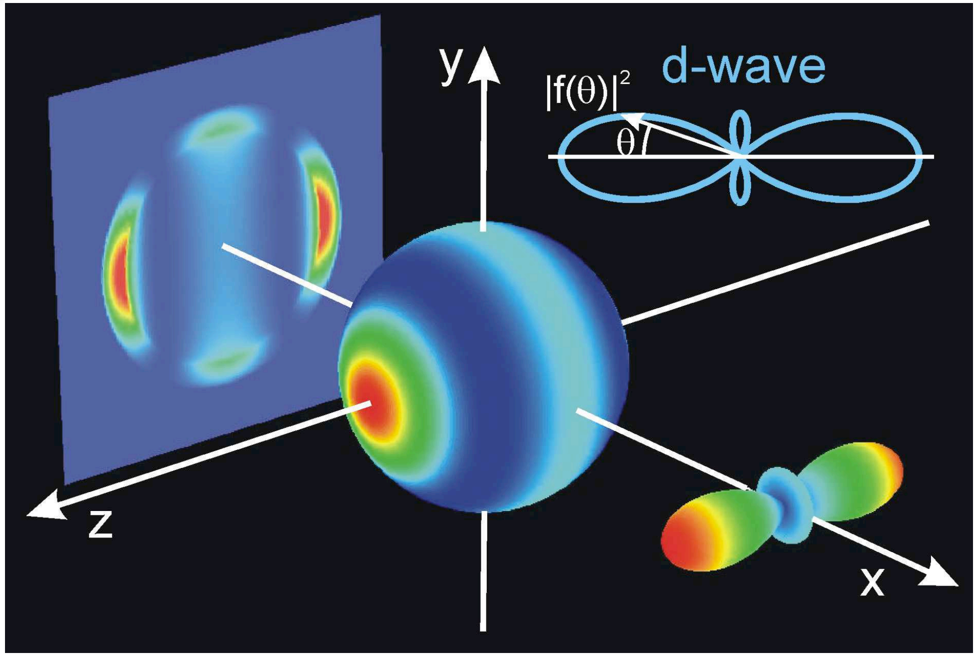

Contributions

- Pristine system for elucidating paradigms of quantum scattering

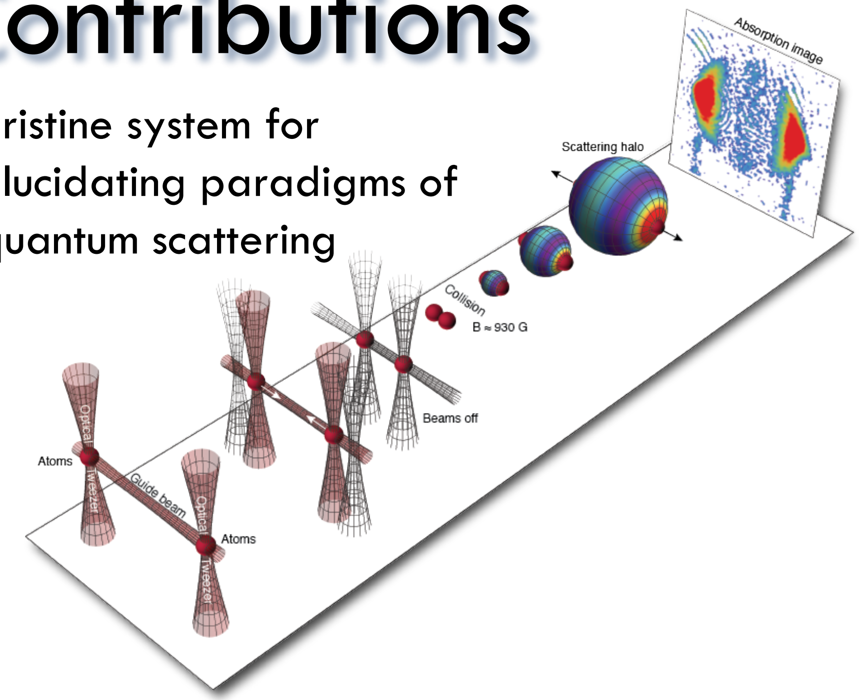

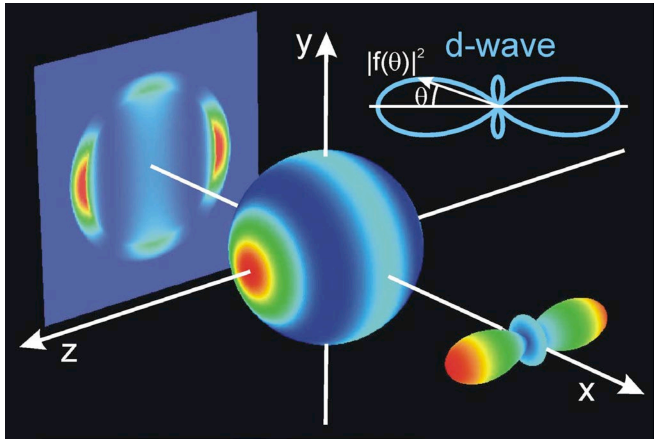

Interplay between S-matrix poles:

- Feshbach resonance + antibound state
- Feshbach resonance + shape resonance

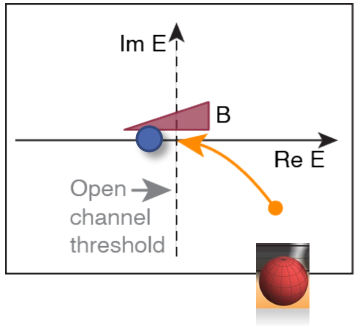

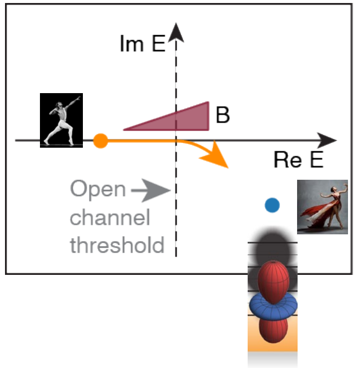

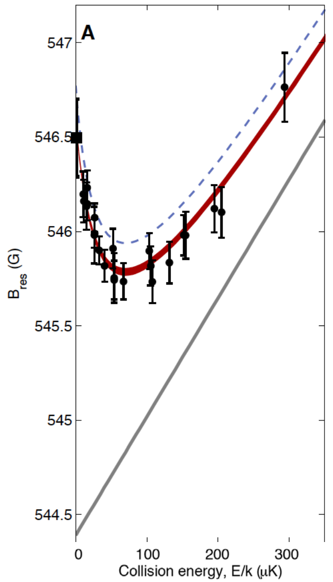

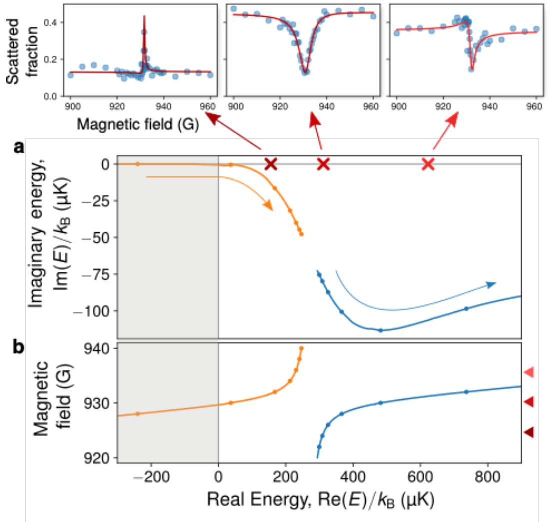

Contributions

- Pristine system for elucidating paradigms of quantum scattering

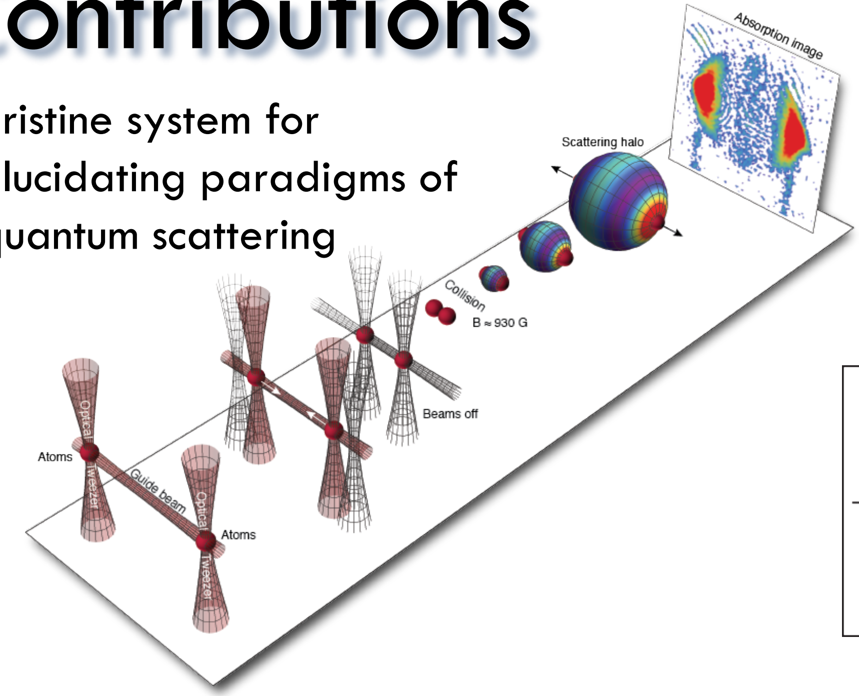

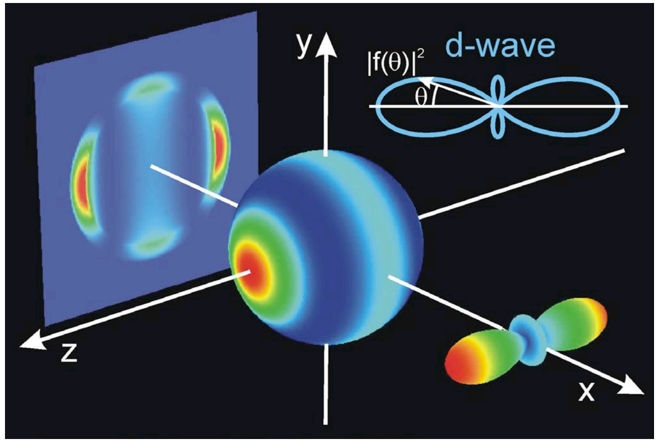

Interplay between S-matrix poles:

- Feshbach resonance + antibound state
- Feshbach resonance + shape resonance

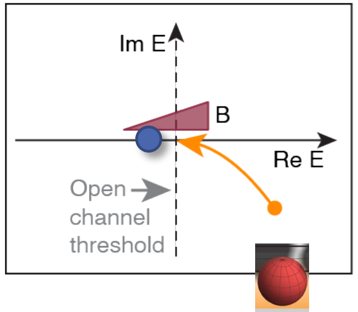

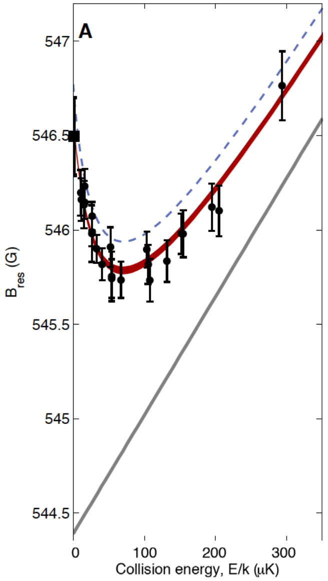

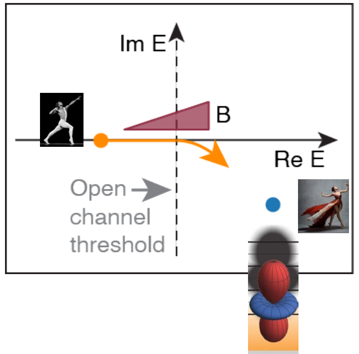

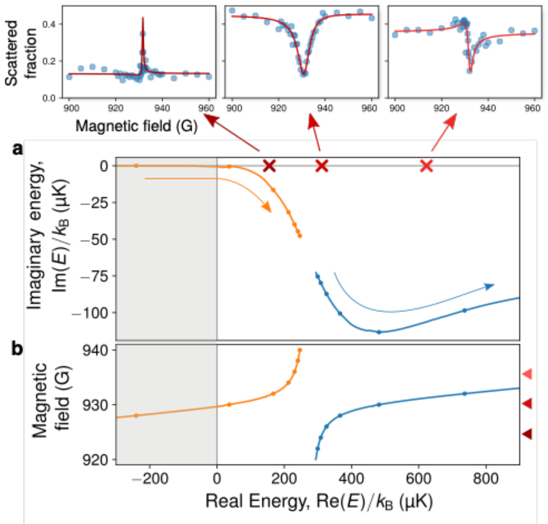

- MQDT analysis

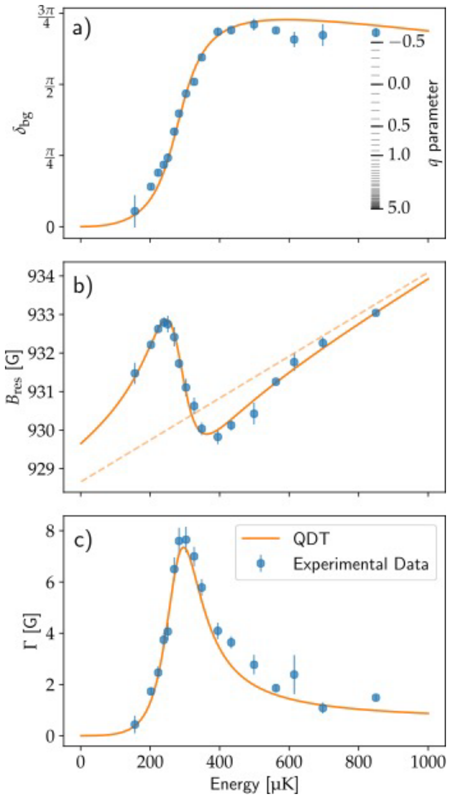

Contributions

- Pristine system for elucidating paradigms of quantum scattering

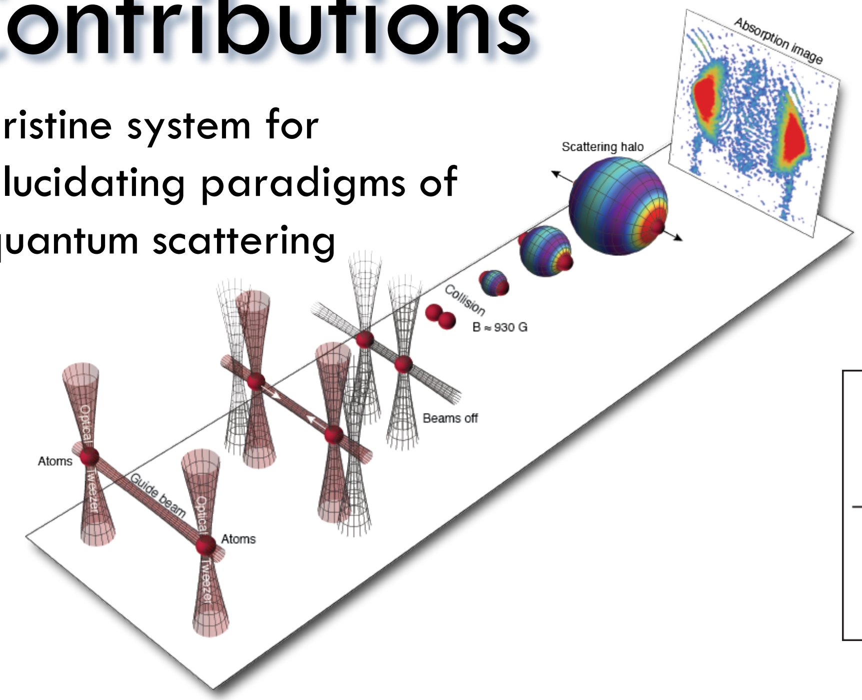

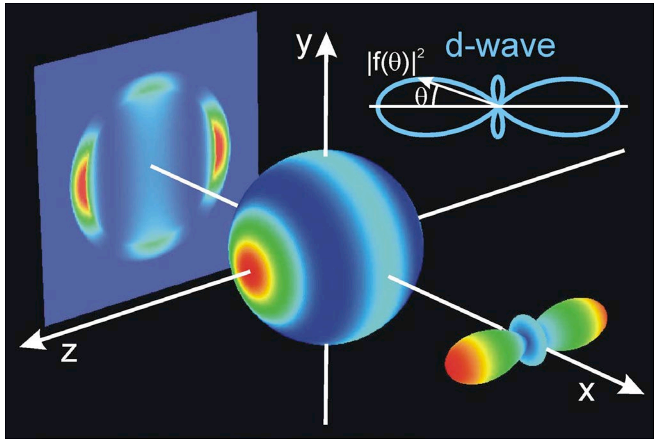

Interplay between S-matrix poles:

- Feshbach resonance + antibound state
- Feshbach resonance + shape resonance

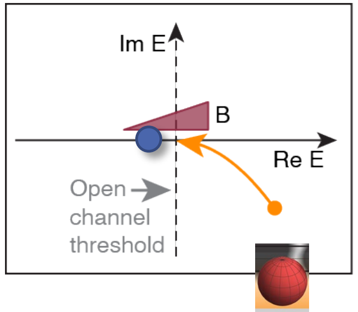

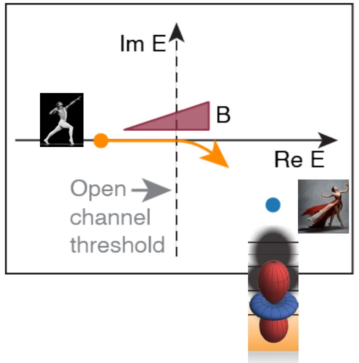

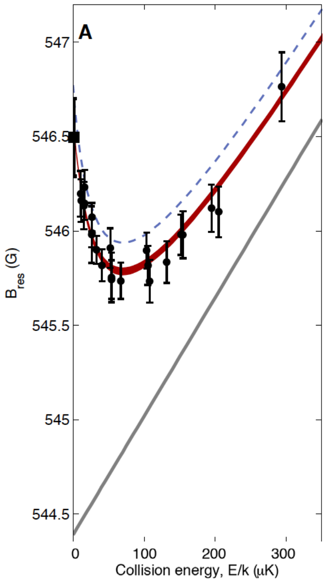

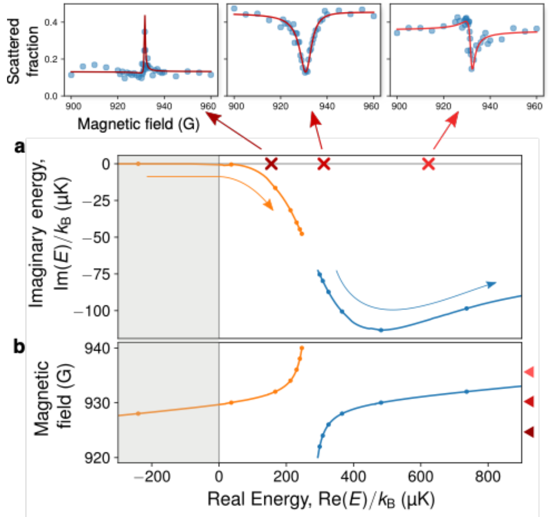

- MQDT analysis

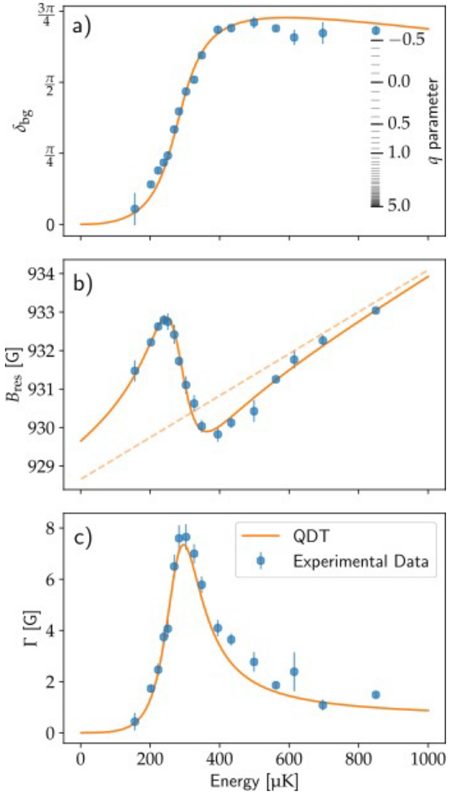

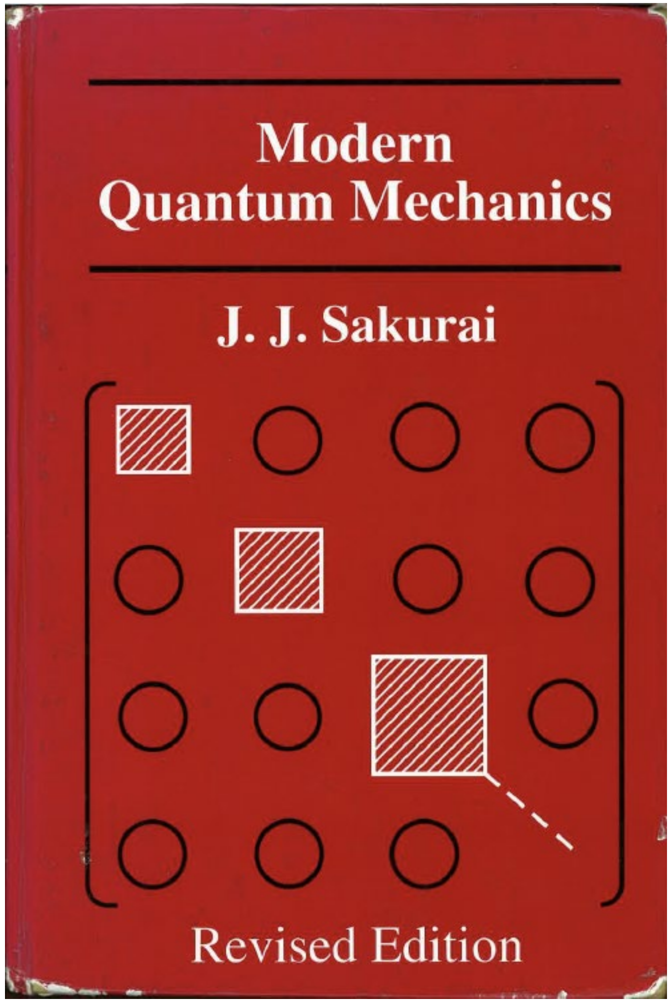

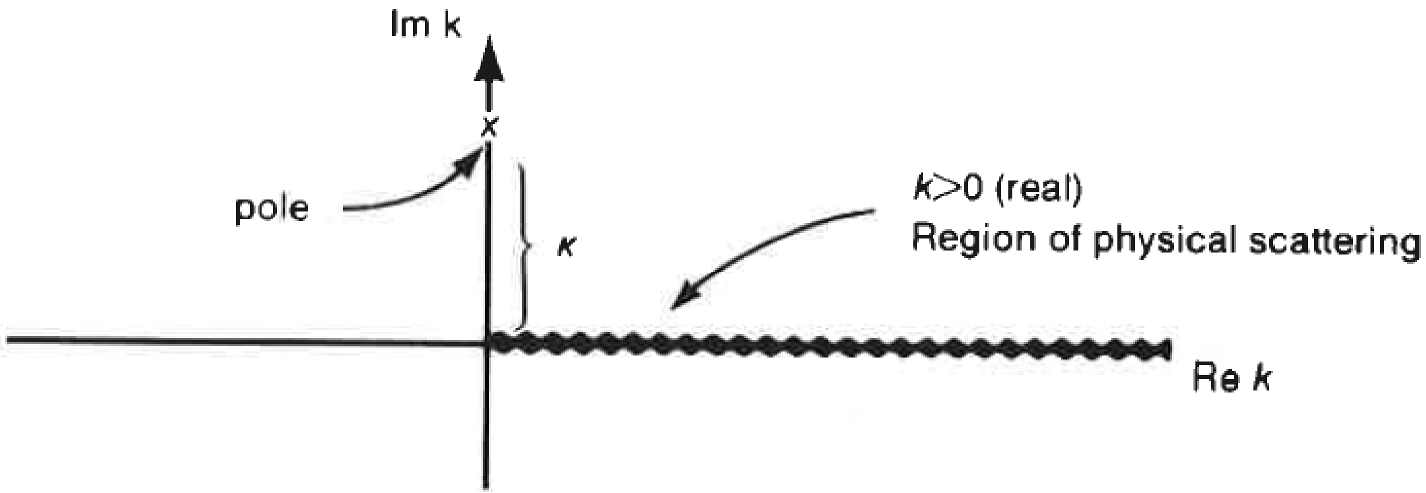

FIGURE 7.10. The complex k-plane with bound-state pole at $k = +i\kappa$.

Non-Hermitian effective Hamiltonian

TABLE I. Classification of S-matrix pole interaction.

	Case I	Case II	Case III
$(\epsilon_1 - \epsilon_2)^2 + 4\omega^2$	Positive	Zero	Negative
Coupling strength ω	$< \frac{1}{4}\lvert\gamma_1 - \gamma_2\rvert$	$= \frac{1}{4}\lvert\gamma_1 - \gamma_2\rvert$	$> \frac{1}{4}\lvert\gamma_1 - \gamma_2\rvert$
Crossing	Real energy $\mathrm{Re}\,\mathcal{E}_+(B_0) = \mathrm{Re}\,\mathcal{E}_-(B_0)$	Poles coincide $\mathcal{E}_+(B_0) = \mathcal{E}_-(B_0)$	Imaginary energy $\mathrm{Im}\,\mathcal{E}_+(B_0) = \mathrm{Im}\,\mathcal{E}_-(B_0)$
Pole trajectories given by Eq. (4) (assuming $E_1 \propto B$ and E_2, γ_1, and γ_2 constant).	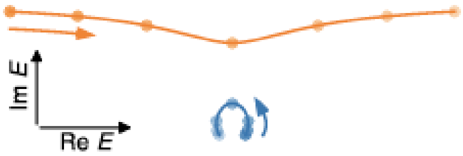	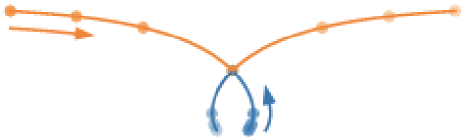	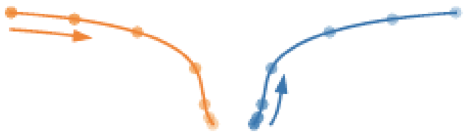

Look at above table in light of what we found for:

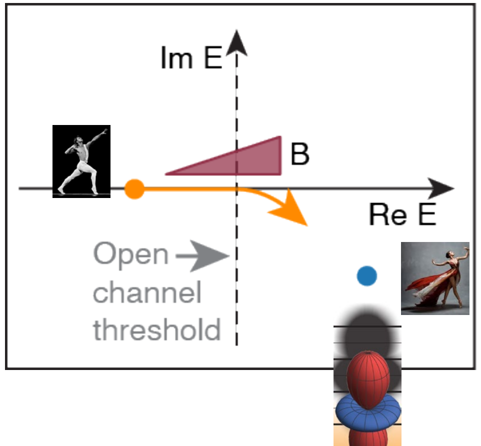

Non-Hermitian effective Hamiltonian

TABLE I. Classification of S-matrix pole interaction.

	Case I	Case II	Case III
$(\epsilon_1 - \epsilon_2)^2 + 4\omega^2$	Positive	Zero	Negative
Coupling strength ω	$< \frac{1}{4}\lvert\gamma_1 - \gamma_2\rvert$	$= \frac{1}{4}\lvert\gamma_1 - \gamma_2\rvert$	$> \frac{1}{4}\lvert\gamma_1 - \gamma_2\rvert$ strong coupling
Crossing	Real energy $\mathrm{Re}\,\mathcal{E}_+(B_0) = \mathrm{Re}\,\mathcal{E}_-(B_0)$	Poles coincide $\mathcal{E}_+(B_0) = \mathcal{E}_-(B_0)$	Imaginary energy $\mathrm{Im}\,\mathcal{E}_+(B_0) = \mathrm{Im}\,\mathcal{E}_-(B_0)$
Pole trajectories given by Eq. (4) (assuming $E_1 \propto B$ and E_2, γ_1, and γ_2 constant).	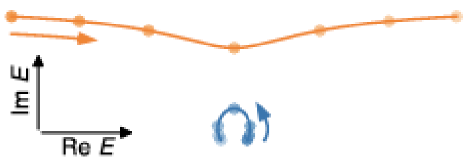	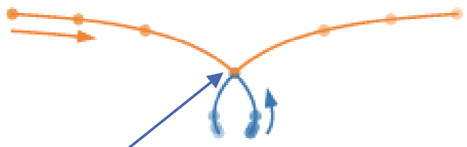	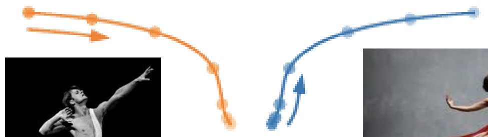

$$H = \begin{bmatrix} \varepsilon_1(B) & \omega \\ \omega & \varepsilon_2(B) \end{bmatrix}$$

$$\mathcal{E}_\pm = \frac{\varepsilon_1 + \varepsilon_2}{2} \pm \frac{1}{2}\sqrt{(\varepsilon_1 - \varepsilon_2)^2 + 4\omega^2}$$

$$\varepsilon_1(B) = E_1(B) - \frac{i}{2}\gamma_1$$

$$\varepsilon_2(B) = E_2(B) - \frac{i}{2}\gamma_2$$

$$E_1(B_0) = E_2(B_0)$$